THE UNIVERSITY OF ALBERTA

RELEASE FORM

NAME OF AUTHOR: David Joseph Swadron

TITLE OF THESIS: Photographic Optics for a 20 Inch Telescope

DEGREE FOR WHICH THESIS WAS PRESENTED: M. Sc.

YEAR THIS DEGREE GRANTED: 1976

THE UNIVERSITY OF ALBERTA

PHOTOGRAPHIC OPTICS FOR A 20 INCH TELESCOPE

by

© DAVID JOSEPH SWADRON

A THESIS

SUBMITTED TO THE FACULTY OF GRADUATE STUDIES AND RESEARCH

IN PARTIAL FULFILLMENT OF THE REQUIREMENTS FOR THE DEGREE

OF MASTER OF SCIENCE

DEPARTMENT OF PHYSICS

EDMONTON, ALBERTA

FALL, 1976

THE UNIVERSITY OF ALBERTA

FACULTY OF GRADUATE STUDIES AND RESEARCH

The undersigned certify that they have read, and recommend to the Faculty of Graduate Studies and Research, for acceptance, a thesis entitled PHOTOGRAPHIC OPTICS FOR A 20 INCH TELESCOPE submitted by David Joseph Swadron in partial fulfillment of the requirements for the degree of Master of Science.

TO MY MOTHER

ABSTRACT

The primary optical aberrations suffered by reflecting telescopes and the effects of these aberrations on the imaging quality of such instruments are discussed. Methods of correcting these aberrations and thus greatly enhancing the photographic usefulness of telescopes are investigated. In particular, designs for three correcting systems to be used on the University of Alberta's new 20 inch telescope are developed; one to be used with the telescope at prime focus, and one for each of the two Cassegrain configurations. The performance of each of the correcting systems is evaluated using a three dimensional ray tracing program, and the results displayed in the form of spot diagrams. The ray tracing programs used in the development of the correcting systems are presented.

ACKNOWLEDGMENTS

I am grateful to Dr. D. P. Hube for having stimulated my interest in astronomy and astronomical optics, and for providing valuable advice throughout his supervision of my research program.

I would also like to thank Dr. J. Winzer for his helpful suggestions and many discussions regarding the work described in this thesis. His expert advice and knowledge of telescopic systems have proven invaluable throughout the development of this work.

I wish to express my appreciation to Mr. B. Arnold, who will be producing the optical systems described in this thesis, for many interesting discussions on optical systems and their production.

I thank the University of Alberta for the financial support that has enabled me to pursue my master's program during the past two years.

Finally, I wish to express my gratitude to my wife, Marilyn, for her help in proof-reading this thesis and checking the accuracy of the equations. I would also like to express my appreciation for her patience and understanding throughout the time I have devoted to this work.

TABLE OF CONTENTS

LIST OF TABLES

LIST OF FIGURES

CHAPTER I

INTRODUCTION

For many years the University of Alberta's principal astronomical research instrument has been a 12" Cassegrain telescope with Dall-Kirkham optics. This telescope has been employed mainly for photometry, as the optics are not entirely satisfactory for deep sky photography. In 1975 construction was initiated on a 20" telescope. This telescope, being constructed at the University of Alberta, is to replace the older instrument. The 12" telescope has been transferred from the observatory to the university campus to facilitate its use as a teaching instrument.

The main component of the new telescope is a 20" f/3 parabolic mirror. To ensure maximum versatility of the new telescope, it has been designed to operate in three different configurations.

For wide field photography and photography of extended deep sky objects the telescope will be used at prime focus. In this mode, the telescope will be capable of photographing a field more than 6 degrees in diameter.

Some photometry, most visual work, and considerable photography will be done with the telescope utilized as an f/8 classical Cassegrain. A large proportion of the telescope's time will be used for photographic observations in this configuration.

The final design, which will be used primarily for photometry and planetary observations, is that of an f/18

classical Cassegrain. In this mode, the telescope can often be used when atmospheric conditions and moon placement do not permit effective use of the other two configurations.

To allow rapid interchange of the optical components three separate tube ends are being constructed for the telescope. This permits rapid change of configuration with a minimum of readjustment and little chance of misalignment or damage to the optics.

The advantage of a parabolic mirror, and the classical Cassegrain configuration, which employs a parabolic primary, is that such telescopes form perfect axial images. This means that, barring poor optical components and atmospheric turbulence, if the telescope is aligned on an object of very small angular width (generally a star) the image formed of that object will be diffraction limited. For a 20" telescope the size of such an image will be about .23 seconds of arc. If, however, the telescope is not aligned with the object (or if the object is of appreciable angular size), the image will be produced off the optical axis at the focal plane and its size will not be diffraction limited. Such an image suffers from the off-axis aberrations known as coma and astigmatism. These aberrations, which are discussed in detail in Chapter II, cause an increase in the image size and a deformation of the image's shape. This destruction of image integrity increases the further off axis that the image formation occurs, and can obliterate much detail at even small distances from the axis.

These off-axis aberrations are not important in photometry as the photometric subjects are usually of very small angular widths (point sources) and the telescope is usually aligned upon the subject, producing an axial image.

Visual work generally only encompasses a narrow cone of light near the optical axis. In any case, eyepieces themselves usually introduce more aberrations than the telescope system, and the eye is not sufficiently accurate to detect small amounts of such aberrations.

These off-axis aberrations become very important, however, in photographic work. Since the photographic plate records the whole field of view of the telescope, and not just the area very near the optical axis, these image errors can produce catastrophic effects, severely limiting the amount of the plate that can be used for accurate measurements. Hundreds or thousands of photographs may be necessary to cover, with good resolution, the same area that one well corrected photograph could. The need to correct these off-axis aberrations thus becomes imperative if scientifically useful photographs are to be obtained from the new telescope.

The photographic requirements for each of the three configurations and the solution of the problems presented by the off-axis aberrations are discussed in the following chapters.

CHAPTER II

ABERRATIONS OF THE CASSEGRAIN TELESCOPE

All practical designs of the Cassegrain telescope are limited in their performance by inherent image aberrations. The primary image aberrations are divided into three characteristic forms, spherical aberration, coma, and astigmatism.

Spherical aberration is characterized by its uniform size over the field, whereas the size of the comatic figure is linearly dependent on the distance from the optical axis, and the size of the astigmatic figure varies as the square of the distance from the axis.

In this chapter we first develop expressions for design relationships in Cassegrain telescopes, and then derive expressions for the aberrations in terms of the design parameters.

2.1 Design Relationships for Two Mirror Telescopes

The combined focal length of a pair of thin lenses (or reflecting surfaces) of focal lengths f_1 and f_2 respectively, separated by a distance d is given by

$$\frac{1}{f} = \frac{1}{f_1} + \frac{1}{f_2} - \frac{d}{f_1 f_2} \qquad (2.1)$$

A ray entering the telescopic system parallel to the optical axis will, after reflection from the primary, intersect the secondary mirror at a height h_s where:

$$h_s = \frac{f_1 - d}{f_1} y = \frac{d+e}{f} y$$

where y is the radial distance from the parallel incident ray to the optical axis. Equating the two expressions for h_s we have:

$$f(f_1 - d) = f_1(d+e)$$

Equation (2.1) can be used to form a third equality:

$$d = f_1 f_2 \left(\frac{1}{f_1} + \frac{1}{f_2} - \frac{1}{f} \right)$$

$$f(f_1 - d) = f\left(f_1 - f_2 - f_1 + \frac{f_1 f_2}{f}\right) = -f_2(f - f_1)$$

We therefore have three equalities:

$$-(f-f_1)f_2 = f_1(d+e) = f(f_1 - d) \qquad (2.2)$$

The last two terms of (2.2) can be separated to express a relationship between d and e:

$$f_1 d + f_1 e = f f_1 - f d$$

$$(f_1 + f)d = f_1(f-e) \qquad (2.3)$$

The radius of the secondary mirror necessary to intercept all the light incident from the primary mirror can also be determined from Figure 1. The necessary radius will be h_s with $y = y'$ (radius

of primary) plus h_ϕ with ϕ = angular radius of the field. Then:

$$h_s = \frac{d+e}{f} y' \qquad\qquad h_\phi = d\phi$$

Therefore, the radius of the secondary is given by:

$$R_s = \frac{d+e}{f} y' + d\phi$$

$$= \frac{f_1+e}{f_1+f} y' + d\phi$$

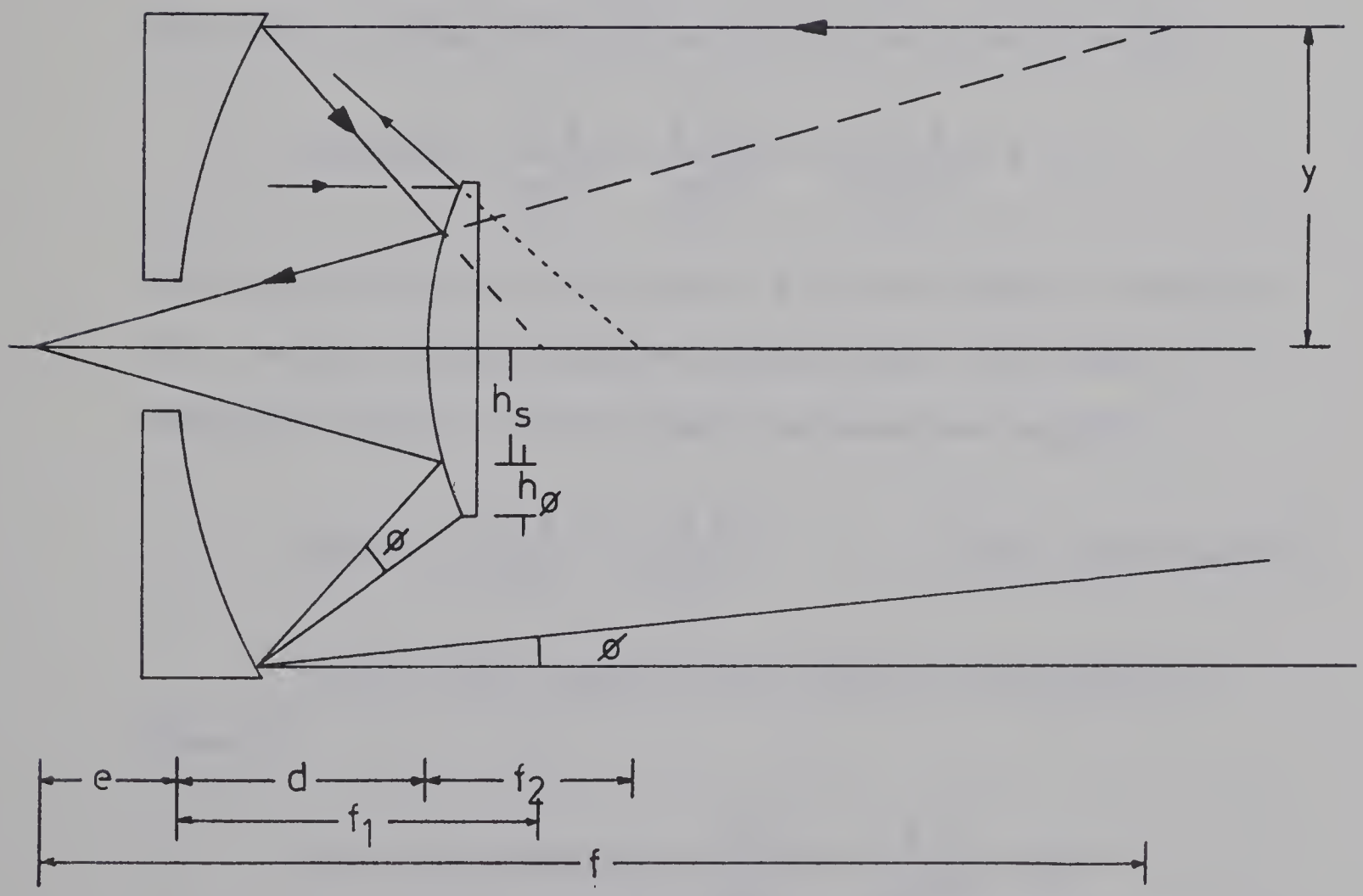

Fig. 1. Design relationships of Cassegrain telescope

2.2 Primary Aberrations of Cassegrain Telescopes

The primary, or Seidel, aberrations for a two mirror system can be determined by retarding lamina analysis (Allen, 1975). Although this system lends itself particularly well to numerical calculations of specific designs, it can also be used to derive the general form of the primary aberrations.

The retarding lamina method of aberration analysis is based on the fact that all conic surfaces can be described by their departure from a spherical surface. This departure from such a spherical surface is called the lamina.

The equation of a sphere with the origin at the pole (the point at which the surface cuts the axis) is given by:

$$x(\text{sphere}) = \left(\frac{1}{2R}\right)y^2 + \left(\frac{1}{8R^3}\right)y^4 + \left(\frac{1}{16R^5}\right)y^6 + \ldots.$$

where x is the depth of the curve, R is the radius of curvature, and y is the distance from the optical axis. For Seidel aberration theory, only the first two terms are required.

$$x(\text{sphere}) = \left(\frac{1}{2R}\right)y^2 + \left(\frac{1}{8R^3}\right)y^4 \qquad \text{(Seidel approximation)}$$

The equivalent equation for a conic of revolution is given by:

$$x(\text{conic of revolution}) = \left(\frac{1}{2R}\right)y^2 + \left(\frac{1}{8R^3}\right)(1-e^2)y^4$$

(Seidel approximation)

where e is the eccentricity of the surface and R is the axial radius

of curvature.

Thus, the departure from a sphere of a conic of revolution is given by:

$$\Delta x = \frac{e^2}{8R^3} y^4$$

Since this lamina is the difference between a sphere and the actual conic figure, if such a lamina were to be physically placed into the system, it would convert the conic into a spherical surface.

It is a well known fact that a spherical surface does not suffer from any off-axis aberrations (coma and astigmatism) but does suffer badly from spherical aberration. This spherical aberration can be corrected without affecting the coma or astigmatism by placing a lamina of positive power at the centre of curvature of the sphere. When this is actually done the lamina is known as a Schmidt plate.

It would therefore be possible to correct all aberrations by supplying each conic surface with the lamina necessary to convert it into a sphere plus a lamina of suitable strength placed at the conic's centre of curvature. As these laminae are not, in fact, present in the actual system it is possible to express the aberrations of the actual system in terms of the "negative" aberration introduced by all the imaginary laminae. This can be done in terms of the retardation caused by each of the laminae in the system.

The extra distance that a wave incident on a conic surface

(as compared to a wave incident on the corresponding spherical surface) must travel is given by:

$$p = 2\Delta x = \frac{e^2}{4R^3} y^4 \qquad (2.5)$$

This distance p, is called the retardation due to the imagined lamina located on the surface of the conic.

From equation (2.5), it is seen that the retardation caused by a lamina is proportional to y^4 (y = distance from the optical axis). This retardation can therefore be written as:

$$p = \beta y^4 \qquad (2.5a)$$

where β is called the lamina power. β is positive for a lamina which retards a wave (corresponding to a physical depression in the surface) and negative for a lamina which advances the wave (corresponding to a physical bulge in the surface). Also, from equation (2.5) we can see that the power of surface laminae for conics of revolution with eccentricity e is

$$\beta_s = \begin{matrix} + \\ - \end{matrix} \frac{e^2}{4R^3} \quad \text{for} \begin{cases} \text{concave} \\ \text{convex} \end{cases} \quad \text{surfaces} \qquad (2.6)$$

It can be shown (Allen, 1975) that the power of the centred lamina of each surface is

$$\beta_c = \begin{matrix} - \\ + \end{matrix} \frac{1}{4R^3 e'^2} \quad \text{for} \begin{cases} \text{concave} \\ \text{convex} \end{cases} \quad \text{surfaces} \qquad (2.7)$$

Here e' is not, in general, equal to the eccentricity of any

mirror but is given by:

$$e' = \frac{oR}{o} = \frac{\text{Object to centre of curvature distance}}{\text{Object to Pole distance}}$$

or equivalently (2.8)

$$e' = \frac{Ri}{i} = \frac{\text{Image to centre of curvature distance}}{\text{Image to pole distance}}$$

In the special case where the surface(s) under consideration form a perfect axial image (such as a paraboloid or classical Cassegrain with parabolic primary and hyberbolic secondary), e = e'.

Figure 2 (which is taken from Allen) demonstrates how the retardation p is related to spherical aberration, coma and astigmatism.

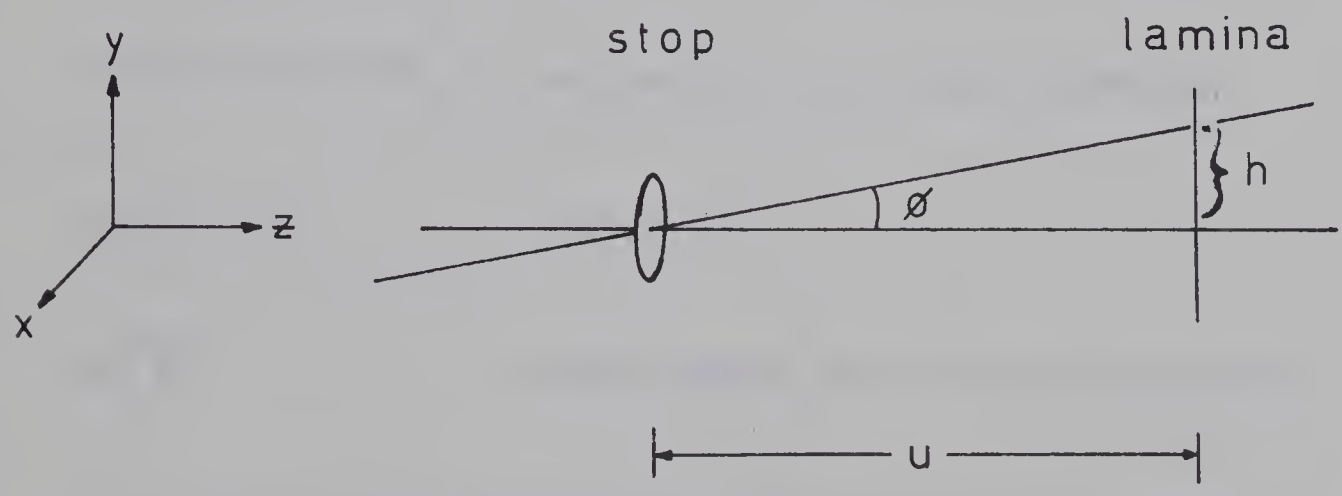

Fig. 2. Laminar retardation

If a light ray in the(y,z) plane, inclined at an angle ϕ to the optical axis, intersects an optical stop at the point

(x,y,0), it will intersect a lamina placed a distance u away at the point (x,y+h,u). The retardation of the wave at the lamina will therefore be given by:

$$p = \beta(x^2 + (y+h)^2)^2$$

$$= \beta(x^2 + y^2 + 2hy + h^2)^2$$

$$= \beta\left[(x^2+y^2)^2 + 4y(x^2+y^2)h + 2(3y^2+x^2)h^2 + 4yh^3 + h^4\right]$$

which can be classified into the Seidel aberrations in the following manner:

$\beta\left[(x^2+y^2)^2\right]$	Spherical aberration
$\beta u\phi\left[4y(x^2+y^2)\right]$	Coma
$\beta u^2\phi^2\left[2(3y^2+x^2)\right]$	Astigmatism and Petzval curvature
$\beta u^3\phi^3\left[4y\right]$	Distortion
$\beta u^4\phi^4$	Phase change (not a true aberration)

To determine the aberrational effect of all the laminae, the powers and positions of all the laminae must be transferred into star space (the space in front of the entrance pupil in which the incident light is neither converging nor diverging). Since the entrance pupil of a Cassegrain system is defined by the

primary mirror, the laminae associated with the primary can be considered to be in star space already. The position and power of the laminae associated with the secondary mirror must, however, be imaged through the primary. Denoting the object positions of the secondary laminae by u, and the image positions in star space by u^*, the simple thin lens formula $\frac{1}{o} + \frac{1}{i} = \frac{1}{f}$ can be used to image the positions through the primary:

$$\frac{1}{u^*} = \frac{1}{f_1} - \frac{1}{u} \tag{2.9}$$

The change to star space also requires a change in the lamina power given by:

$$\beta^* = \beta\left(\frac{u}{u^*}\right)^4 \tag{2.10}$$

Once all the lamina powers and positions have been imaged into star space, they can be added together to determine the aberrations. The various forms of aberration are denoted by:

Spherical aberration	$\Sigma\beta$	
Coma	$\Sigma\beta u$	(2.11)
Astigmatism	$\Sigma\beta u^2$	

The traditional coefficients B, F, and C (Schwarschild, 1905) which express the magnitudes of the aberrations are related by the formulae:

$$B = -4\Sigma\beta$$

$$F = -4\Sigma\beta u$$

$$C = -4\Sigma\beta u^2$$

In the following derivation, the retarding lamina method is used to determine the aberrations of a Cassegrain system in terms of the design parameters.

The subscripts 1 and 2 refer to the primary and secondary mirror respectively, while the subscripts s and c refer to the surface and centred lamina. The superscript * refers to values taken in star space.

The origin of the co-ordinate system is taken as the pole of the primary, with distances in Figure 3 being positive to the right.

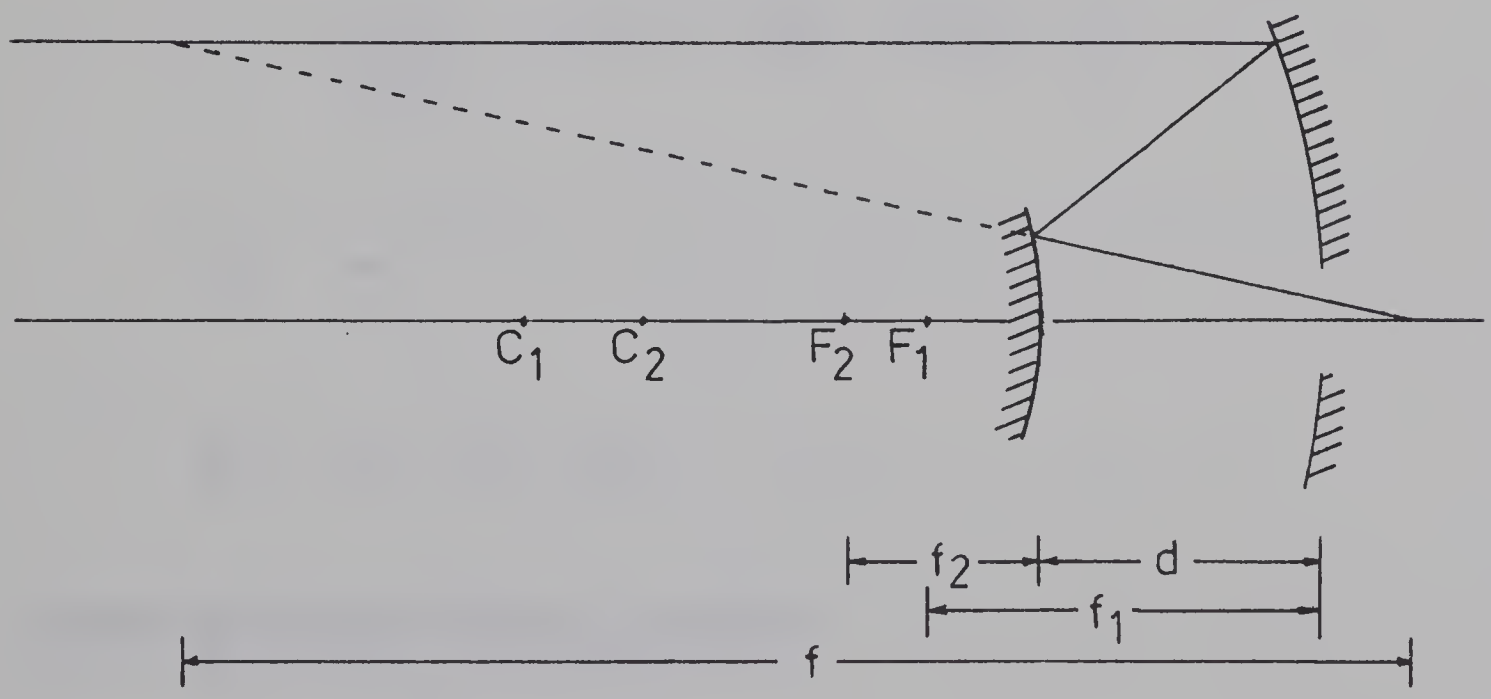

Fig. 3. Laminae positions in Cassegrain telescopes

C_1 and C_2 are the centres of curvature of the primary and secondary

mirrors. F_1 and F_2 are the focii of the two mirrors.

Laminae associated with the primary:

$$\beta_{1s} = \frac{e_1^2}{4R_1^3} = \frac{e_1^2}{4(2f_1)^3} = \frac{e_1^2}{32f_1^3}$$

$$= -\frac{b_1}{32f_1^3} \quad (b = \text{asphericity factor} = -e^2)$$

$$\beta^*_{1s} = \beta_{1s} = -\frac{b}{32f_1^3}$$

$$\beta^*_{1c} = \beta_{1c} = -\frac{1}{4R_1^3 e_1'^2} = -\frac{1}{32f_1^3 e_1'^2}$$

$$= -\frac{1}{32f_1^3} \quad \text{since } e' = \frac{R_1 - i}{i} = \frac{R_1 - f_1}{f_1} = \frac{f_1}{f_1} = 1$$

$$u^*_{1s} = u_{1s} = 0$$

$$u^*_{1c} = u_{1c} = -R = 2f_1$$

Laminae associated with the secondary:

$$\beta_{2s} = -\frac{e_2^2}{4R_2^3} = \frac{b_2}{32f_2^3}$$

$$u_{2s} = -d$$

Using equations (2.9) and (2.10) to transform these into star space,

$$\frac{1}{u^*_{2s}} = -\frac{1}{f_1} - \frac{1}{u} = -\frac{1}{f_1} + \frac{1}{d} = \frac{f_1 - d}{f_1 d}$$

$$u^*_{2s} = \frac{f_1 d}{f_1 - d}$$

$$\beta^*_{2s} = -\frac{e_2^{\,2}}{32 f_2^{\,3}} \frac{u^4}{u^*} = -\frac{e_2^{\,2}}{32 f_2^{\,3}} \frac{-d(f_1-d)}{f_1}^4$$

Using $f_2 = -\dfrac{f(f_1-d)}{(f-f_1)}$ from equation (2.2),

$$\beta^*_{2s} = -\frac{e_2^{\,2}}{32} \frac{(f-f_1)^3(f_1-d)}{f^3 f_1^{\,4}} = \frac{b_2}{32} \frac{(f-f_1)^3(f_1-d)}{f^3 f_1^{\,4}}$$

$$\beta_{2c} = \frac{1}{4R_2^{\,3} e_2'^{\,2}}$$

$$e_2' = \frac{R_2 - i}{i} = \frac{\text{Image to centre of curvature distance}}{\text{Image to Pole distance}}$$

$$= \frac{d + e - 2f_2}{d + e} \quad \text{(note: } f_2 \text{ is negative)}$$

using $d + e = -\dfrac{(f-f_1)f_2}{f_1}$,

$$e_2' = \frac{-2f_2 - \lceil (f-f_1)f_2 \rfloor / f_1}{-\lceil (f-f_1)f_2 \rfloor / f_2}$$

Therefore, $\beta_{2c} = -\dfrac{(f+f_1)}{32(f+f_1)f_2^3}$

$$u_{2c} = -(d-2f_2)$$

Transforming β_{2c} and u_{2c} into star space,

$$\frac{1}{u^*_{2c}} = -\frac{1}{f_1} - \frac{1}{u_{2c}} = -\frac{1}{f_1} + \frac{1}{d-2f_2} = \frac{f_1-(d-2f_2)}{f_1(d-2f_2)}$$

$$u^*_{2c} = \frac{f_1(d-2f_2)}{f_1-(d-2f_2)}$$

$$\beta^*_{2c} = \beta_{2c}\left(\frac{u_{2c}}{u^*_{2c}}\right)^4 = -\left(\frac{1}{32}\frac{f-f_1}{f+f_1}\right)^2 \frac{1}{f_2^3}\left(\frac{(d-f_2)(f_1-(d-2f_2))}{f_1(d-2f_2)}\right)^4$$

$$= -\frac{1}{32}\left(\frac{f-f_1}{f+f_1}\right)^2 \frac{1}{f_2^3}\left(\frac{f_1-d+2f_2}{f_1}\right)^4$$

Using $f_1 - d = \dfrac{-(f-f_1)f_2}{f}$,

$$\beta^*_{2c} = -\frac{1}{32}\left(\frac{f-f_1}{f+f_1}\right)^2 \frac{1}{f_2^3}\left(\frac{-(f-f_1)f_2+2f_2f}{f_1f}\right)^4$$

$$= -\frac{1}{32}\left(\frac{f-f_1}{f+f_1}\right)^2 \frac{1}{f_2^3}\left(\frac{f_1f_2+f_2f}{f_1f}\right)^4$$

$$\beta^*_{2c} = -\frac{1}{32}\left(\frac{f-f_1}{f+f_1}\right)^2 \frac{f_2}{f_1^4 f^4}(f+f_1)^4$$

and using $f_2 = \dfrac{-f(f_1-d)}{f-f_1}$,

$$\beta^*_{2c} = \frac{1}{32}\left(\frac{f-f_1}{f+f_1}\right)^2 \frac{(f_1-d)}{f_1^4 f^3(f-f_1)}(f+f_1)^4$$

$$= \frac{(f-f_1)(f_1-d)(f+f_1)^4}{32 f_1^4 f^3}$$

$$= \frac{1}{32}\left(\frac{f+f_1}{f-f_1}\right)^2 \frac{(f_1-d)(f-f_1)^3}{f_1^4 f^3}$$

The results are summarized in Table 1. Combining the values in this table, one obtains (after considerable algebraic manipulation and reduction):

$$\beta^* = -\frac{(1+b_1)}{32 f_1^3} + \frac{1}{32}\left[b_2 + \left(\frac{f+f_1}{f-f_1}\right)^2\right]\frac{(f-f_1)^3(f_1-d)}{f^3 f_1^4}$$

$$\beta^* u^* = -\frac{1}{16 f^2} - \frac{1}{32}\left[b_2 + \left(\frac{f+f_1}{f-f_1}\right)^2\right]\frac{(f-f_1)^3 d}{f^3 f_1^3}$$

$$\beta^* u^{*2} = -\frac{f_1(f-d)}{8f^2(f_1-d)} + \frac{1}{32}\left[b_2 + \left(\frac{f+f_1}{f-f_1}\right)^2\right]\frac{(f-f_1)^3 d^2}{8 f^3 f_1^2(f_1-d)}$$

Lamina	β^*	u^*
1s	$\frac{-b}{32f_1^3}$	0
1c	$\frac{-1}{32f_1^3}$	$2f_1$
2s	$\frac{b_2}{32}\frac{(f-f_1)^3(f_1-d)}{f^3f_1^4}$	$-\frac{f_1 d}{f_1-d}$
2c	$\frac{1}{32}\left(\frac{f+f_1}{f-f_1}\right)^2\frac{(f_1-d)}{f_1^4 f^3}(f-f_1)^3$	$-\frac{f_1(d-2f_2)}{f_1-(d-2f_2)}$

(2.12)

Table 1. Laminae powers and positions

Using the traditional coefficients B, F, and C, the aberrations are given by:

$$B = \frac{1+b_1}{8f_1^3} - \left[b_2 + \left(\frac{f_1+f}{f-f_1} \right)^2 \right] \frac{(f-f_1)^3(f_1-d)}{8f^3 f_1^4}$$

$$= \frac{1+b_1}{8f_1^3} - \left[b_2 + \left(\frac{f+f_1}{f-f_1} \right)^2 \right] \frac{(f-f_1)^3(f_1+e)}{8f^3 f_1^3 (f+f_1)}$$

$$F = \frac{1}{4f^2} + \left[b_2 + \left(\frac{f+f_1}{f-f_1} \right)^2 \right] \frac{(f-f_1)^3 d}{8f^3 f_1^3} \qquad (2.13)$$

$$= \frac{1}{4f^2} + \left[b_2 + \left(\frac{f+f_1}{f-f_1} \right)^2 \right] \frac{(f-f_1)^3 (f-e)^2}{8f^3 f_1 (f+f_1)(f_1+e)}$$

$$C = \frac{f_1(f-d)}{2f^2(f_1-d)} - \left[b_2 + \left(\frac{f+f_1}{f-f_1} \right)^2 \right] \frac{(f-f_1)^3 d^2}{8f^3 f_1^2 (f_1-d)}$$

$$= \frac{f^2+f_1 e}{2f^2(f_1+e)} - \left[b_2 + \left(\frac{f+f_1}{f-f_1} \right)^2 \right] \frac{(f-f_1)^3 (f-e)^2}{8f^3 f_1 (f+f_1)(f_1+e)} \; *$$

2.3 Size of Aberrations at the Focal Plane

The size of the aberrations at the focal plane (in angular measure) are given by (Gascoigne, 1968):

Angular diameter of spherical aberration = $\frac{1}{2}By^3$

Angular length of coma figure = $3Fy^2\phi$

Angular diameter of astigmatic blur circle = $2Cy\phi^2$

One can therefore use the equations of the previous section to numerically determine the size of image aberration

---

* The first term in the corresponding equation in Gascoigne (1968) is in error by a factor $(f^2+f_1 e)/f(f+e)$.

for any system.

The size of the comatic and astigmatic aberrations for a system consisting of a single parabolic mirror are plotted as a function of the semi angular field in Figures 4 and 5. It is seen that both coma and astigmatism are very strongly dependent on the focal ratio of the mirror, being very extreme for fast systems. It is also seen that, for a single mirror, it is the coma that limits the size of the usable photographic field.

Dr. W. Baade, in studies made during preparations for the construction of the Hale telescope, concluded that the usable field of a large parabolic mirror was limited to the area in which the comatic figure was less than 1.5 seconds of arc in size. This value has been considered unduly severe by many. On the basis of a somewhat more generous figure of 2.5 seconds of arc, the useful field of an f/3 paraboloid is only 4 minutes of arc in diameter. For a 20 inch diameter primary mirror, this corresponds to an area at the focal plane only 0.063 inch in diameter.

The aberrations for a two mirror system are dependent on the figure of the secondary. For a classical Cassegrain, which forms a perfect image on the optical axis, $b_2 = -\left[(f+f_1)/(f-f_1)\right]^2$ and the second terms in equations (2.13) become zero. Thus, the equation for coma remains unchanged, and the Cassegrain system has the same coma as a parabola with the same effective focal length.

The equation for astigmatism is:

$$C = \frac{f_1(f-d)}{2f^2(f_1-d)} = \frac{f^2+f_1e}{2f^2(f_1+e)} \quad .$$

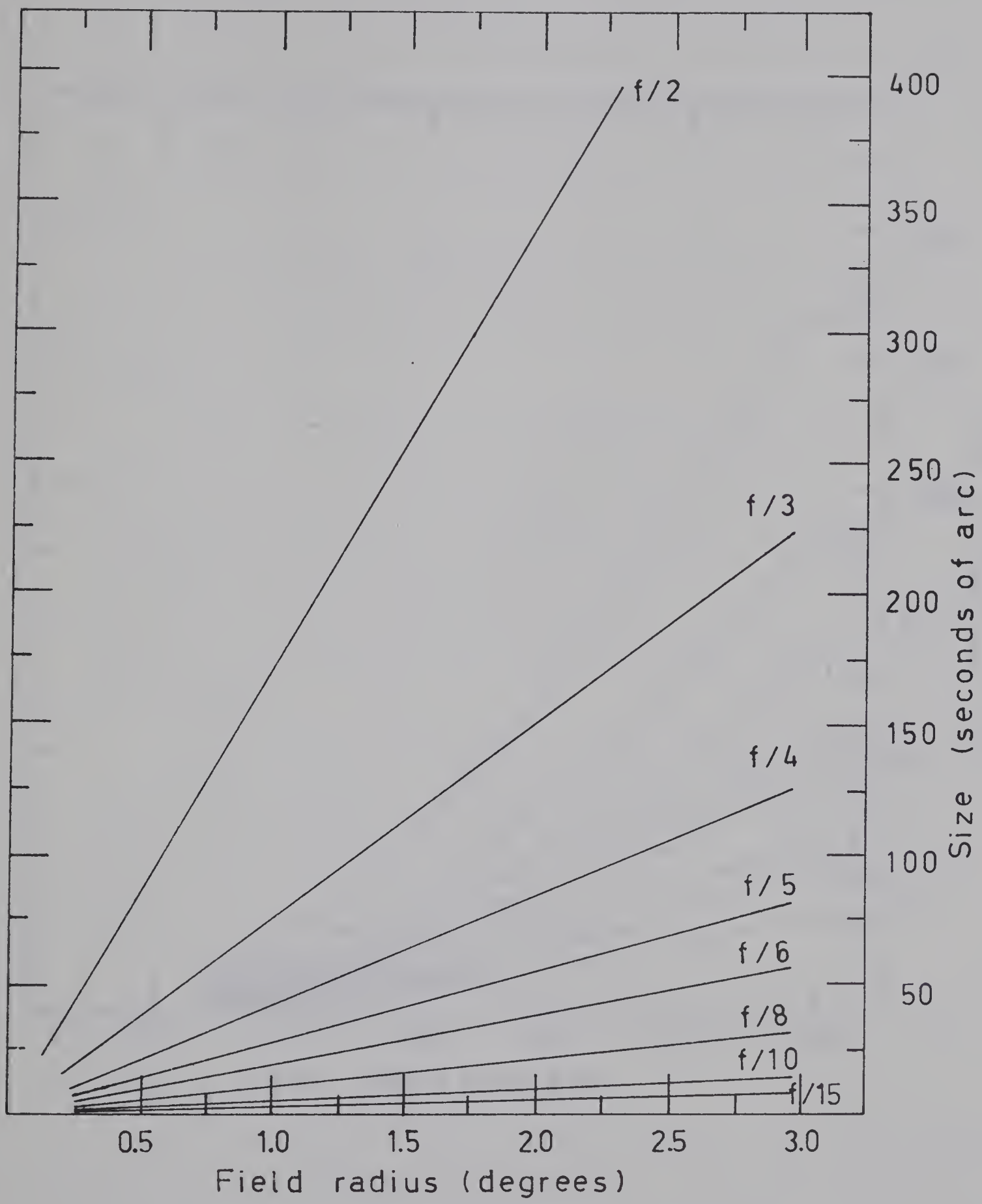

Fig 4. Coma of a parabolic mirror

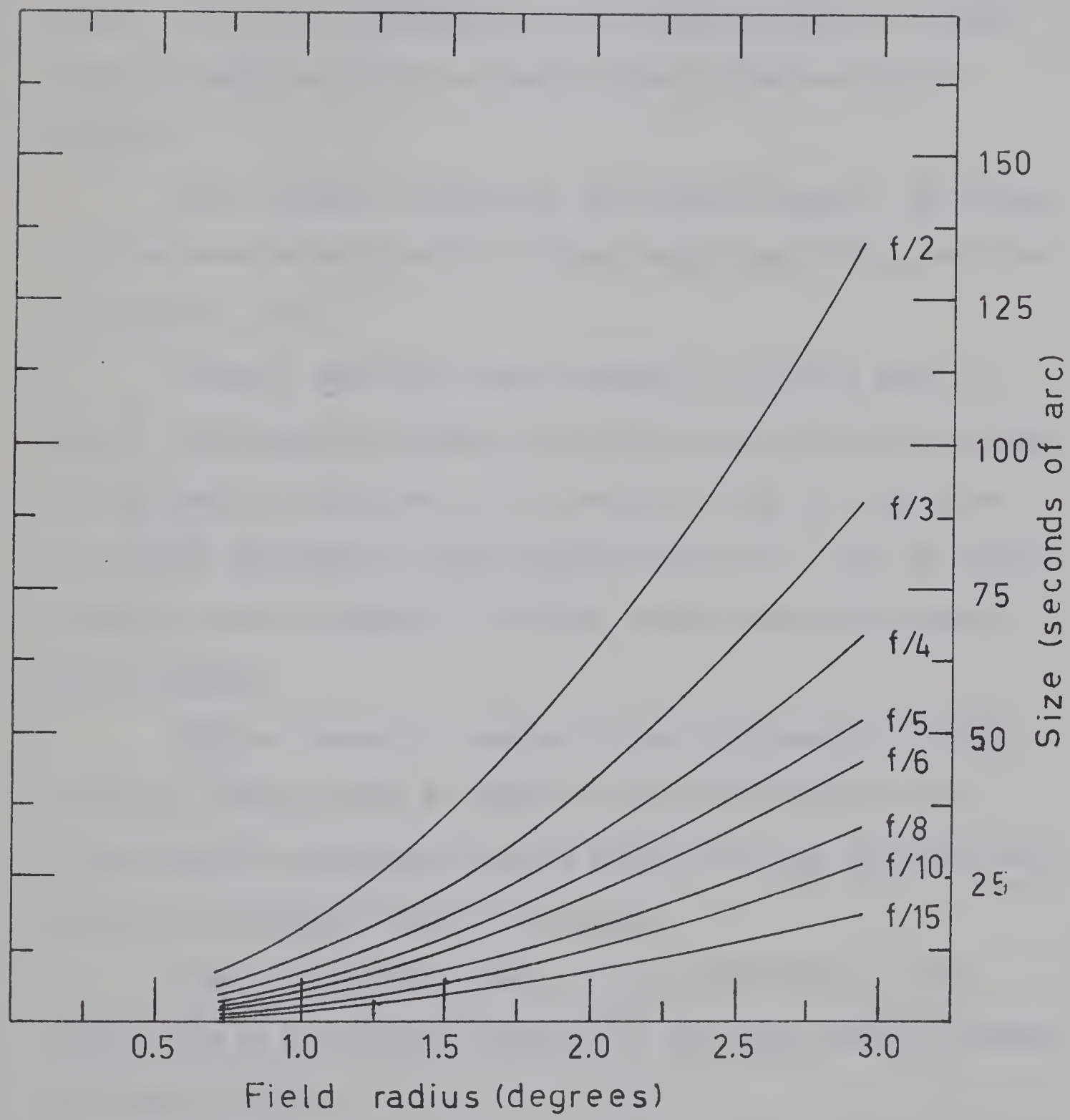

Fig. 5. Astigmatism of a parabolic mirror

With the approximation that $e \ll f$ this can be written as $C \approx \frac{1}{2f_1}$ which means that the astigmatism of a Cassegrain system is approximately the same as the astigmatism of the system's primary alone. Thus, the astigmatism of a two mirror system is several times as large as that of a single mirror of the same focal length.

Spot diagrams, indicating the size and shape of the images for the uncorrected telescope systems being constructed, are shown in Figures 6 - 8.

Figure 6 shows the images formed at the prime focus of the 20 inch diameter f/3 paraboloid. The characteristic fan shape of the comatic aberration is very evident. Near the edge of a 4 x 5 inch photographic plate (corresponding to a field of angular radius of about 3 degrees) the image is well over 300 seconds of arc in length.

Figure 7 shows the images for the f/8 Cassegrain configuration. Although coma is evident (particularly close to the optical axis), astigmatism and the effects of field curvature can be seen at distances away from the axis.

Figure 8 shows the images for the f/18 system. Very little coma is in evidence, and most of the image spread is caused by field curvature.

In all figures the spot diagrams represent the images formed at the edge of a field of angular radius ϕ. The diagrams were produced with the aid of the ray tracing computer program described in Appendix II.

Fig. 6. Images of uncorrected f/3 mirror

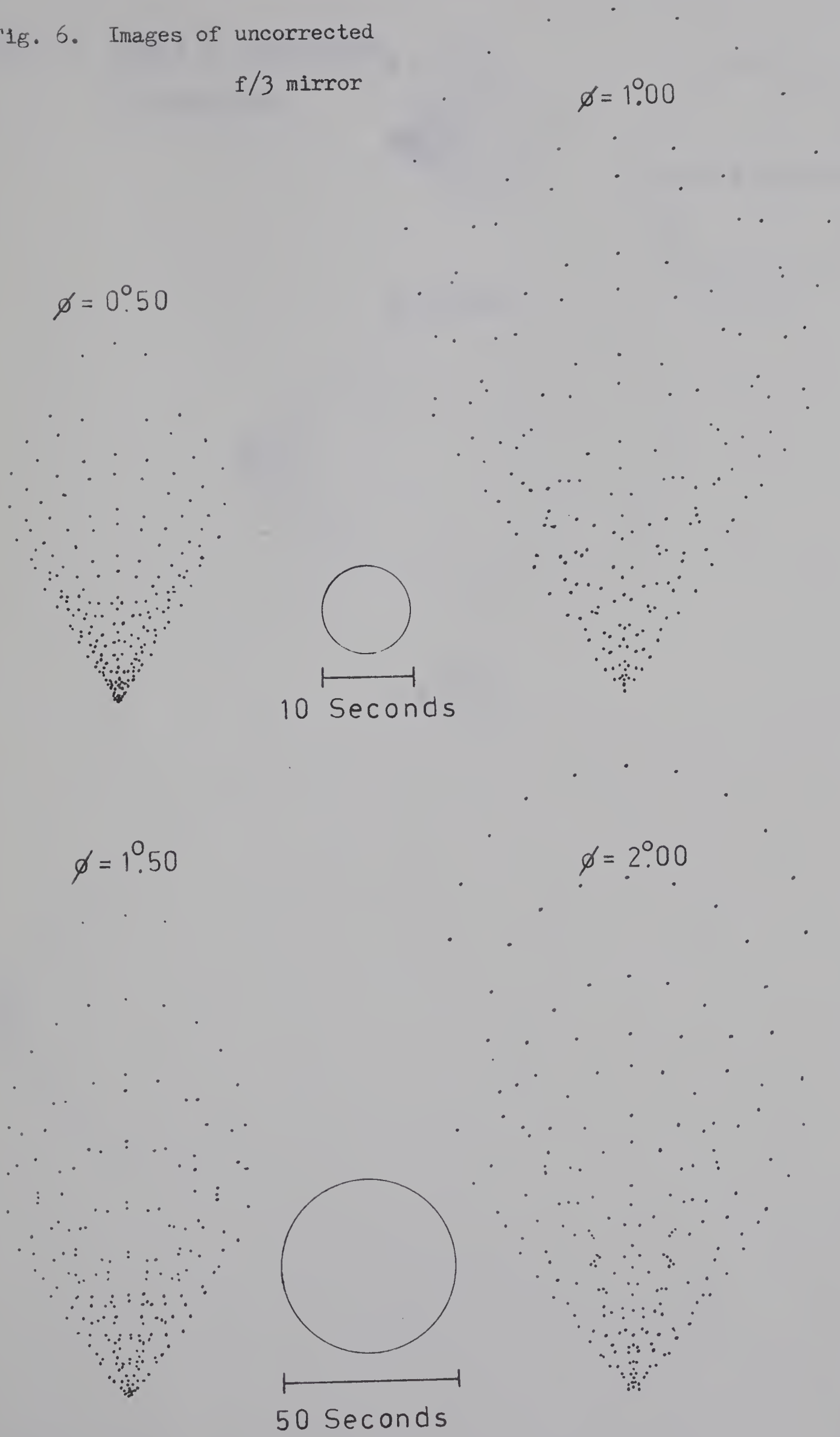

Fig. 7. Images of uncorrected f/8 Cassegrain

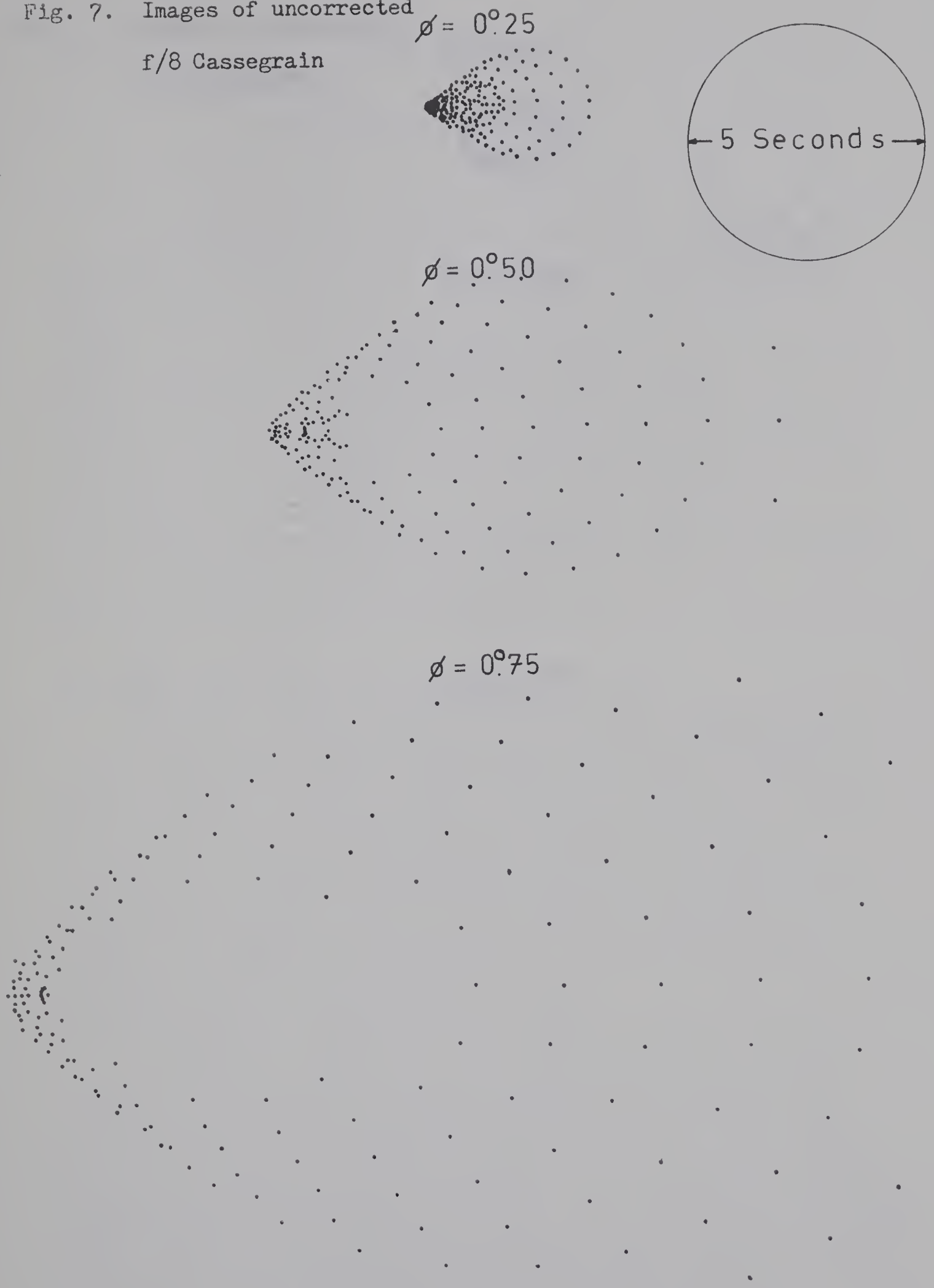

Fig. 8. Images of uncorrected f/18 Cassegrain

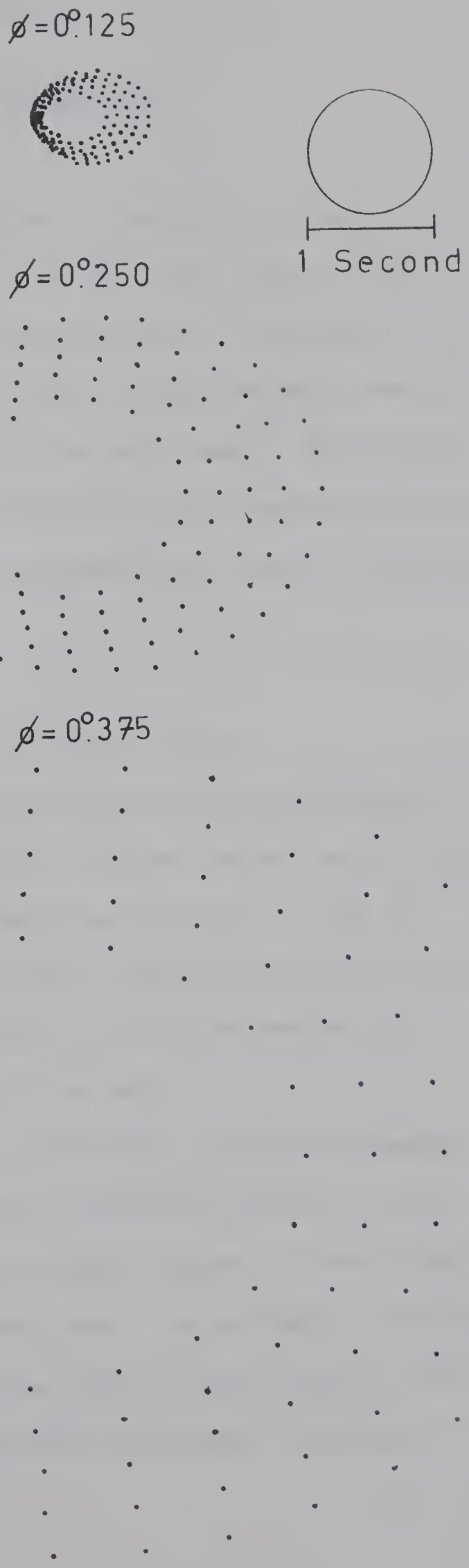

CHAPTER III

CORRECTION OF ABERRATIONS

The aberrations described in the previous chapter place severe limits on the size of field that will produce useful images. When a telescope is being used for photography, it is highly desirable to extend this area of good imagery, even if it entails a slight degradation of the axial image. Many methods of correcting the aberrations of reflecting telescopes, as well as alternate aberration free configurations, have been developed in the last half century.

3.1 Historical Outline of Correcting Systems

It has long been realized that the great advantage of a parabolic mirror is its ability to produce perfect axial images. Therefore, much of the early work was done with a view to providing a correcting system which could give reasonably good images over fairly large fields, yet could be removed when critical definition was required on axis.

One of the first to consider this problem was Sampson (1913). He attempted to correct spherical aberration, coma, and field curvature by using an afocal system of three closely spaced lenses in the convergent beam. The stringent requirements that he placed on the correcting system (close spacing of all three lenses and very small surface curvatures) precluded

satisfactory correction and led him to suggest the use of a primary which departed quite drastically from a parabola.

The first correctors for parabolic mirrors actually to be employed were designed by Ross (1935) in the 1930's. In his first designs, Ross used an afocal pair of lenses to correct the coma. The pair consisted of one positive and one negative element composed of the same glass in contact. This introduced considerable spherical aberration (about 10 seconds of arc for the 200 inch Hale telescope) which Ross considered a necessary evil.

Ross later introduced a third element, a strongly curved meniscus lens placed between the mirror and the afocal pair, designed to reduce the spherical aberration.

In 1946 Baker (1953) devised a novel extension of Ross's original solution which eliminated not only coma, but astigmatism and spherical aberration as well. In place of Ross's afocal pair, Baker used an achromatic doublet of slightly positive power. The positive power of the achromat flattened the field of the parabola,with the coma and astigmatism being removed by the bending and axial placement of the doublet. The spherical aberration introduced by this doublet was countered by a full aperture aspheric plate placed near the primary's focal plane. This design produces very good images over an extremely large field, but is impractical for very large apertures as it requires a correcting plate almost as large as the primary mirror.

In the last few decades many designs employing three or more spherically surfaced elements have been proposed and built for existing parabolic telescopes. The proliferation of such correcting systems has been greatly facilitated by the advent of large high speed computers capable of quickly and accurately assessing the effects of the large number of parameters introduced by systems composed of many elements.

In 1953 Meinel (1953) proposed the use of aspherically figured plates in the converging beam to correct the primary mirror's aberrations. Such systems, composed of several such elements, have been employed in large telescopes, although usually in conjunction with a hyperbolic primary.

If the requirement of perfect axial images is dropped, several additional methods of correction are possible.

The simplest and most effective system yet devised was first produced by Bernhardt Schmidt in 1931. Although similar systems had been proposed by others, it was Schmidt's genius as an optician which allowed him to actually produce such a system.

The Schmidt camera is based on the principal that a sphere, having no axis, has no off-axis aberrations. If a stop is placed at the centre of curvature, the system still has no unique axis. Hence, any element placed at this stop will not introduce coma or astigmatism, but can be designed to eliminate spherical aberration. Such a Schmidt plate has a fourth order curve with the figure given by $\Delta t = \frac{y^4}{4(n-1)R^3}$, Δt being the differential thickness of the plate. A second order curve of opposite sign is

usually superimposed to minimize chromatic effects.

Despite excellent performance over wide fields, the Schmidt camera suffers from several disadvantages. To prevent the introduction of off-axis aberrations, the corrector must be positioned at the centre of curvature of the primary. This means that the tube of the Schmidt must be at least twice as long as that of a conventional prime focus telescope, and any dome designed to house the instrument must have four times the surface area.

The correcting plate, which has an aperture two thirds as large as the primary, is expensive and difficult to fabricate. Also, since the corrector plate is the effective entrance pupil of the system, the system's clear aperture is only two thirds that of the primary, and the Schmidt utilizes only four ninths of the area (and hence light) that an equivalent primary, working alone, does.

One further difficulty with the Schmidt camera is that the focal plane, which is located in a rather inaccessible position between the corrector plate and the mirror, is strongly curved. This necessitates either the bending of the photographic plates, or the use of a field flattener which compromises the integrity of the images. Because of the awkward placement of the focus the Schmidt does not lend itself to photometry.

In spite of these problems, the Schmidt camera is unsurpassed in the production of well corrected wide field photographs, and many major Schmidt systems have been constructed.

Several variations of the Schmidt have been developed in an attempt to overcome its shortcomings. Particular effort has been expended in flattening the focal plane and making it more accessible. Most of these designs involve turning the Schmidt into a Cassegrain, which, unfortunately, introduces aberrations anew. One effective solution, known as the Maksutov telescope (1944), replaces the Schmidt corrector with a deeply curved meniscus lens which not only solves the focal plane problems, but also reduces the physical length of the telescope.

The solution which has been adopted for most large telescopes constructed recently has been to match a hyperbolic primary mirror with a strongly eccentric hyperbolic secondary, with the result that both spherical aberration and coma are eliminated at the Cassegrain focus. This system, a variation of which was investigated by Schwarzschild in 1905, was studied by Chrétien in 1922, and examples were built by Ritchey in the 1920's. One major disadvantage of the Ritchey-Chrétien configuration is that it cannot be used at prime focus (or any but its designed Cassegrain focus) without correction, as the primary suffers from considerable spherical aberration. This spherical aberration can be corrected however, and overall correction at prime focus can actually be accomplished more easily than with a paraboloid.

3.2 Aspheric Correctors

One method of correcting the aberrations of a mirror or system of mirrors is to place one or more aspherically surfaced

glass plates into the system. The Schmidt correcting system is the simplest example of such a system. In the following we develop the expressions necessary for the designing of such systems.

The methods used are essentially the same as in Chapter II, except that, as aberration producing laminae are actually being added to the system, the signs of all laminae powers must be reversed.

Since the speed of light is reduced in glass, somewhat thicker elements than the imagined laminae of the previous chapter must be used. The velocity of light in a non-magnetic transparent material is c/n (n = index of refraction), and the optical path distance through a glass plate of thickness Δx is n x. Therefore a retardation p is obtained if one surface of the glass plate is figured to the profile:

$$A_4 = \frac{p}{4(n-1)y^4}$$

where (from equation (2.5a)):

$$p = \beta y^4$$

As shown in the previous chapter, the effects of spherical aberration, coma, and astigmatism can be determined by summing the powers (β) and positions (u) of all the laminae in the system.

Using the precepts of the previous chapter and the fact that the power of each lamina can be expressed in terms of the

fourth order figure on each aspheric glass plate ($\beta = \frac{p}{y}_4 = 4(n-1)A_4$), the effect of a number of such plates on a system can be easily determined.

If several aspheric plates of strength β_i are placed in star space (in front of the system's entrance pupil) at distances l_i from the entrance pupil, their effects on the primary aberrations are given by (in terms of the traditional coefficients B, F, and C):

$$\begin{aligned} &\text{Spherical aberration} && B = -\sum_i 4(n_i-1)A_{4,i} \\ &\text{Coma} && F = -\sum_i 4(n_i-1)A_{4,i}l_i \qquad (3.1) \\ &\text{Astigmatism} && C = -\sum_i 4(n_i-1)A_{4,i}l_i^2 \end{aligned}$$

In the Schmidt camera, one such plate is employed. In general, however, the use of several such plates is undesirable, as they must be full aperture plates, and hence are large and expensive and cause considerable vignetting.

A much more attractive solution is to place them close to the focal plane in the convergent cone of light. This solution allows the diameter of the correctors to be much smaller, but involves considerably deeper figuring of the surfaces.

As indicated in Chapter II, the effect of a plate located at a point G in the convergent beam, a distance g from the focal plane of the system, will have the same effect as a plate of strength $(g/f)^4$ located at the image point of G in star space.

For a Cassegrain system, with the aspheric plates placed between the secondary mirror and the focal plane, the image

positions of the plates are given by

$$-f\left(\frac{f}{g_i} + \frac{(d-f_2)}{f_2}\right)$$

and the effects of such a system of aspheric plates on the primary aberrations of the system are given by the following expressions:

$$\text{Spherical aberration} \quad B = -\Sigma 4(n_i-1)A_{4,i}\left(\frac{g_i}{f}\right)^4$$

$$\text{Coma} \quad F = +\Sigma 4(n_i-1)A_{4,i}\,\frac{g_i^4}{f^3}\left(\frac{f}{g_i} + \frac{d-f_2}{f_2}\right) \qquad (3.2)$$

$$\text{Astigmatism} \quad C = -\Sigma 4(n_i-1)A_{4,i}\,\frac{g_i^4}{f^2}\left(\frac{f}{g_i} + \frac{d-f_2}{f_2}\right)^2$$

A preliminary design for a correcting system can be accomplished by combining the above equations with equations (2.13) and either solving all equations simultaneously, or, if there are not enough free parameters, minimizing the equations to produce the least amount of aberration possible. The three equations to be solved are:

$$B = \frac{1+b_1}{8f_1^3} - \left[b_2 + \left(\frac{f+f_1}{f-f_1}\right)^2\right]\frac{(f-f_1)^3(f_1-d)}{8f^3f_1^4}$$

$$-\Sigma 4(n_i-1)A_{4,i}\left(\frac{g_i}{f}\right)^4 = 0$$

$$F = \frac{1}{4f^2} + \left[b_2 + \left(\frac{f+f_1}{f-f_1}\right)^2 \right] \frac{(f-f_1)^3 d}{8f^3 f_1^3}$$

$$+ \Sigma 4(n_i-1)A_{4,i} \frac{g_i^4}{f^3}\left(\frac{f}{g_i} + \frac{d-f_2}{f_2}\right) = 0 \qquad (3.3)$$

$$C = \frac{f_1(f-d)}{2f^2(f_1-d)} - \left[b_2 + \left(\frac{f+f_1}{f-f_1}\right)^2 \right] \frac{(f-f_1)^3 d^2}{8f^3 f_1^2 (f_1-d)}$$

$$- \Sigma 4(n_i-1)A_{4,i} \frac{g_i^4}{f^2}\left(\frac{f}{g_i} + \frac{d-f_2}{f_2}\right)^2 = 0$$

3.3 Spherically Surfaced Correctors

Another method of correcting the primary aberrations of a reflecting telescope is through the use of spherically surfaced lenses. The Seidel aberration coefficients for such a lens system are given by the following formulae (the stop of the system is taken as the first surface of the first lens):

Spherical aberration	$S_I = \Sigma A$
Coma	$S_{II} = \Sigma AB$
Astigmatism	$S_{III} = \Sigma AB^2$ (3.4)
Field curvature	$S_{IV} = \Sigma P$
Distortion	$S_V = \Sigma B(AB^2+P)$

where:

$$A_i = Q_i^2 h_i^4 \left(\frac{1}{n_{i-1} s_i} - \frac{1}{n_i s_i'} \right)$$

$$B_i = - \frac{1}{Q_i h_i^2} - \sum_{p=1}^{i-1} \frac{d_p}{n_p h_p h_{p+1}} = - \frac{1}{Q_i h_i^2} - E_i \qquad (3.5)$$

$$P_i = \frac{1}{r_i} \left(\frac{1}{n_i} - \frac{1}{n_{i-1}} \right)$$

$$Q_i = n_{i-1} \left(\frac{1}{r_i} - \frac{1}{s_i} \right) = n_i \left(\frac{1}{r_i} - \frac{1}{s_i'} \right)$$

In the above formulae, r_i is the radius of curvature of the i^{th} surface, n_{i-1} and n_i the indices of refraction on either side of it and s_i, s_i' the conjugate focal distances at the surface of a paraxial ray traced through the system. h_i is the height at the i^{th} surface of a marginal ray traced through the system, and d_p is the axial distance between surfaces.

A complete geometric derivation of formulae (3.5) is to be found on pages 24 - 28 of Whittaker (1907).

Spherical elements are most effectively employed at the prime focus, usually in the form of an afocal doublet. Since, however, the aberrations from equations (3.4) are expressed for a stop at the lens system, and the mirror aberrations are expressed for a stop at the mirror, the stop positions must be made to coincide before their effects can be compared. The only variable

which is not stop invariant in equations (3.5) is E_i in the equation for B_i, and a simple change of E_i to $E_i - dE_i$ is all that is involved in a change of stop position. Equations (3.4) can then be re-expressed as:

$$S_I' = S_I$$

$$S_{II}' = S_{II} + S_I dE$$

$$S_{III}' = S_{III} + 2S_{II}dE + S_I(dE)^2 \qquad (3.6)$$

$$S_{IV}' = S_{IV}$$

$$S_V' = S_V + (S_{IV} + 3S_{III})dE + 3S_{II}(dE)^2 + S_I(dE)^3$$

The spherical aberration of a parabolic mirror is zero, and the coma, which is therefore independent of the stop position, is equal to $-2h^2/R_m^2$. The astigmatism is dependent on the stop position, and the new stop position can be chosen so that the mirror's astigmatism is zero.

The equations which must be solved to eliminate spherical aberration, coma, and astigmatism are then:

$$S_I'' = S_I' = S_I = 0$$

$$S_{II}'' = S_{II}' - 2h^2/R_m^2 = S_{II} + S_I dE - 2h^2/R_m^2 = 0 \qquad (3.7)$$

$$S_{III}'' = S_{III}' = S_{III} + 2S_{II}dE + S_I(dE)^2 = 0$$

where $dE = -R_m^2/2h^2(R_m - 2d)$ for a parabolic mirror (Wynne 1949).

It is not, in fact, possible to solve all three of these

equations using only a pair of lenses, and correction for spherical aberration, which is necessarily introduced if coma and astigmatism are to be completely eliminated, is usually sacrificed. If complete correction is to be obtained at least one additional (usually large) element must be added.

3.4 Relative Advantages of Spherical and Aspheric Elements

Both spherically and aspherically surfaced elements enjoy some relative advantages and suffer from some disadvantages.

Spherically surfaced elements are the easiest surfaces to produce, and can be polished to very high tolerances. Aspheric surfaces, on the other hand, are expensive and very difficult to fabricate, and the exact curves necessary for optimum performance are almost impossible to generate.

Spherical elements can, in some cases, be used to alter the Petzval sum and thus flatten the focal plane. Aspheric elements, being essentially flat plates of zero power, do not have this ability, and in systems employing aspherics, an additional field flattening lens, with its intrinsic aberration, must be added to the system. Thus, in general, systems employing aspherics will require one more element than those using spherical elements.

Spherical elements are also less sensitive to misalignment than are aspheric elements. Aspheric elements are particularly affected by lateral misalignment if there are several correctors in the system.

One other advantage of spherical elements is that a system

of spherical lenses can often be placed closer to the focal plane than an aspheric system. This reduces the diameter of the corrector and increases the amount of light incident on the primary mirror.

The primary advantage of aspheric correctors lies in the fact that, being flat and thin, they introduce very little chromatic aberration. Spherical elements, even if achromatized, suffer from quite large refractive errors, and are very wavelength dependent. This is particularly true if they are used in fast systems.

Another major advantage of aspherics is that, not needing achromatization, any glass may be used. Thus, the index of refraction and dispersion need not be considered, and a glass may be chosen for its transmission and weathering characteristics, as well as its workability.

Aspherics generally suffer less from higher order aberrations than do spherically surfaced elements. This is not true however, unless the fourth order curves on the correctors are very shallow.

For the reasons outlined here, an aspheric correcting system was chosen for the f/8 configuration. This correcting system is described in detail in the following chapter.

CHAPTER IV

F/8 CASSEGRAIN CORRECTING SYSTEM

The classical Cassegrain focus has attendant comatic and astigmatic aberration which must be corrected if a sizable portion of the field is to be used for photography. The problems associated with the f/8 configuration and the correcting system which will be employed are described below.

4.1 Classical Cassegrain Configuration

The curve on the secondary mirror and the separation between the secondary and primary for a classical Cassegrain configuration can be determined from the equations derived in Chapter II:

$$\frac{1}{f} = \frac{1}{f_1} + \frac{1}{f_2} - \frac{1}{f_1 f_2} \qquad (2.1)$$

$$d(f+f_1) = f_1(f-e) \qquad (2.3)$$

$$f_1(d+e) = f(f_1-d) = -(f-f_1)f_2 \qquad (2.2)$$

where:

f = effective focal length of the system (160")

f_1 = focal length of the primary mirror (60")

f_2 = focal length of the secondary mirror

d = separation of the secondary from the primary

e = distance behind primary of the Cassegrain focus

Choosing e = 12".5 and solving for d and f_2 one obtains values of d = 40".227 and f_2 = 31".63.

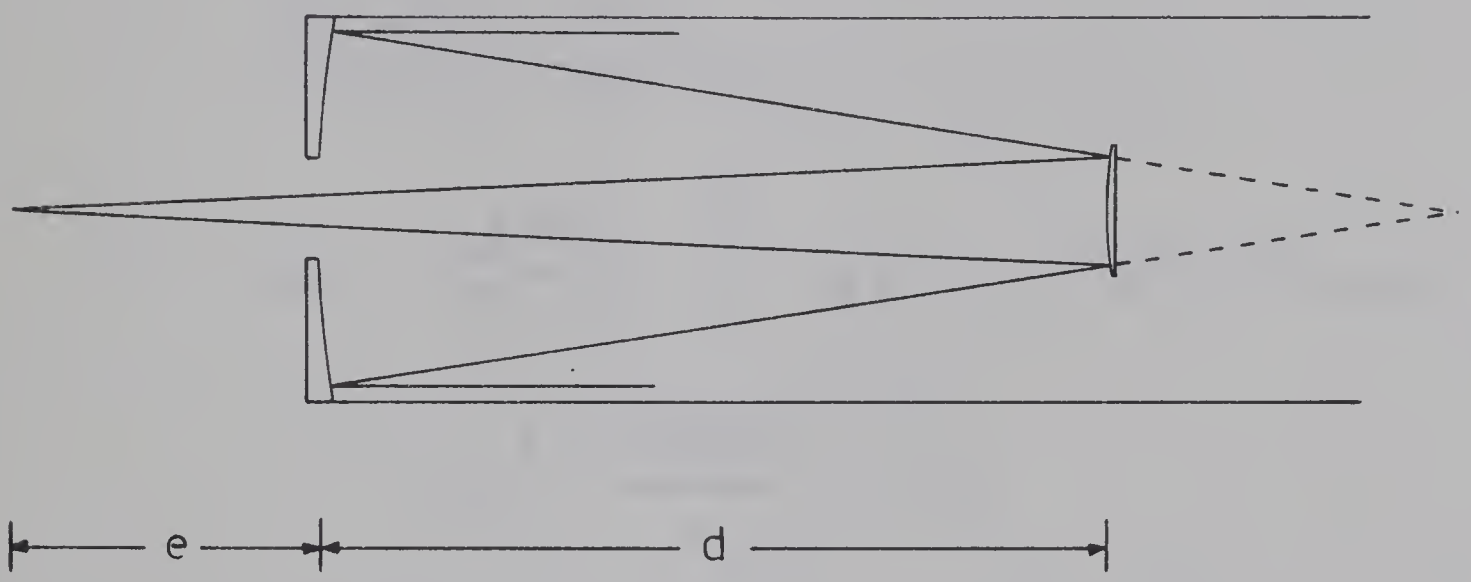

Fig. 9. Classical Cassegrain system

The curve on the hyperbolic secondary can be found by considering the form of a hyperboloid.

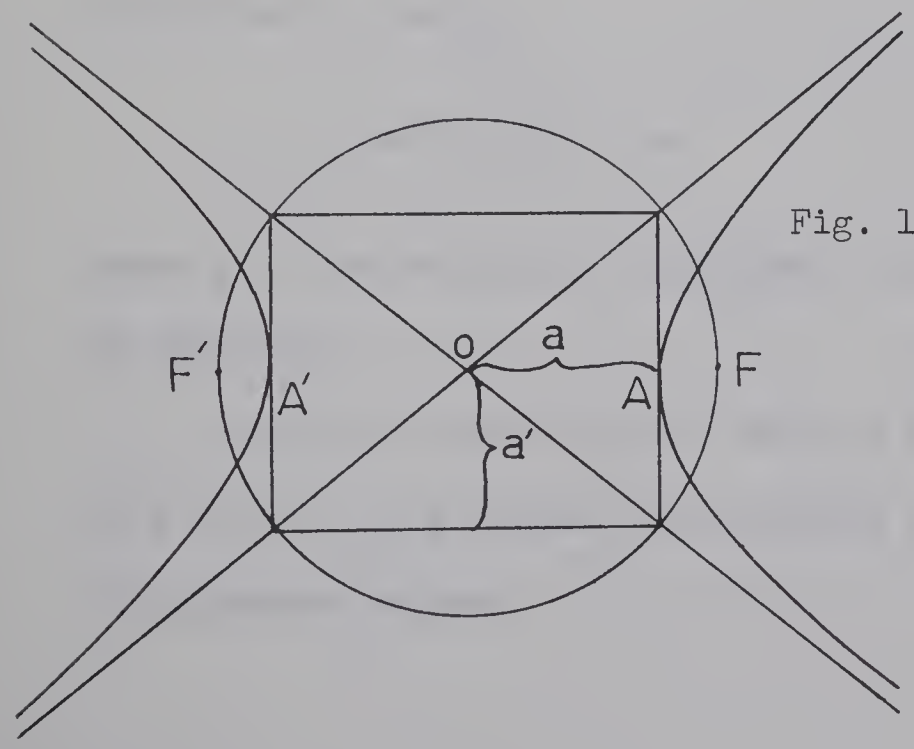

Fig. 10. Dimensions of the hyperbola

$$\frac{(z-z_o)^2}{a^2} - \frac{(x^2+y^2)}{a'^2} = 1$$

$c = (a^2+a'^2)^{\frac{1}{2}} = OF = 36''.25$

a = semi-major axis = $OA = c - AF = 16''.4772$

a' = semi-minor axis = $(c^2-a^2)^{\frac{1}{2}} = 32''.288728$

e = eccentricity = $c/a = 2.20$

b = asphericity factor = $-e^2 = -4.84$

Using $z_o = d-a$, the hyperbolic equation becomes:

$$\frac{(z-(d-a))^2}{a^2} = \frac{(x^2+y^2)}{a'^2} = 1$$

$$\text{and} \quad z = a\left(\frac{x^2+y^2}{a^2} + 1\right)^{\frac{1}{2}} + (d-a) = \frac{a}{a'}(x^2+y^2+a'^2)^{\frac{1}{2}} + (d-a)$$

$$\text{but} \quad \frac{a}{a'} = \frac{(c^2-a^2)^{\frac{1}{2}}}{a} = (e^2-1)^{\frac{1}{2}}$$

and for our system

$$z = \left(\frac{x^2+y^2+a'^2}{e^2-1}\right)^{\frac{1}{2}} + (d-a) = \left(\frac{x^2+y^2+1042.562}{3.84}\right)^{\frac{1}{2}} + 23.75$$

The diameter necessary for the secondary mirror can be determined by using:

$$D = (d+e)2y\left(\frac{1}{f}\right) + 2d\phi$$

where y is the radius of the primary and ϕ is the angular radius of the field.

For our system ($y=10''$) using a slightly exaggerated value of $\phi = 1^\circ$ (0.0175 radians) one obtains a diameter of $8''.00$ for the secondary mirror.

4.2 Aberrations of the Uncorrected System

The aberrations of a Cassegrain system are given by:

Spherical aberration:

$$B = \frac{1+b_1}{8f_1^3} - \left[b_2 + \left(\frac{f+f_1}{f-f_1} \right)^2 \right] \frac{(f-f_1)^3(f_1-d)}{8f^3 f_1^4}$$

$$= \frac{1+b_1}{8f_1^3} - \left[b_2 + \left(\frac{f+f_1}{f-f_1} \right)^2 \right] \frac{(f-f_1)^3(f_1+e)}{8f^3 f_1^3 (f+f_1)}$$

Coma:

$$F = \frac{1}{4f^2} + \left[b_2 + \left(\frac{f+f_1}{f-f_1} \right)^2 \right] \frac{(f-f_1)^3 d}{8f^3 f_1^3}$$

$$= \frac{1}{4f^2} + \left[b_2 + \left(\frac{f+f_1}{f-f_1} \right)^2 \right] \frac{(f-f_1)^3 (f-e)^2}{8f^3 f_1 (f+f_1)(f_1+e)}$$

Astigmatism:

$$C = \frac{f_1(f-d)}{2f^2(f_1-d)} - \left[b_2 + \left(\frac{f+f_1}{f-f_1} \right)^2 \right] \frac{(f-f_1)^3 d^2}{8f^3 f_1^2 (f_1-d)}$$

$$= \frac{f^2+f_1 e}{2f^2(f_1+e)} - \left[b_2 + \left(\frac{f+f_1}{f-f_1} \right)^2 \right] \frac{(f-f_1)^3 (f-e)^2}{8f^3 f_1 (f+f_1)(f_1+e)}$$

For a classical Cassegrain the asphericity of the hyperbolic secondary, b_2, is equal to $-\left(\frac{f+f_1}{f-f_1} \right)^2$ and the aberration equations reduce to:

$$B = \frac{1+b_1}{8f_1^3} = 0 \quad (b_1 = -1 \text{ for a paraboloid})$$

$$F = \frac{1}{4f^2}$$

$$C = \frac{f_1(f-d)}{2f^2(f_1-d)} = \frac{f^2+f_1e}{2f^2(f_1+e)}$$

For the system under consideration, f = 160", f_1 = 60", and e = 12".5. Substituting these into the aberration equations, the numerical values of the aberration coefficients are found to be:

$$B = 0$$

$$F = 9.76525 \times 10^{-6}$$

$$C = 7.0986 \times 10^{-3}$$

and using the equations from Chapter II (with $\phi = 1^\circ = 3600$ seconds) the size of the aberrations near the edge of a 4 x 5 inch plate are found to be:

Angular diameter of spherical aberration blur circle

$$= \tfrac{1}{2}By^3 = 0$$

Angular length of coma figure = $3Fy^2\phi$ = 10.55 arc seconds

Angular diameter of astigmatic blur circle = $2Cy\phi^2$

= 8.92 arc seconds

There is an additional large off-axis image spread due to curvature of the field (about 15 seconds of arc at 1° off axis). The total image size at the edge of a 1° radius field is therefore

about 30 seconds of arc.

4.3 Correcting System

As most photography will be done at the f/8 focus, a dependable correcting system is a necessity.

While a correcting system composed entirely of spherical elements is possible, any such configuration will be accompanied by some chromatic aberration. Essentially no such aberration is introduced by a system composed of aspheric elements. Therefore, if a simple corrector composed of aspherics is possible, it would be preferable to one composed of spherical elements.

Large amounts of both comatic and astigmatic aberration must be corrected in the f/8 Cassegrain. Since correction of coma and astigmatism requires aspheric curves of opposite sign, at least two aspheric elements will be required.

For a correcting system composed of two aspherics in the convergent beam designed to eliminate coma and astigmatism the equations to be solved are:

$$F = \frac{1}{4f^2} + 4(n_1-1)A_{4,1}\frac{g_1}{f}^4\left(\frac{f}{g_1} + \frac{d-f_2}{f_2}\right)$$

$$+ 4(n_2-1)A_{4,2}\frac{g_2}{f}^4\left(\frac{f}{g_2} + \frac{d-f_2}{f_2}\right) = 0$$

$$C = \frac{f_1(f+d)}{2f^2(f_1-d)} - 4(n_1-1)A_{4,1}\frac{g_1}{f^2}^4\left(\frac{f}{g_1} + \frac{d-f_2}{f_2}\right)$$

$$- 4(n_2-1)A_{4,2}\frac{g_2}{f^2}^4\left(\frac{f}{g_2} + \frac{d-f_2}{f_2}\right) = 0$$

Using $\alpha = \frac{f}{g_2} + \frac{d-f_2}{f_2}$, $\beta = \frac{f}{g_1} + \frac{d-f_2}{f_2}$, and setting F = C = 0, one obtains:

$$A_{4,1} = \frac{2f_1(d-f) + f\alpha(d-f_1)}{16(n_1-1)g_1^4(f_1-d)\beta(\alpha-\beta)}$$

$$A_{4,2} = -\frac{f + 16(n_1-1)A_{4,1}g_1^4}{16(n_2-1)g_2^4}$$

The amount of spherical aberration introduced by the two aspheric elements (in seconds of arc) is given by:

$$\text{Angular diameter} = 2y^3\left((n_1-1)A_{4,1}\left(\frac{g_1}{f}\right)^4 + (n_2-1)A_{4,2}\left(\frac{g_2}{f}\right)^4\right)$$

The above equations obviously admit of a large range of solutions with the positioning of the two correcting elements varying from the focal plane to the secondary mirror. There are, however, several practical limitations to be considered.

The correctors cannot be placed too close to the secondary mirror. Firstly, if either element is placed more than a few inches in front of the primary mirror, some light incident on the secondary from the primary will be cut off by the corrector, altering its path and introducing a large error. If either aspheric

is placed in front of the primary care must be taken to preclude this possibility. Secondly, since spherical aberration increases as the focal plane - corrector separation increases, a practical limit is set by the amount of spherical aberration considered acceptable. Since spherical aberration distributes the light fairly uniformly, an arbitrary upper limit of one second of arc would seem reasonable.

On the other hand, the correctors cannot be placed too close to the focal plane as the depth of the fourth order curve increases rapidly with decreasing focal plane - corrector separation, becoming infinite at the focal plane. A deep aspheric curve not only introduces great difficulties in testing and production of the element, but introduces large higher order aberrations, primarily due to refraction and differential thickness. This is particularly important in the case of the corrector on which the light is first incident. This is because the theory on which aspheric correctors are based assumes that the refraction at each element is very small, and the point of intersection of the light ray by subsequent aspheric surfaces is not appreciably altered. If this is not the case, and appreciable refraction occurs at the first corrector, problems arise. Such refraction by a previous element can be corrected for any one angle of incident light by superimposing a suitable sixth order curve on the element, but correction for all incident angles does not appear possible.

The separation between the two elements is also quite important. The smaller the separation between the two elements,

the deeper the aspheric curves become, yet an increase in the separation results in an enhancement of the spherical aberration.

Corrector curves were calculated for all integral values of g_1 and g_2 such that $g_2 < g_1 \leq 15"$ along with the resultant spherical aberration of each pair. The results are shown in Figure 11 on the following page.

On the basis of preliminary ray tracing a total aspheric depth of 1.0×10^{-3} inches for the first element and 1.0×10^{-1} inch for the second element were chosen as the most extreme curves that could be expected to yield good correction relatively free of higher order aberrations. Assuming a diameter of six inches for each aspheric, these correspond to maximum fourth order coefficients of:

$$A_{4,1} = -1.23 \times 10^{-5}$$

$$A_{4,2} = 1.23 \times 10^{-3}$$

The shaded area in Figure 11 shows the values of g_1 and g_2 for which the conditions

(i) spherical aberration $\leq$ 1 second of arc

((ii) $A_{4,1} \geq -1.23 \times 10^{-5}$

(iii) $A_{4,2} \leq 1.23 \times 10^{-3}$

are satisfied.

After ray tracing several of the solutions in and near this region it appeared that the solution at $g_1 = 15"$

Fig. 11. Spherical aberration for f/8 aspheric plate corrective system

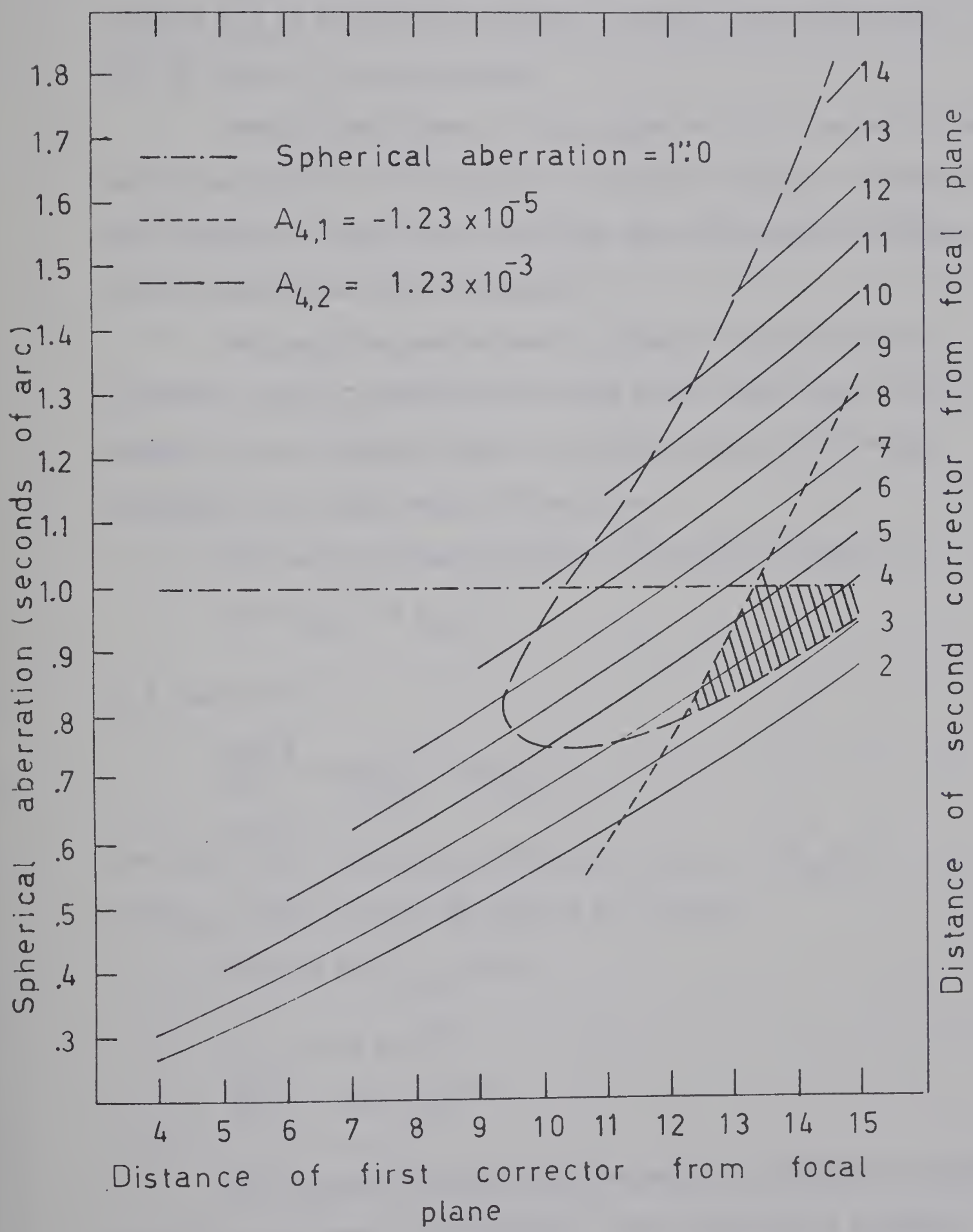

($A_{4,1} = -5.933 \times 10^{-5}$) and $g_2 = 3''$ ($A_{4,2} = 1.418 \times 10^{-3}$) provided the best potential for image correction. This placed the first element 2".5 in front of the primary and the second 9".5 behind, or 3".0 in front of the focal plane.

Second order curves of sign opposite to the aspheric curves were superimposed on the elements in order to minimize refractive and chromatic effects and to decrease the differential thickness of the elements as much as possible.

Following the method used on Schmidt corrector plates (Linfoot, 1955) a neutral zone at 65% of the plate radius was chosen for the initial design. A neutral zone at this radius minimizes the actual depth of the curve.

The surface equation of the i^{th} element is given by:

$$\Delta t = A_{4,i} r^4 + A_{2,i} r^2$$

and therefore:

$$\frac{d(\Delta t)}{dr} = 4A_{4,i} r^3 + 2A_{2,i} r$$

Setting $\frac{d(\Delta t)}{dr} = 0$ for the neutral zone, $A_{2,i} = -2A_{4,i} r_n^2$ with $r_n = 1".95$ for the 65% zone on a 6" plate.

Solving for $A_{2,i}$ gives:

$$A_{2,1} = 4.5 \times 10^{-4}$$

$$A_{2,2} = -1.10 \times 10^{-2}$$

Since aspheric plates are incapable of altering the Petzval sum, it is necessary to introduce a third spherically surfaced

element to flatten the focal plane.

The Petzval sum over i surfaces, which is equivalent to the reciprocal of the radius of field curvature is given by:

$$P = \sum_{j=2}^{i} \frac{\phi_j}{n_{j-1} n_{j+1}}$$

where ϕ_j is the power of the j^{th} surface and n_{j-1}, n_{j+1} the indices of refraction before and after the surface. For reflecting surfaces, $n_{j-1} = -n_{j+1} = -1$ and $\phi = 1/f_\infty$. Thus, for our Cassegrain system, the Petzval sum is equal to $\frac{1}{f_1} + \frac{1}{f_2} = -0.01494$ and our focal plane has a radius of curvature of -66".92. To correct this curvature, a plano-convex lens with P = +0.01494 is necessary. Assuming crown glass (n = 1.517) the power of the element must be:

$$\phi = n_1 n_2 P = 0.02266$$

and using $\phi = (n-1)\left(\frac{1}{r_1} - \frac{1}{r_2}\right)$ with $r_2 = \infty$ the radius of the first surface must be 22".8.

This element should be placed as close to the focal plane as possible to minimize aberrations introduced by it. The aspheric elements could be redesigned to take the additional residual aberrations into account, but as these image errors are relatively small, correction for them was effected during the final ray tracing of the system.

A summary of the preliminary correcting system is given in Table 2 on the following page.

Element	Distance from focal plane	Surface equation
1st aspheric corrector	15"	$\Delta t = -5.933 \times 10^{-5} r^4 + 4.5 \times 10^{-4} r^2$
2nd aspheric corrector	3"	$\Delta t = 1.418 \times 10^{-3} r^4 - 1.1 \times 10^{-2} r^2$
field flattener	1"	$\Delta t = (22.8 - (519.84 - r^2)^{\frac{1}{2}})$

Table 2. Preliminary f/8 corrector design

Before final testing and optimization of the system can be accomplished, suitable glass types and thicknesses for each element must be chosen. Since the aspherics and field flattener can be designed for any index of refraction, crown glass of refractive index 1.517 (Schott type BK7 (517642)) was chosen for all three elements. This glass has good strength, weathering, and transmission characteristics. Each element should be as thin as possible to reduce absorption and higher order aberrations, yet thick enough to prevent flexure and prohibitive fabrication problems. With these criteria in mind, an axial thickness of 0".20 was chosen for all three elements.

4.4 Computer Optimization of the Correcting System

The solution described in the previous section provides only a preliminary design, and extensive optimization must be performed to correct for the effects of element thickness, surface to surface refraction, and higher order aberrations.

The optimization was accomplished using an interactive, three dimensional, surface to surface ray trace program (see Appendix II). On the basis of results from this program, parameters were semi-empirically altered until the smallest and most uniform image patterns possible were obtained. Several of the surface equations were appreciably changed.

Specifications for the optimized system are shown in Table 3, and are followed by a comparison of the uncorrected and corrected

images. Finally, a profile of the correcting surface of each aspheric surface is presented. Spot diagrams of the corrected images for various angle can be found in Appendix I.

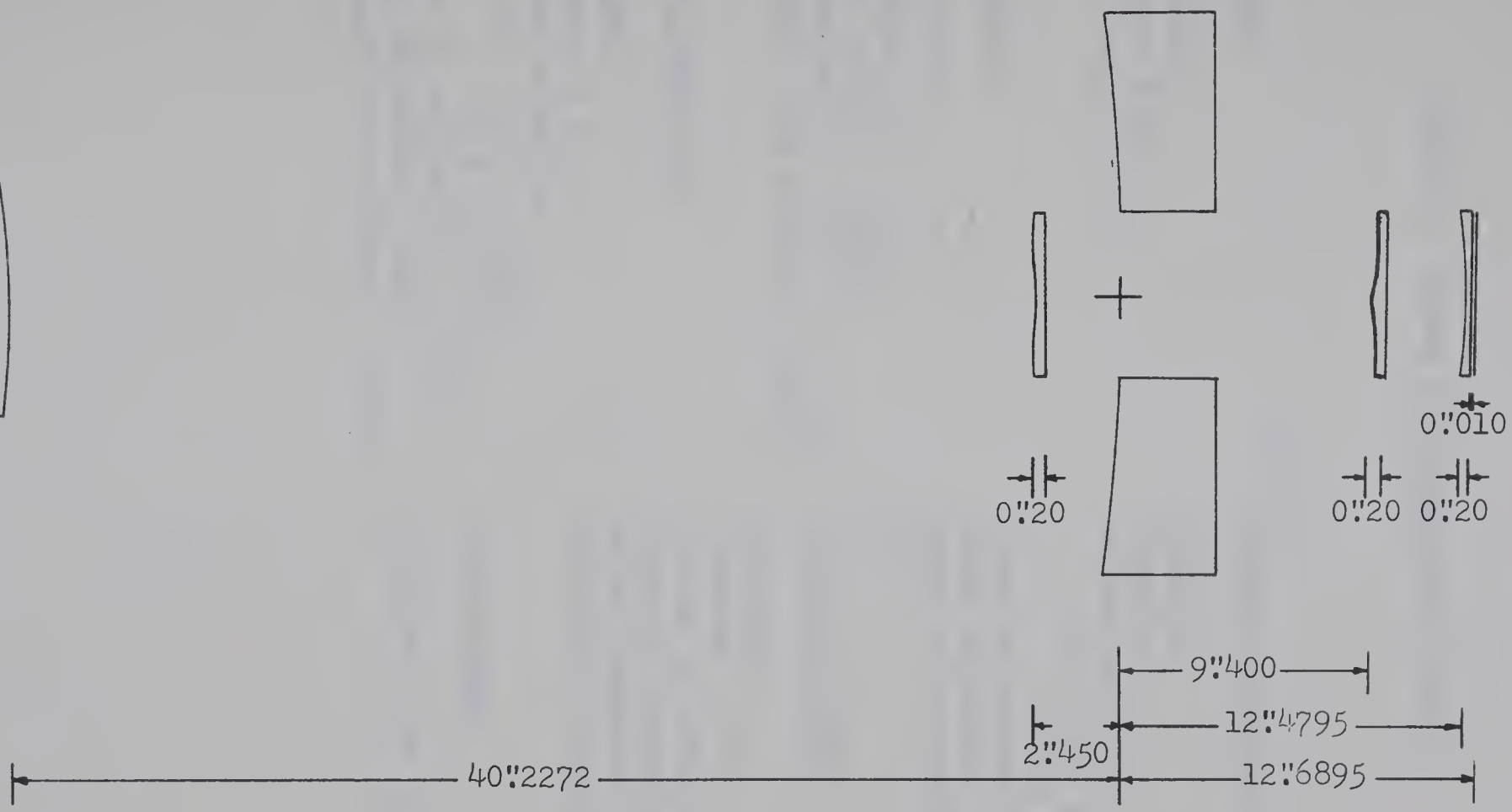

Fig. 12 Optimized f/8 Cassegrain system

Table 3. Final f/8 Cassegrain design

Primary

Paraboloid
diameter = 20"
focal length = 60"

Secondary

Hyperboloid
diameter = 8"
focal length = -31.63
eccentricity = 2.20
distance from primary = 40.227

First corrector

Aspheric
diameter = 6"
surface equation:

$$\Delta t = -5.9 \times 10^{-5} r^4 + 4.5 \times 10^{-4} r^2$$

index of refraction = 1.517
axial thickness = 0.20
distance from primary = 2.450

Second corrector

Aspheric
diameter = 6"
surface equation:

$$\Delta t = 1.359 \times 10^{-3} r^4 - 9.9 \times 10^{-3} r^2$$

index of refraction = 1.517
axial thickness = 0.20
distance from primary = -9.40

Field flattener

Spherical
diameter = 6"
radius of curvature = 23.0
index of refraction = 1.517
axial thickness = 0.20
distance from primary = -12.4795

Focal plane

distance from primary = -12.6895

Fig. 13. Optimized f/8 Cassegrain system image comparison

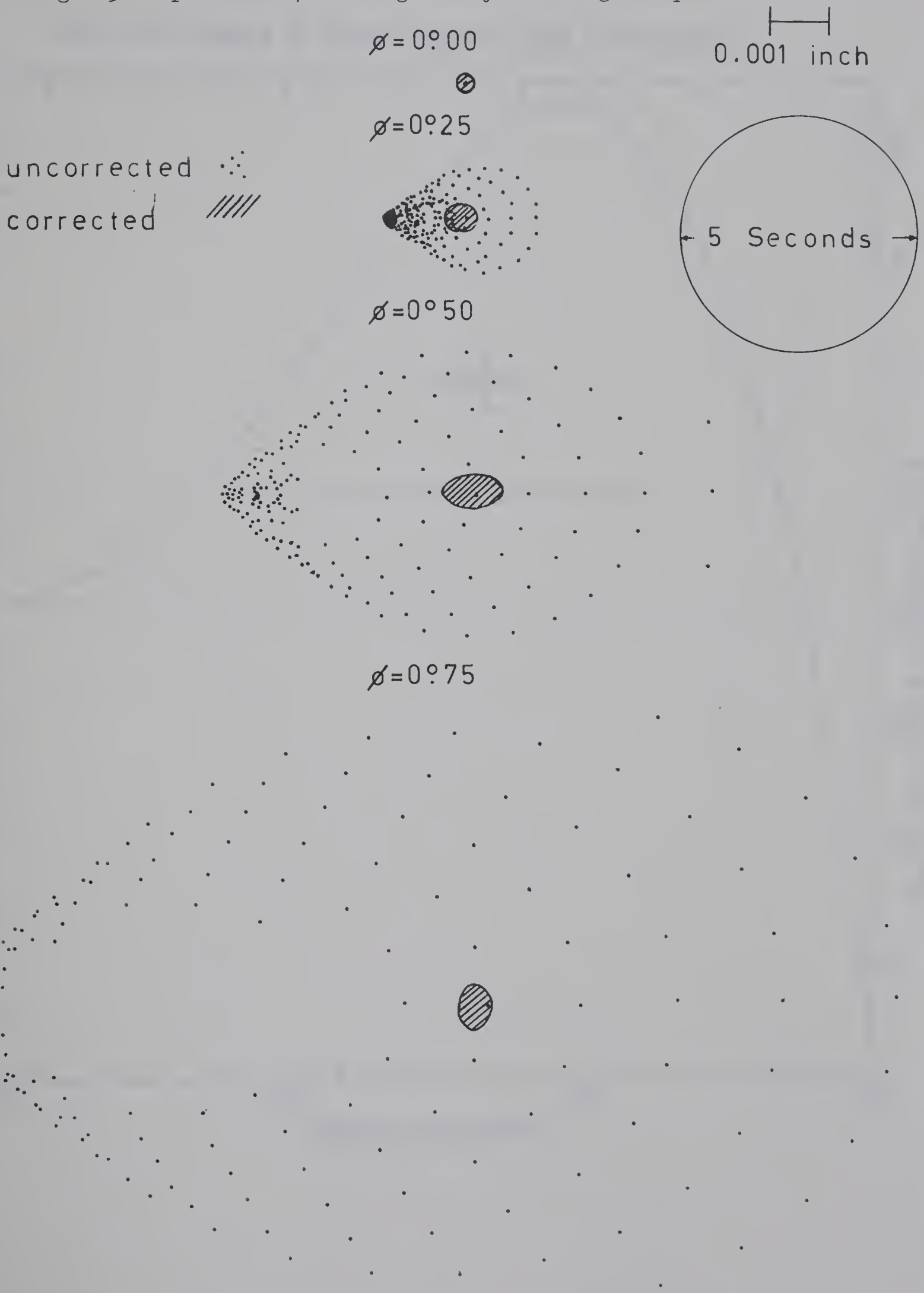

Fig. 14. Profile of first aspheric plate (f/8 system)

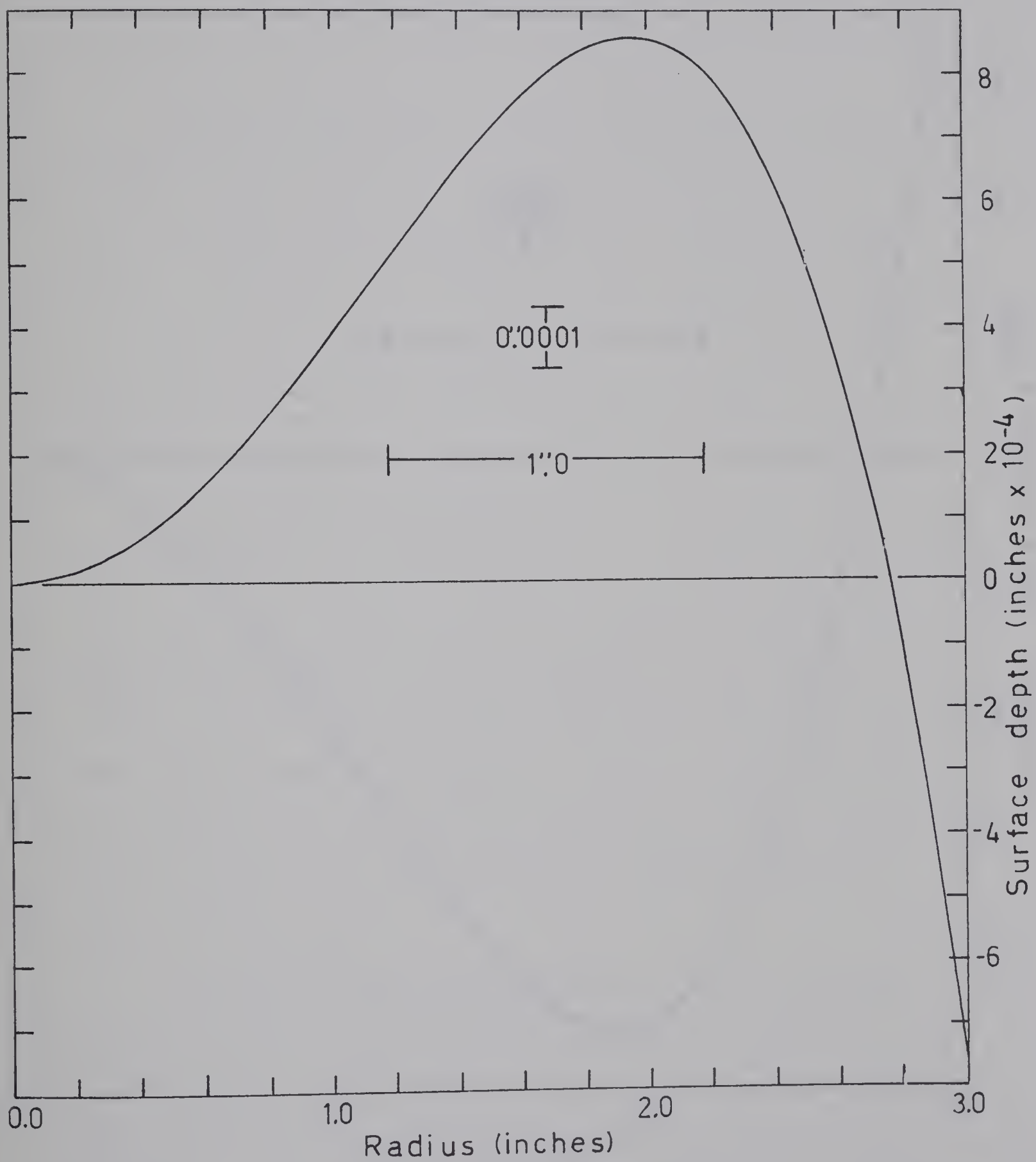

Fig. 15. Profile of second aspheric plate (f/8 system)

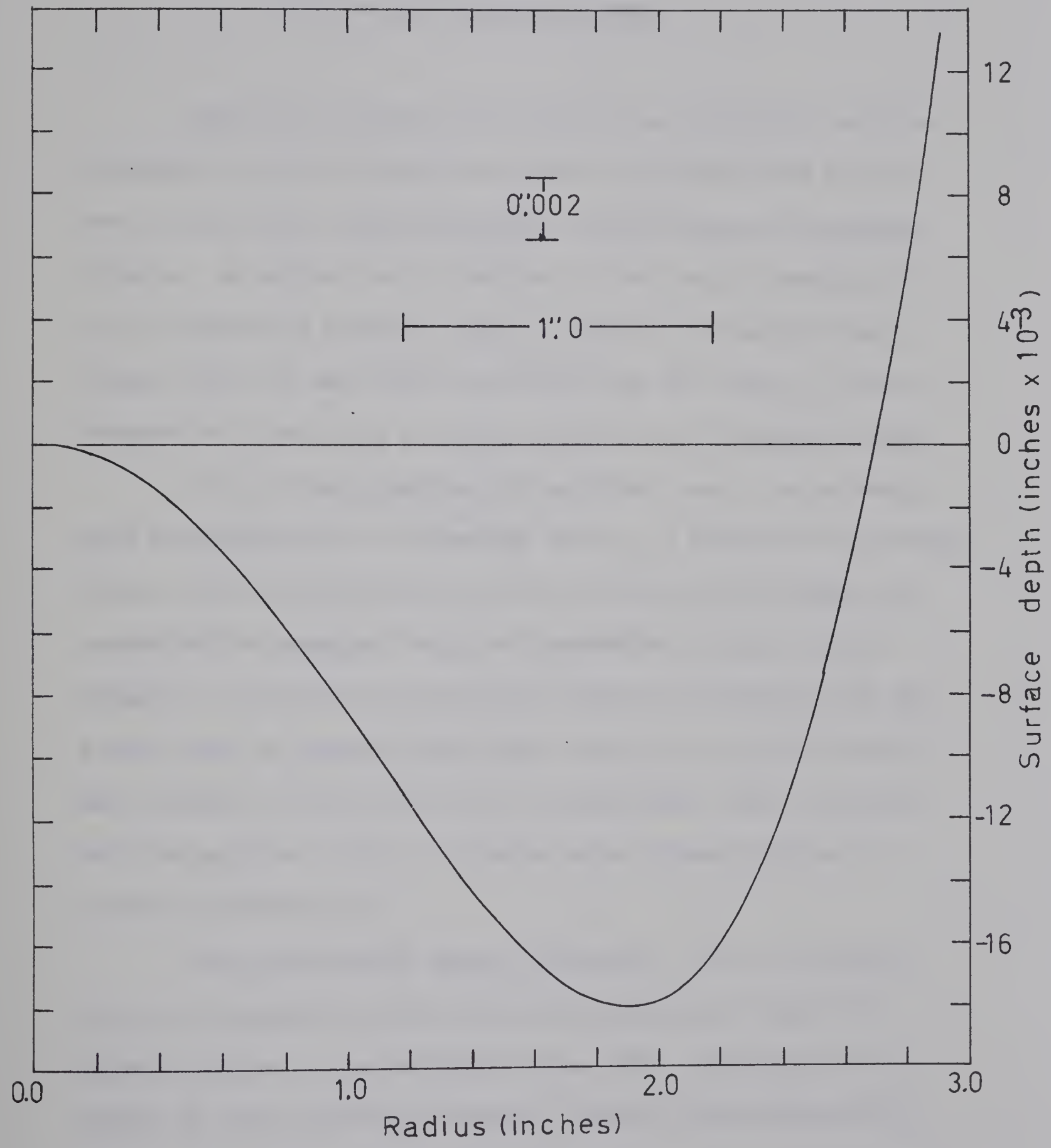

CHAPTER V

PRIME FOCUS CORRECTING SYSTEM

While all photometry and much of the photography will be undertaken at the f/8 Cassegrain focus, the prime focus will be used for all wide field photography and photography of extended objects. As pointed out in Chapter II, the image aberrations of an f/3 paraboloid severely limit the size of the usable field; indeed, only one inch from the optical axis the image of such an uncorrected primary has a spread of more than 75 seconds of arc!

To be of any practical use at prime focus, the telescope must be equipped with a correcting system. A simple Ross corrector (Ross, 1935) in the form of an afocal doublet, while simple and economical to construct, would be inadequate for such a fast primary. The uncorrected spherical aberration introduced by such a pair would be prohibitively large. Also, as an afocal doublet has no effect on the Petzval sum, an additional field flattener would be required. Thus, a somewhat more elaborate system is needed for correction.

Two possibilities present themselves. One is the possibility of correcting the aberrations by placing a number of aspheric plates in the convergent beam. The other would be to employ the Baker Reflector-Corrector (Baker, 1953) mentioned in Chapter III. Each of these possibilities has relative advantages and disadvantages.

5.1 Aspheric Prime Focus Correctors

If a number of aspheric plates are placed in the convergent light cone of a primary mirror, at distances g_i from the focal plane, the equations governing the primary aberrations are given by combining equations (2.13) and (3.2) and setting $f_2 = d = \infty$:

$$B = \frac{1+b_1}{8f} - 4(n_i-1)A_{4,i}\left(\frac{g_i}{f}\right)^4 \qquad (b_1 = -1 \text{ for a paraboloid})$$

$$F = \frac{1}{4f^2} + 4(n_i-1)A_{4,i}\left(\frac{g_i}{f}\right)^3 (f-g_i)$$

$$C = \frac{1}{2f} - 4(n_i-1)A_{4,i}\left(\frac{g_i}{f}\right)^2 (f-g_i)^2$$

A preliminary design may be obtained by setting $B = F = C = 0$ and solving for $A_{4,i}$ and g_i. Some practical limitations must be considered however. A plate positioned at a distance g from the focal plane must have a radius of at least $f\phi + gy'/f$ where y' is the radius of the primary and ϕ is the angular radius of the field. For the system under consideration ϕ is about 3 degrees, f is 60 inches, and y is 10 inches. If the first correcting plate is placed $\frac{1}{4}f$ or 15 inches in front of the focal plane, the required radius will be 5.7 inches or .57y. This will result in the blockage of 32.5% of the light incident on the primary. It can be seen that a value of about $g = \frac{1}{4}f$ can be considered a practical upper limit for the placement of the correcting system.

The three equations for spherical aberration, coma, and

astigmatism cannot all be set equal to zero and solved simultaneously for the case of one aspheric plate in the convergent beam.

For two aspherics in front of the focal plane the equations to be solved are:

$$B = -4(n_1-1)A_{4,1}\left(\frac{g_1}{f}\right)^4 - 4(n_2-1)A_{4,2}\left(\frac{g_2}{f}\right)^4 = 0$$

$$F = \frac{1}{4f^2} + 4(n_1-1)A_{4,1}\left(\frac{g_1}{f}\right)^3 (f-g_1) + 4(n_2-1)A_{4,2}\left(\frac{g_2}{f}\right)^3 (f-g_2) = 0$$

$$C = \frac{1}{2f} - 4(n_1-1)A_{4,1}\left(\frac{g_1}{f}\right)^2 (f-g_1)^2 - 4(n_2-1)A_{4,2}\left(\frac{g_2}{f}\right)^2 (f-g_2)^2 = 0$$

Solving these equations simultaneously yields the solutions:

$$A_{4,1} = \frac{(n_2-1)}{(n_1-1)} A_{4,2}\left(\frac{g_2}{g_1}\right)^4$$

$$A_{4,2} = \frac{g_1}{16(n_2-1)g_2^3(g_2-g_1)}$$

$$g_1 = \pm g_2$$

Obviously, no usable system is available for a configuration using two plates. For the solution in which $g_1 = g_2$ the fourth order coefficient of the second plate goes to infinity. In the case of $g_1 = -g_2$ one is faced with the rather intractable necessity of placing one of the correctors in the light beam behind the focal plane!

It would therefore seem that the minimum number of aspheric plates necessary for complete correction is three.

In a system encompassing three aspheric surfaces in the convergent beam, the relevant equations necessary for aberration elimination are:

$$B = 4(n_1-1)A_{4,1}\left(\frac{g_1}{f}\right)^4 + 4(n_2-1)A_{4,2}\left(\frac{g_2}{f}\right)^4 + 4(n_3-1)A_{4,3}\left(\frac{g_3}{f}\right)^4 = 0$$

$$F = \frac{1}{4f^2} + 4(n_1-1)A_{4,1}\left(\frac{g_1}{f}\right)^3(f-g_1) + 4(n_2-1)A_{4,2}\left(\frac{g_2}{f}\right)^3(f-g_2)$$

$$+ 4(n_3-1)A_{4,3}\left(\frac{g_3}{f}\right)^3(f-g_3) = 0$$

$$C = \frac{1}{2f} - 4(n_1-1)A_{4,1}\left(\frac{g_1}{f}\right)^2(f-g_1)^2 - 4(n_2-1)A_{4,2}\left(\frac{g_2}{f}\right)^2(f-g_2)^2$$

$$- 4(n_3-1)A_{4,3}\left(\frac{g_3}{f}\right)^2(f-g_3)^2 = 0$$

The solution of the three equations for $A_{4,1}$, $A_{4,2}$, and $A_{4,3}$ yields:

$$A_{4,1} = -\frac{1}{(n_1-1)}\left\{A_{4,2}(n_2-1)\left(\frac{g_2}{f}\right)^4 + A_{4,3}(n_3-1)\left(\frac{g_3}{f}\right)^4\right\}$$

$$A_{4,2} = -\frac{1}{(n_2-1)}\left\{\frac{-A_{4,3}(n_3-1)g_3^3(g_3-g_1) + g_1/16}{g_2^3(g_2-g_1)}\right\}$$

$$A_{4,3} = \frac{g_1^2 - g_2^2}{16(n_3-1)g_3^2\left[g_2g_3(g_2-g_3) - g_1(g_2^2-g_3^2) + g_1^2(g_2-g_3)\right]}$$

We therefore have three free parameters, corresponding to the positioning of each of the three elements. The spacing of these elements is not completely arbitrary, but is subject to some restrictions. In particular, the closer any two elements, or any element and the focal plane, approach each other, the more extreme becomes the figuring of the fourth order curve. This results in larger higher order aberrations and less effective correction. It has been suggested (Schulte, 1966b) that equal element spacing produces the optimum correction. Some ray tracing performed on the system under consideration, using other than equal spacing, seems to confirm this.

With this assumption, and the previously assumed restriction of $g \leq \frac{1}{4}f$, the obvious design is one with the elements placed at $g_1 = 15"$, $g_2 = 10"$, $g_3 = 5"$.

With the choice of crown glass (n = 1.517), the fourth order curve coefficients become:

$$A_{4,1} = 1.612 \times 10^{-4}$$

$$A_{4,2} = -9.671 \times 10^{-4}$$

$$A_{4,3} = 2.418 \times 10^{-3}$$

The required radii of these plates are 5.7, 4.8, and 4.0 inches, respectively.

In addition to these aspheric plates, a field flattener of crown glass with a radius of curvature of 20."448 is necessary to flatten the focal plane.

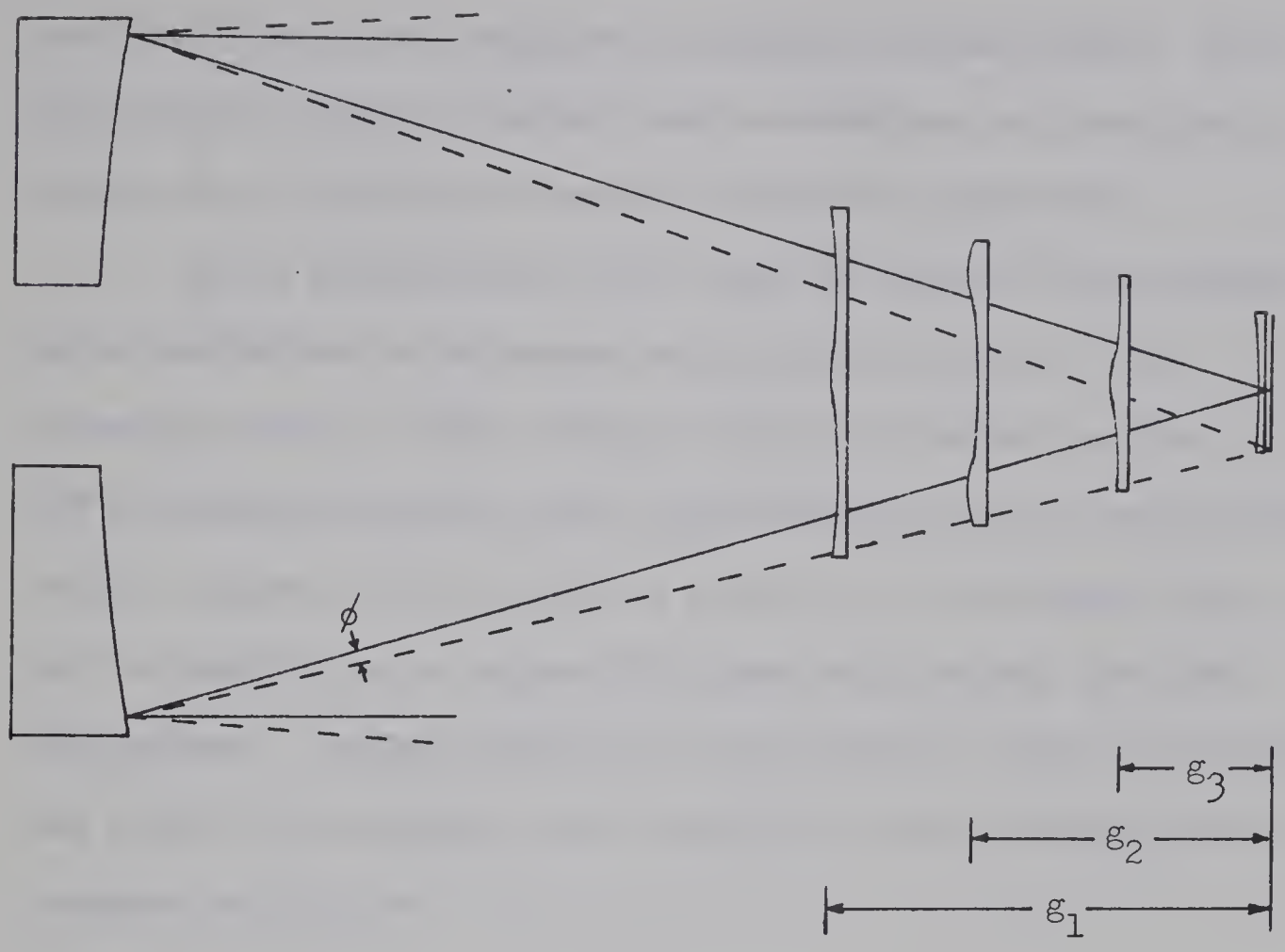

Fig. 16. Aspheric prime focus corrector

Attempts to optimize this system met with limited success. Image sizes across the field were reduced to several seconds of arc in size. This represents an improvement of a few orders of magnitude, but not as much improvement as desired.

The difficulty in achieving very small images is attributed to the higher order aberrations introduced by the large fourth order figures on the plates.

The aspheric depths of the plates are 0.16, 0.51, and 0.62 inches, respectively, and the angles between the normal to the optical axis and the front face of each plate (at the plate's edge) are 6.6, 23.2, and 31.8 degrees. These are hardly the

idealized flat plates supposed by retarded lamina theory. It is quite easy to envision higher order aberrations, as described in Section 4.3, limiting the amount of correction possible.

It is interesting to note that the cause of these higher order aberrations is dependent on the physical size of the telescope system. Thus, although sufficient correction for the 20" f/3 parabolic mirror under consideration does not seem possible using a system of three aspheric plates in the convergent beam, it may be possible for a larger f/3 system with exactly the same proportions. Design parameters of two systems, a 20" f/3 telescope and a 100" f/3 telescope, with exactly the same proportions are compared in Table 4.

Table 4

Aspheric parameters of correcting systems for 20" and 100" telescopes

Parameter	20" Telescope	100" Telescope
f	60"	300"
g_1	15"(r = 5".7)	75"(r=15".7)
g_2	10"(r = 4".8)	50"(r=11".5)
g_3	5"(r = 4".0)	25"(r= 7".4)
$A_{4,1}$	1.612×10^{-4}	1.289×10^{-6}
$A_{4,2}$	-9.671×10^{-4}	-7.737×10^{-6}
$A_{4,3}$	2.418×10^{-3}	1.934×10^{-5}
θ_1	$6^{\circ}.6$	$0^{\circ}.12$
θ_2	$23^{\circ}.2$	$2^{\circ}.7$
θ_3	$31^{\circ}.8$	$16^{\circ}.6$

The quantity which is most responsible for higher order aberrations is θ_i, the angle, at the edge of the plate, between the plate face and the normal to the optical axis. In particular, θ_1 and θ_2 are the most critical. It is noted that both θ_1 and θ_2 are more than an order of magnitude smaller in the 100" system than they are in the 20" system. In both systems, the plate sizes were chosen to completely illuminate a 4 x 5 inch plate at the focal plane.

One other form of three plate corrector was considered. This consisted of one full aperture correcting plate placed near the focal plane, and two smaller plates in the convergent beam. For such a system the equations for correction are:

$$B = -4(n_1-1)A_{4,1}\left(\frac{g_1}{f}\right)^4 - 4(n_2-1)A_{4,2}\left(\frac{g_2}{f}\right)^4 - 4(n_f-1)A_{4,f} = 0$$

$$F = \frac{1}{4f^2} + 4(n_1-1)A_{4,1}\left(\frac{g_1}{f}\right)^3(f-g_1) + 4(n_2-1)A_{4,2}\left(\frac{g_2}{f}\right)^3(f-g_2)$$

$$- 4(n_f-1)A_{4,f}g_f = 0$$

$$C = \frac{1}{2f} - 4(n_1-1)A_{4,1}\left(\frac{g_1}{f}\right)^2(f-g_1)^2 - 4(n_2-1)A_{4,2}\left(\frac{g_2}{f}\right)^2(f-g_2)^2$$

$$- 4(n_f-1)A_{4,f}g_f^2 = 0$$

where the subscript f refers to the full aperture corrector and g_f

is the distance of the full aperture corrector from the primary.

Simultaneous solution of the three equations yields:

$$A_{4,2} = (g_1^2 g_f^2 - 2g_f g_1^2 f + g_1^2 f^2 - f^4)/\{16(n_2-1)g_2^2(g_2 f^4 - g_1 f^4 - g_2^2 f^3 + g_1^2 f^3 + g_1 g_2^2 f^2 + g_f g_2^2 f^2 - g_1^2 g_2 f^2 - g_f g_1^2 f^2 - 2g_f g_1 g_2^2 f + 2g_f g_1^2 g_2 f - g_f^2 g_1^2 g_2 + g_f^2 g_1 g_2^2)\}$$

$$A_{4,1} = -\frac{1}{(n_1-1)}\left\{\frac{A_{4,2}(n_2-1)(g_2^3 f^2 - g_2^4 f + g_f g_2^4) + \frac{f^2}{16}}{g_1^3 f^2 - g_1^4 f + g_f g_1^4}\right\}$$

$$A_{4,f} = -\frac{1}{(n_f-1)}\left\{A_{4,1}(n_1-1)\left(\frac{g_1}{f}\right)^4 + A_{4,2}(n_2-1)\left(\frac{g_2}{f}\right)^4\right\}$$

Choosing crown glass (n = 1.517) and arbitrary element positions of $g_f = f = 60''.0$, $g_1 = 10''.0$, and $g_2 = 5''.0$, one obtains for the fourth order coefficients:

(i) $A_{4,f} = 1.399 \times 10^{-7}$

(ii) $A_{4,1} = -2.418 \times 10^{-4}$

(iii) $A_{4,2} = 9.671 \times 10^{-4}$

In this system, the full aperture corrector is mainly responsible for the removal of the spherical aberration introduced by the two plates in the convergent beam. The two plates in the convergent beam remove the coma and astigmatism. An additional field flattening lens with a radius of curvature of 20''.45 is

required near the focal plane.

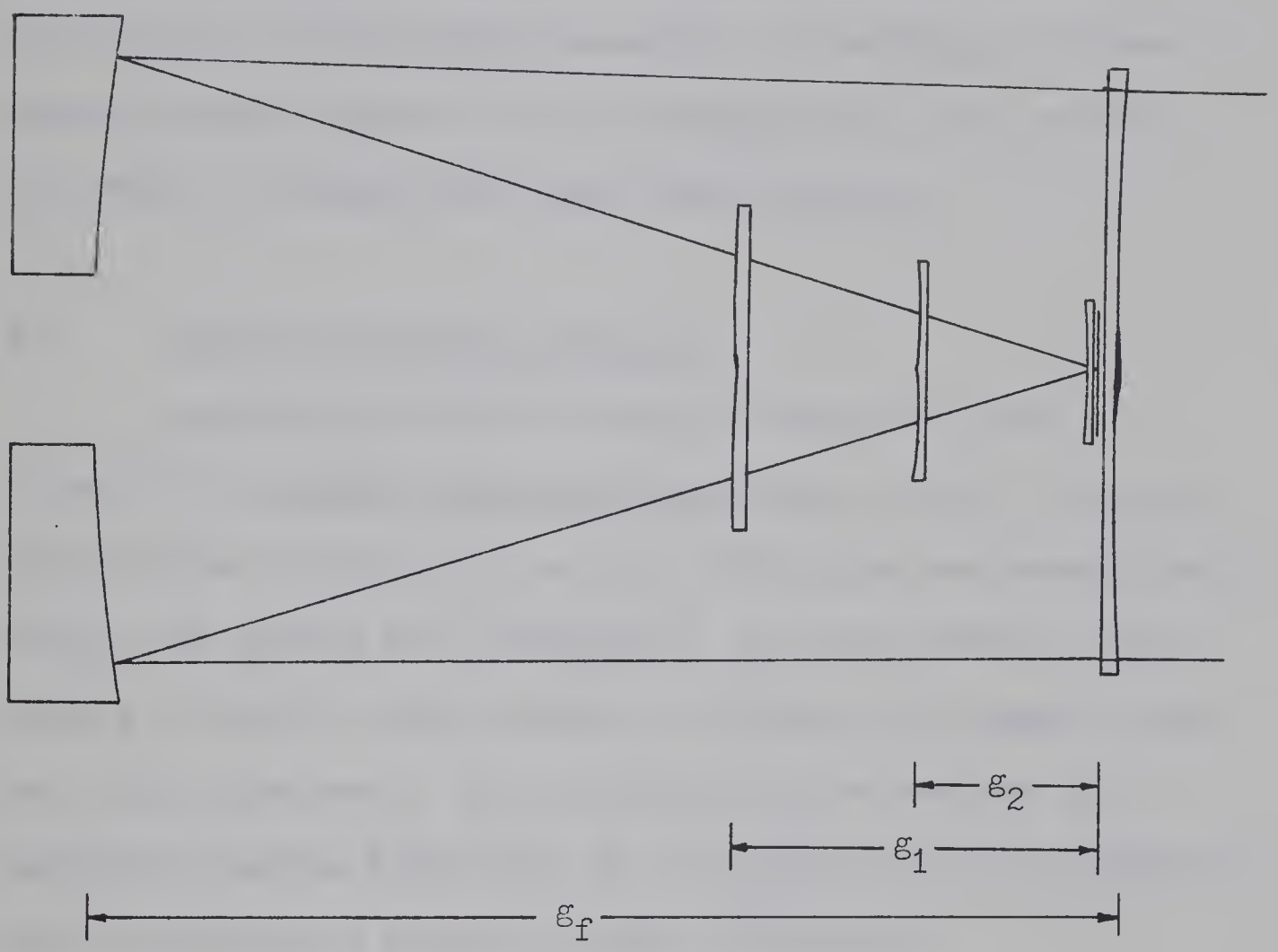

Fig. 17. Prime focus corrector with full aperture plate

Some preliminary ray tracing of this design suggested that fairly good correction could be obtained. Final optimization of this design was not, however attempted. The reason that this was not done is that a simpler, more easily constructed system, the Baker Reflector-Corrector, is already in existence.

While the last system proposed could achieve good correction, its value is largely compromised by the vignetting caused by the full aperture plate. Although the Baker design is attended by the

same problem, the coma and astigmatism are removed by an achromatic doublet, not by two aspheric plates. This doublet is much simpler and less expensive to construct, and is less sensitive to misalignment and temperature expansion. In addition, the Baker design does not require a field flattening lens, thus reducing the number of elements (and light loss) required.

5.2 The Baker Reflector-Corrector

Construction details of Baker's design are given in volume III of Amateur Telescope Making (Baker, 1953). Although instructions are given for scaling, difficulties are encountered if large, fast systems are contemplated. For such systems, direct scaling of Baker's system results in elements with negative edge and axial thicknesses. This difficulty can be overcome by assigning adequate thicknesses to all elements and then performing minor modifications during the final optimization.

The Reflector-Corrector is essentially a non-afocal Ross corrector with an additional element (the full aperture aspheric plate) added to eliminate the spherical aberration. By giving the doublet a slight positive power, it is possible to negate the Petzval curvature of the primary. Since the lens system is no longer afocal, however, the pair must be achromatized. This is accomplished by the choice of glasses and relative power of each lens in the system.

The coma and astigmatism of the primary are removed by the bending of the doublet and its axial placement. The positive

power of the doublet has the effect of reducing the system's focal length. The focal ratio of the system being considered is reduced from f/3 to f/2.65.

Baker, in his original design, used a cemented doublet. To prevent difficulties arising from different coefficients of expansion in the larger system being constructed, a separated doublet is used.

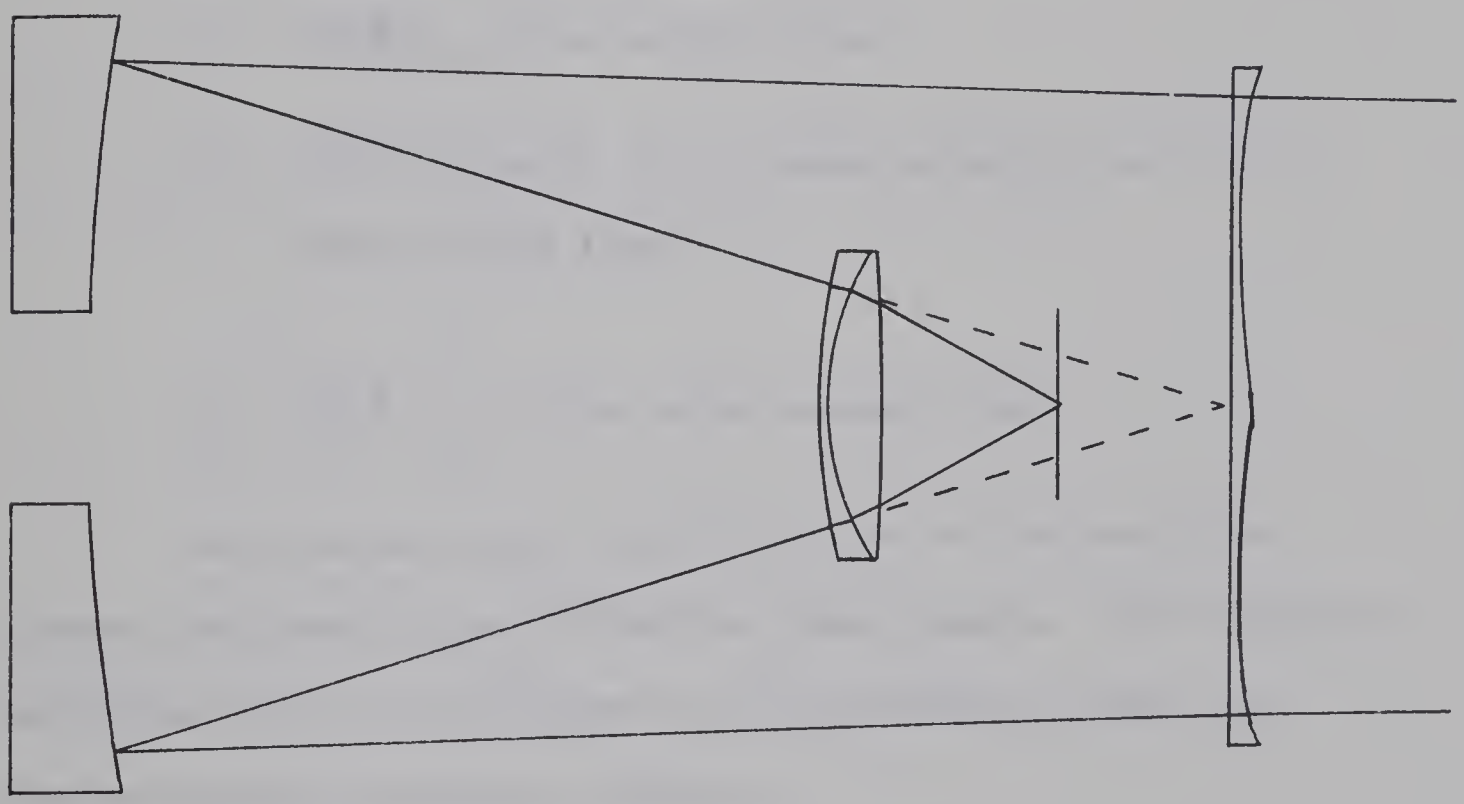

Fig. 18. Reflector-Corrector

The condition to be fulfilled for achromatization of a pair of thin lenses is given by:

$$\frac{\phi_1}{v_1} + \frac{\phi_2}{v_2} = 0$$

where ϕ_i is the power of each lens, and v_i is a quantity known as the constringency or dispersion of the glass:

$$v = \frac{n_{\lambda 1} - 1}{n_{\lambda 2} - n_{\lambda 3}}$$

In the equation for v, $\lambda 1$ is the wavelength about which the pair is to be achromatized, and $\lambda 2$ and $\lambda 3$ are the long and short wavelengths at which chromatism is to be corrected.

The wavelengths chosen for achromatization were:

$\lambda 1 = 4350\text{Å}$ (λ_g, blue mercury line)

$\lambda 2 = 5650\text{Å}$ (midpoint of λ_e, green mercury line, and λ_d, yellow helium line)

$\lambda 3 = 3650\text{Å}$ (λ_I, ultra violet mercury line)

The glasses chosen were Schott type F4 for the flint element and Schott type BK7 for the crown element. The indices of refraction for the two glasses at the wavelengths chosen for achromatization are shown in Table 5.

Table 5

Indices of Refraction for Doublet Glasses

Wavelength (Å)	Index of Refraction	
	Flint (F4)	Crown (BK7)
3650	1.6622	1.5363
4350	1.6383	1.5267
5650	1.6186	1.5178

Using the values from Table 5, $v_1 = 14.640$ and $v_2 = 28.470$. The ratio of powers of the two elements necessary for achromatization is:

$$\frac{\phi_1}{\phi_2} = -\frac{v_1}{v_2} = -.5142$$

In addition, the elimination of the Petzval curvature requires that:

$$P = \frac{\phi_1}{n_1} + \frac{\phi_2}{n_2} - \frac{1}{f_m} = 0$$

where f_m is the focal length of the primary mirror. Inserting the equality $\phi_1 = -.5142\phi_2$ and solving, one obtains:

(i) $\phi_1 = -.025$

(ii) $\phi_2 = .049$

The necessary placement and bending of the lens can be determined using the equations of Section 3.3:

Spherical aberration: S_I

Coma: $S_{II} + 2S_I dE - 2h^2/R_m^2$ (3.7)

Astigmatism: $S_{III} + 2S_{II}dE + S_I(dE)^2$

with S_I, S_{II}, S_{III}, and dE being determined from equations (3.4):

$$S_I = \Sigma A; \quad S_{II} = \Sigma AB; \quad S_{III} = \Sigma AB^2$$

with (3.5):

$$A_i = Q_i^2 h_i^4 \left(\frac{1}{n_{i-1} s_i} - \frac{1}{n_i s_i'} \right)$$

$$B_i = - \frac{1}{Q_i h_i^2} - \sum_{p=1}^{i-1} \frac{d_p}{n_p h_p h_{p+1}} = - \frac{1}{Q_i h_i^2} - E_i$$

$$Q_i = n_{i-1} \left(\frac{1}{r_i} - \frac{1}{s_i} \right) = n_i \left(\frac{1}{r_i} - \frac{1}{s_i'} \right)$$

$$dE = - \frac{R_m^2}{2h^2 (R_m - 2d)}$$

The notation is the same as that used in Chapter III.

The positioning and radii of curvature of the element surfaces must be chosen so that coma and astigmatism are zero. Although the above equations could, in principle, be solved in closed form, the most practical form of solution is graphical.

A position for the lens element is chosen, and the coefficients of coma and astigmatism calculated for several different lens curvatures. If this procedure is repeated for several different axial positions of the lens system and the results then plotted, the correct positioning of the doublet and radii of curvature of the lens surfaces can be found by inspection.

In Figure 19 the astigmatic and comatic coefficients are plotted as functions of the radius of curvature of the first lens surface. Three different positions of the lens system are

Fig. 19. Coma and astigmatism of achromatized doublet

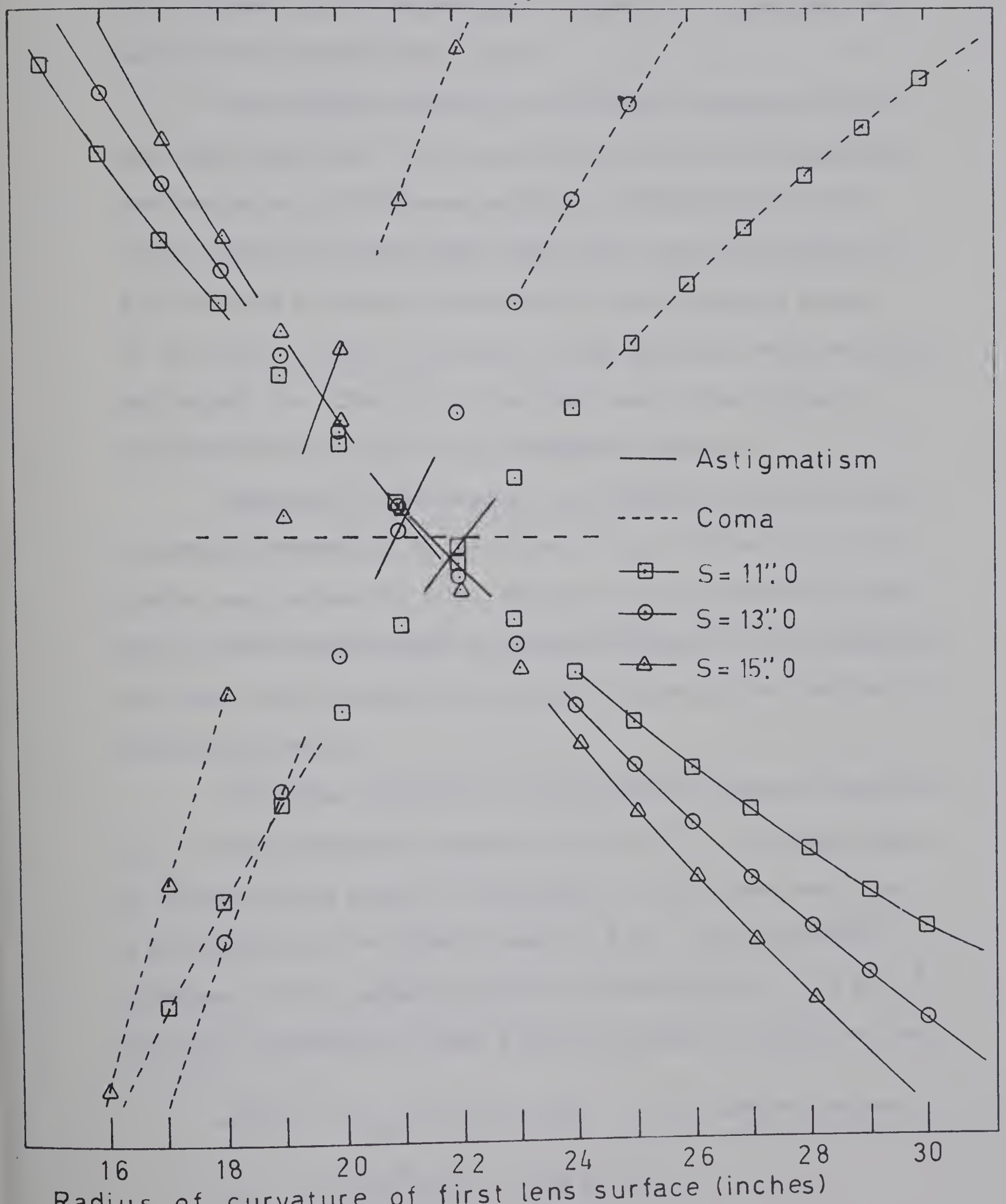

shown in the figure; s_1 = 11".0, 13".0, and 15".0. S_1 represents the distance that the correcting lens system is placed from the paraboloid's original focal plane.

The horizontal dashed line in Figure 19 represents zero coma and astigmatism. For correction, both coma and astigmatism must become zero at the same position. Interpolation of the values presented in the graph suggest that this will happen for $s_1 \approx$ 12".2 and a radius of curvature for the first lens surface of about 21".6. Since the powers of each lens have been previously determined, the curvature of the first lens surface uniquely specifies the curvature of all subsequent surfaces.

Evaluation of the comatic and astigmatic coefficients for a system corresponding to the values of s_1 = 12".2 and r_1 = 21".6 yields small values for both. Although these values are non-zero, they are much smaller than the expected effects of lens thicknesses and higher order aberrations, and these values can be used for a preliminary design.

The Seidel coefficient of the residual spherical aberration, S_I, for this preliminary design is 6.67×10^{-3}. To correct this, an aspheric plate placed at the primary's focal plane must cause a retardation (at the plate's edge) of $S_I/8$. The differential thickness of this aspheric plate can be expressed as $\Delta t = A_{4,f} y^4$. Since the retardation of such a plate is given by $\Delta t(n-1)$ we have:

$$\Delta t(n-1) = A_{4,f} y'^4 (n-1) = S_I/8 \qquad (y' = \text{system aperture})$$

$$A_{4,f} = S_I/(8y'^4(n-1)) = 3.09 \times 10^{-7}$$

In actual performance, the system will suffer less vignetting if the full aperture plate is placed at approximately the same position as the lens system, rather than at the focal plane of the primary. This will result in a change in the fourth order figure on the full aperture plate, but this change is small and can be accomplished during the optimization of the system.

The particulars of the preliminary design, as derived from Seidel aberration theory, are summarized below.

Fourth order curve on aspheric plate: $A_{4,f} = 3.09 \times 10^{-7}$

Distance of lens system from primary: $f\text{-}s_1 = 47''.8$

Radii of curvature of flint element surfaces: $r_1 = 21''.6$

$r_2 = 11''.5$

Radii of curvature of crown element surfaces: $r_3 = 11''.5$

$r_4 = -127''.8$

Distance of focal plane from lens system; $s'_3 = 9''.45$

Focal length of complete system: $f\text{-}s_1 + s'_3 = 57''.25$

A comparison of this preliminary design to the final optimized design (Table 6) reveals that the changes necessary to correct for the lens thicknesses and higher order aberrations are remarkably small.

5.3 Computer Optimization of the Reflector-Corrector

The initial design used in the optimization procedure was a scaled model of Baker's published design. Larger lens thicknesses and separation between the components of the lens pair necessitated changing several of the surfaces and distances. A small second order curve was superimposed on the aspheric corrector to minimize chromatic effects and further optimize performance.

Optimization of the system and generation of spot diagrams were accomplished using a ray trace program described in Appendix II.

The finalized design gives extremely good monochromatic correction. At the designed wavelength 4358Å (n_g, blue mercury line) the system produces images smaller than one second of arc over a 6 degree field. This represents a reduction in the area of images near the edge of the field by a factor of almost 100,000.

Good correction is achieved at all wavelengths from below 3500Å to above 6000Å. However, there is a shift with wavelength of the focal plane position. The total shift between 3650Å and 5461Å is 0.008 inches. Thus, optimum performance will be achieved if this system is used in conjunction with filters.

Specifications of the finalized design are given in Table 6. A comparison of the uncorrected and corrected image sizes is shown in Figure 21, and the profile of the full aperture corrector is given in Figure 22.

Spot diagrams of the corrected images are presented in Appendix I.

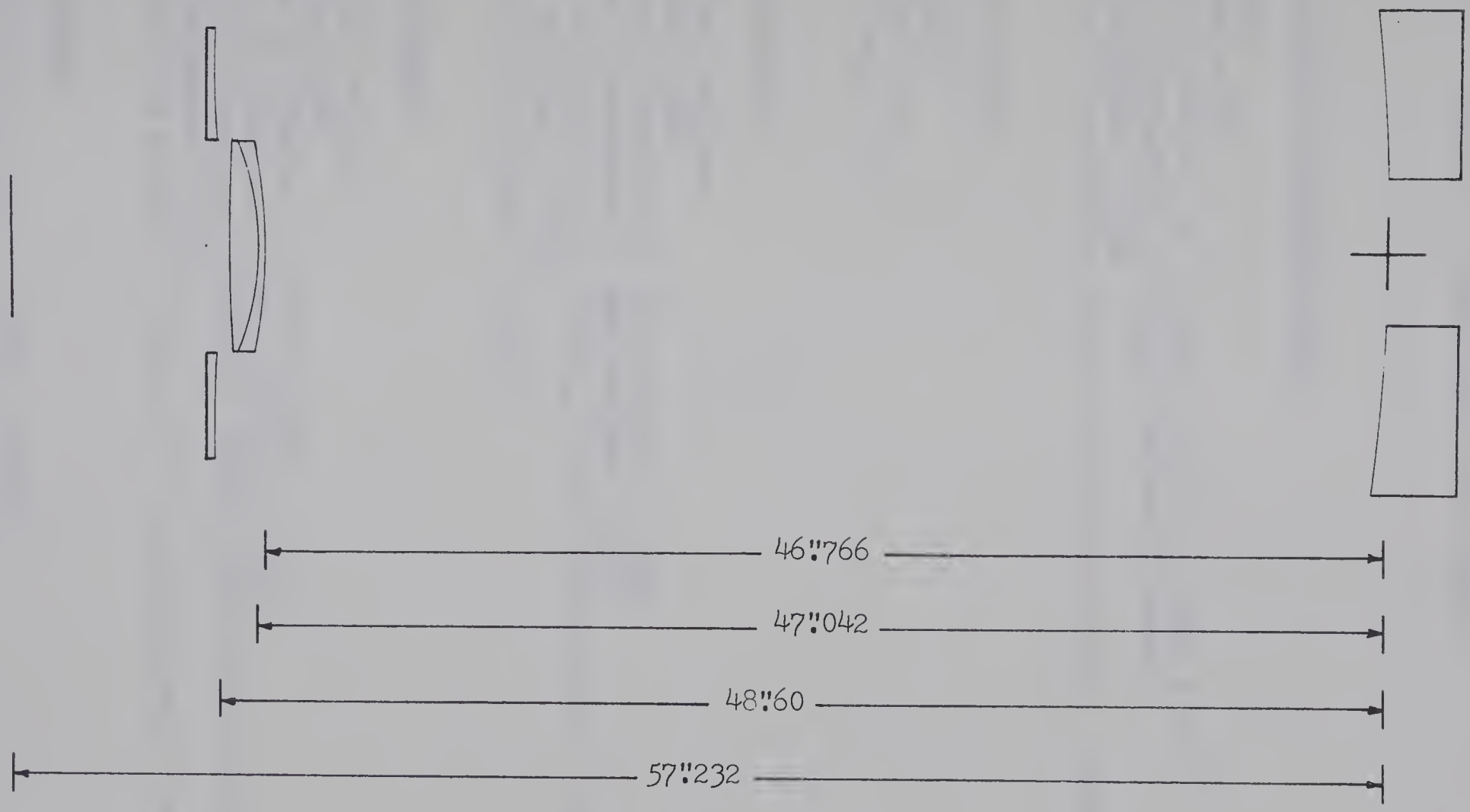

Fig. 20. Optimized prime focus system

Table 6. Final Prime Focus Design

Full aperture correcting plate

Aspheric
diameter = 18"
surface equation: $\Delta t = 3.296 \times 10^{-7} r^4 - 4.5336 \times 10^{-5} r^2$
index of refraction = $1.522 n_d$ (opthomalic crown)
axial thickness = 0".50
distance of correcting (back) surface from primary = 48".60

Primary mirror

Paraboloid
diameter = 20"
focal length = 60"

Flint element

Spherical surfaces
diameter = 8".8
radius of curvature of front surface = 21".87
radius of curvature of rear surface = 11".61
index of refraction = $1.61659 n_d$ (Schott glass type F4 (617366))
axial thickness = 0".275
distance from primary = 46".766

Crown element

Spherical surfaces
diameter = 8".8
radius of curvature of front surface = 11".61
radius of curvature of rear surface = -130".0
index of refraction = $1.51680 n_d$ (Schott glass type BK7 (517642))
axial thickness = 1".00
distance from primary = 47".042 (0".001 spacing between elements)

Focal plane

Distance from primary = 57".232 (4358Å)

Fig. 21. Comparison of corrected and uncorrected prime focus images

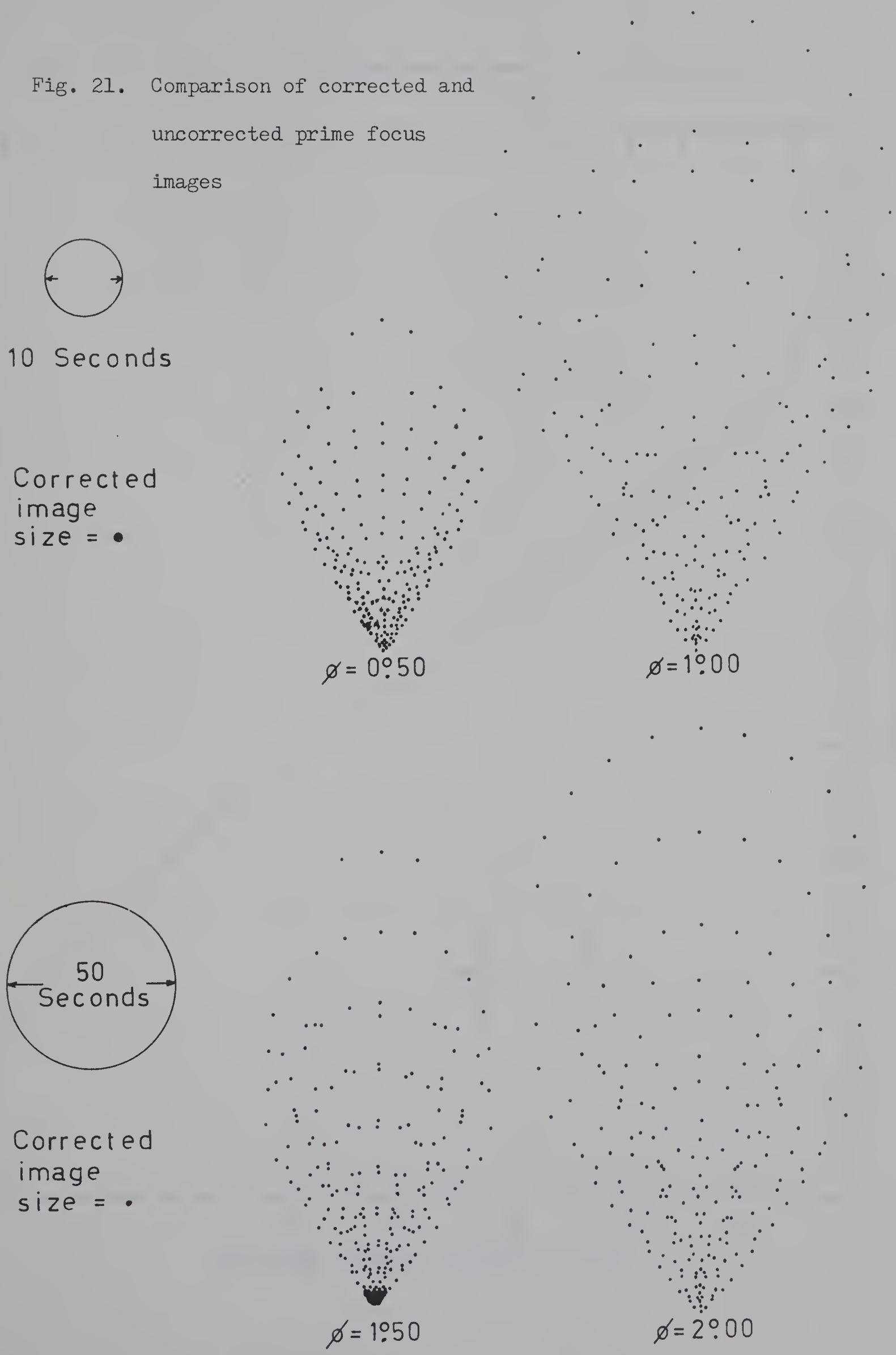

Fig. 22. Profile of full aperture aspheric correcting plate

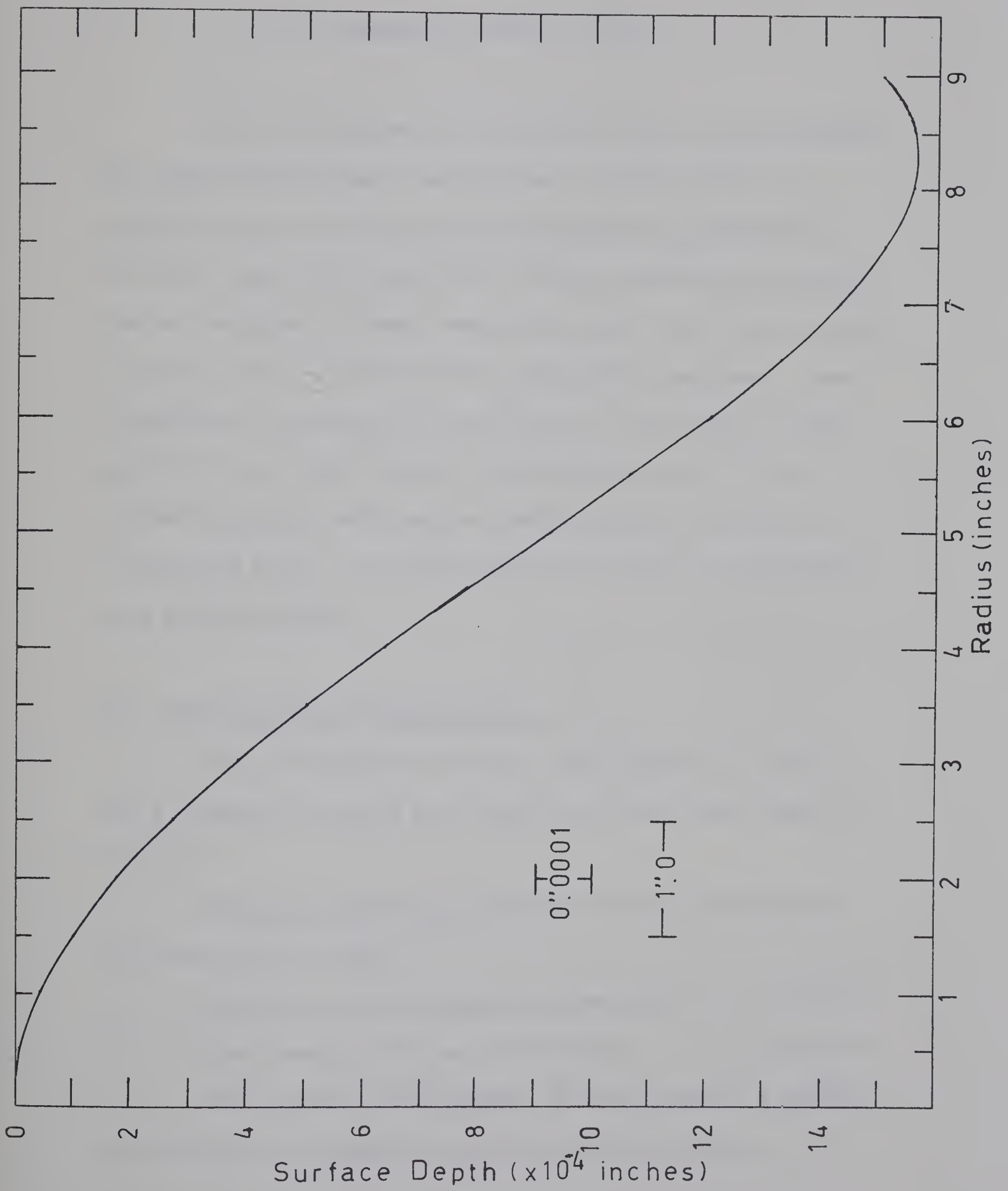

CHAPTER VI

F/18 CASSEGRAIN CORRECTING SYSTEM

The f/18 Cassegrain configuration will be used primarily for lunar and planetary observations. In this context the necessity of an elaborate correction system is questionable. At such a large focal ratio, the off-axis aberrations are small, and as the planets subtend very small angles, they can be placed near the centre of the field for photographic purposes. Lunar observations represent the only occasion during which a large portion of the field would be considered necessary. Thus a correcting system would only be justifiable if it could be constructed simply and inexpensively and could be incorporated in a single element.

6.1 F/18 Cassegrain Specifications

The f/18 system will have a focal length, f, of 360" and a separation between the primary mirror and focal plane, e, of 12".5.

Using the equations of Section 4.1 the parameters of the system can be found:

Separation between primary and secondary = d = 49".64286

Focal length of the secondary mirror = f_2=-12".42857

The equation of the surface of the hyperbolic secondary can also be found using the equations of that section.

Semi-major axis = a = 25".892857

Semi-minor axis = a' = 25".369715

Eccentricity = $\underline{e} = (a^2+a'^2)^{\frac{1}{2}}/a = 1.40$

Asphericity factor = $b_2 = -\underline{e}^2 = -1.96$

and the equation of the hyperbolic surface is given by:

$$z = \left(\frac{x^2+y^2+a'^2}{\underline{e}^2-1}\right)^{\frac{1}{2}} + (d-a)$$

$$= \left(\frac{x^2+y^2+643.622}{.96}\right)^{\frac{1}{2}} + 23.75$$

The diameter necessary for the secondary mirror, given by $D = (d+e)2y(1/f) + 2d\phi$ where y is the system's aperture (10") and ϕ is the radius of the field (0.5 degrees or 0.00873 radians), is about 4.32 inches. The actual obstruction will be considerably larger however, as necessary light baffling will cause the effective light blockage to be enhanced greatly over that which the size of the secondary would indicate.

6.2 F/18 Aberration Correction

The sizes (in seconds of arc) of the comatic and astigmatic aberrations are given by (Section 2.3):

Angular length of the coma figure $= 3Fy^2\phi$

Angular diameter of the astigmatic blur circle $= 2Cy\phi^2$

where F and C are given by (for a classical Cassegrain configuration):

$$F = \frac{1}{4f^2}$$

$$C = \frac{f_1(f-d)}{2f^2(f_1-d)}$$

At the edge of the field (about $0^{\circ}.5$ from the optical axis) this corresponds to a comatic figure of about 1.0 second of arc in length and an astigmatic figure of 2.2 seconds of arc in diameter. Examination of Figure 8 at the end of Chapter II reveals that the images are much larger than indicated by the aberrations. The cause of these large images is the extreme Petzval curvature of the system. The focal plane has a radius of curvature of only -15".6575.

Since the radius of curvature of the focal plane is the most serious defect of the system, any correction attempt must be aimed primarily at the elimination of this curvature. The requisite for a flat field of focus is a Petzval sum of zero:

$$P = \frac{1}{f_1} + \frac{1}{f_2} + \frac{\phi}{n} = 0$$

where ϕ is the power and n the index of refraction of a field flattening lens placed near the focal plane. Choosing crown glass (n = 1.517) and making the second surface of the lens plane to minimize the introduction of additional aberrations, a first surface radius of curvature of 5".342 is necessary to flatten the field.

Since astigmatism is closely related to field curvature, it was considered possible that the astigmatism could be removed by altering the radius of curvature of the field flattening element. Computer investigation of several different radii of curvature showed this to be so. Maximum overall correction was obtained for a radius of curvature of 4".79. It was found necessary to make the axial thickness of the lens small (0".10) and the lens-focal plane separation very small (0".01) for optimum images. Further computer ray tracing showed that good correction was obtainable for lens-focal plane separations of up to 0".10, but that correction fell off rapidly for larger separations. Similarly, it was found that the lens thickness could be increased by a factor of two without severe image degradation, although this necessitated a change in the radius of curvature.

Design specifications are given in Table 7 and a comparison of the corrected and uncorrected images is shown in figure 23.

Spot diagrams of the corrected images are presented in Appendix I. Examination of these images reveals that a large proportion of the residual aberration is comatic. Due to the specialized requirements of the f/18 system, the images are not uniform over the entire field, but increase in size with distance from the optical axis. The central image is still diffraction limited in size. This allows critical work, under fine seeing conditions, to be done without the necessity of removing the corrector. The images near the edge of the field, already under

one second of arc in diameter, can be somewhat further reduced in size, at the expense of the central image, by a change in focus.

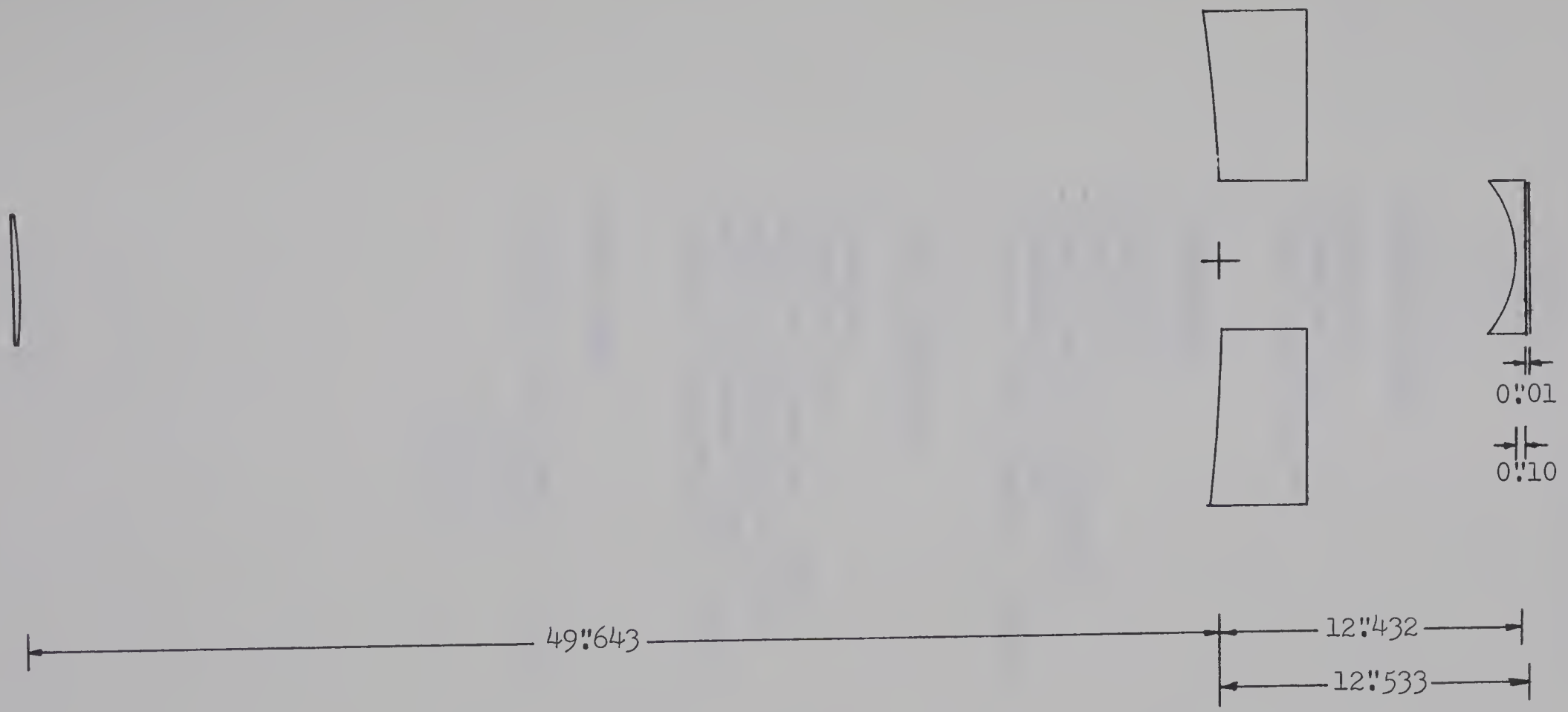

Fig. 23. Optimized f/18 Cassegrain

Table 7. Final F/18 Cassegrain Design

Primary mirror

Paraboloid
diameter = 20"
focal length = 60"

Secondary

Hyberboloid
diameter = 4.5"
focal length = -12".42857
eccentricity = 1.40
distance from primary = 49".643

Field flattener

Spherical
diameter = 6"
radius of curvature = 4".79
index of refraction = 1.517
axial thickness = 0".10
distance from primary = 12".432

Focal plane

distance from primary = -12".533

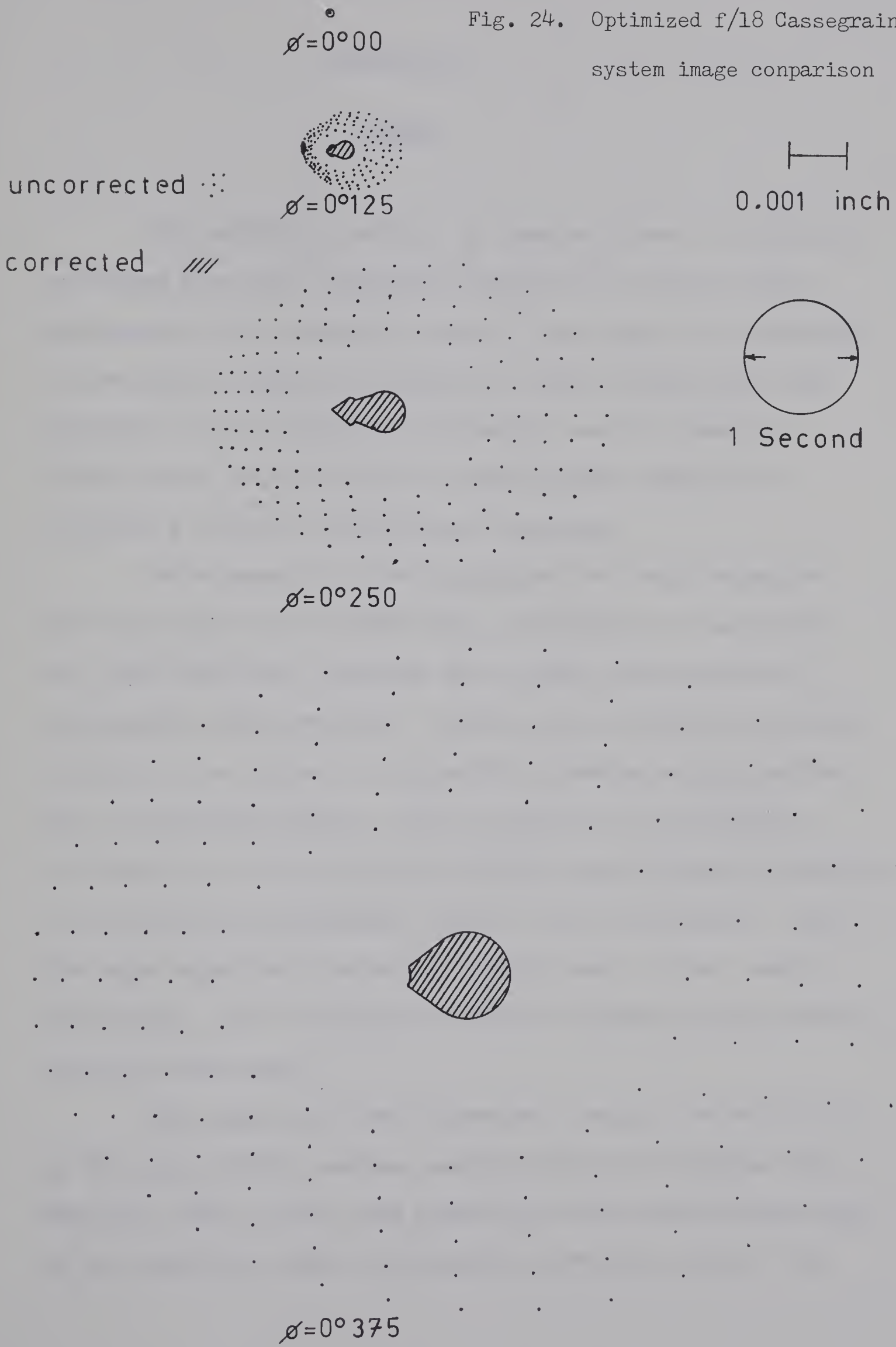

Fig. 24. Optimized f/18 Cassegrain system image conparison

CHAPTER VII

SUMMARY

The aberrations suffered by classical forms of reflecting telescopes have been investigated and means of achieving large photographic fields relatively free of these aberrations discussed. In particular, designs for corrective optical systems have been developed for the University of Alberta's new 20" telescope. These systems, when constructed, should greatly enhance the telescope's value as a photographic instrument.

The advances in correcting systems for large telescopes have been many since the first Ross correctors were constructed, and today most large telescopes are equipped with some form of photographic field corrector. In recent years advances in optical technology have allowed the production of precision non-spherical and non-parabolic surfaces, with the result that non-classical configurations of telescopes with highly aspheric mirrors, resulting in well-corrected photographic fields, have been possible. Most of the large telescopes constructed recently have, in fact, been of such designs, with the Ritchey-Chrétien or modified Ritchey-Chrétien being the most common.

Most moderately sized telescopes, however, are still built in the more versatile and more easily constructed classical form. Moreover, there are very many moderately sized systems extant which do not possess any form of photographic correcting system. The

majority of these telescopes could benefit greatly from the addition of a corrective system. Such systems can be designed using the methods discussed in this work. The expense and difficulty of constructing such a corrector is more than offset by the increased usefulness of the new system.

BIBLIOGRAPHY

Allen, C. W., 1975, Vistas in Astro., 19, 179

Baker, J. G., Amateur Telescope Making, 3 (Scientific American, 1953), p. 1

Baker, J. G., 1969, IEEEE Trans., AES-5, 2, 261

Boutry, G. A., 1961, Instrumental Optics, translated by R. Auerbach (Interscience Publishers Inc., New York, 1962)

Bowen, I. S., 1960, Stars and Stellar Systems, 1, 43

Bowen, I. S., 1967, Q. J. R. Astr. Soc., 8, 9

Bowen, I. S., 1967, An. Rev. Astr. & Astrophys., 5, 45

Brewer, S. H., 1975, J. Opt. Soc. Am., 66, 8

Buchroeder, R. A., 1972, Applied Optics, 11, 2968

Burch, C. R., 1942, Mon. Not. R. Astr. Soc., 102, 159

Burch, C. R., 1943, Proc. Phys. Soc., 55, 29

Code, A. C., 1973, An. Rev. Astr. & Astrophys., 10, 239

Crawford, D. L. (ed), 1966, The Construction of Large Telescopes, (I. A. U. Symposium no. 27), (Academic Press, London and New York, 1966)

Gascoigne, S. C. B., 1965, Observatory, 85, 79

Gascoigne, S. C. B., 1968, Q. J. R. Astr. Soc., 9, 98

Gascoigne, S. C. B., 1973, Applied Optics, 12, 1419

Klein, M. V., 1970, Optics, (John Wiley and Sons, Inc. , New York, London, Sydney, Toronto, 1970)

Köhler, H., 1968, Applied Optics, 7, 241

Korsch, D., 1972, Applied Optics, 11, 2986

Linfoot, E. H., 1943, Mon. Not. R. Astr. Soc., 103, 210

Linfoot, E. H., 1945, Proc. Phys. Soc., 62, 199

Linfoot, E. H., 1955, Recent Advances in Optics, (Oxford University Press, London, 1955)

Maksutov, D. D., 1944, J. Opt. Soc. Am., 34, 270

Meinel, A. B., 1953, Astrophys. J., 118, 335

Odgers, G. J., 1967, Applied Optics, 6, 1635

Rosin, S., 1961, J. Opt. Soc. Am., 51, 331

Rosin, S., 1964, Applied Optics, 3, 151

Ross, F. E., 1935, Astrophys. J., 81, 156

Sampson, R. A., 1913, Phil.Trans. R. Soc., 213, 149

Schulte, D. H., 1963, Applied Optics, 2, 141

Schulte, D. H., 1966, Applied Optics, 5, 309

Schulte, D. H., 1966b, Applied Optics, 5, 313

Schwarzschild, K., 1905, Astron. Mit. Koniglichen Sternwarte, 10, 1, (Gottingen)

Stein, W. A., and Woolf, N. J., 1971, Applied Optics, 10, 655

Wallin, W., 1951, J. Opt. Soc. Am., 41, 1029

Waland, R. L., 1961, J. Opt. Soc. Am., 51, 359

Wayman, P. A., 1950, Proc. Phys. Soc., B63, 553

Wetherell, W. B., and Rimmer, M. P., 1972, Applied Optics, 11, 2817

Wilson, R. N., 1968, Applied Optics, 7, 253

Whittaker, E. T., 1907, The Theory of Optical Instruments, (Cambridge University Press, London, 1905)

Wyman, C. L., and Korsch, D., 1974, Applied Optics, 13, 2402

Wyman, C. L., and Korsch, D., 1974, Applied Optics, 13, 2064

Wynne, C. G., 1947, Mon. Not. R. Astr. Soc., 107, 356

Wynne, C. G., 1949, Proc. Phys. Soc., B62, 772

Wynne, C. G., 1951, Proc. Phys. Soc., 65, 429

Wynne, C. G., 1956, Rep. Prog. Phys., 19, 298

Wynne, C. G., 1961, Optica Acta, 8, 255

Wynne, C. G., 1965, Applied Optics, 4, 1185

Wynne, C. G., 1967, Applied Optics, 6, 1227

Wynne, C. G., 1968, Astrophys. J., 152, 675

Wynne, C. G., 1972, Progress in Optics, 10, 139

APPENDIX I

IMAGES OF THE FINALIZED DESIGNS

In this appendix, spot diagrams of the images produced by the finalized designs are presented.

Figure 25 shows the images of the Reflector-Corrector at the designed wavelength of 4358Å over a 6 degree field. At the edge of a 6 degree field, the image is 2.8 inches from the centre of the photographic plate. In Figure 26, a comparison is made between the images produced at three different wavelengths; 3650Å, 4358Å, and 5461Å. The effect of changing focus is shown in Figure 27, with the images at 5461Å being shown for three different focal plane positions; 57.233, 57.234, and 57.235 inches.

The images of the corrected f/8 Cassegrain system over a 1.50 degree field are shown in Figure 28.

Figure 29 shows the corrected images of the f/18 Cassegrain system over a 0.75 degree field.

Each of the dots in the spot diagrams represents an equal area, or equivalently, an equal amount of light, at the entrance pupil of the system.

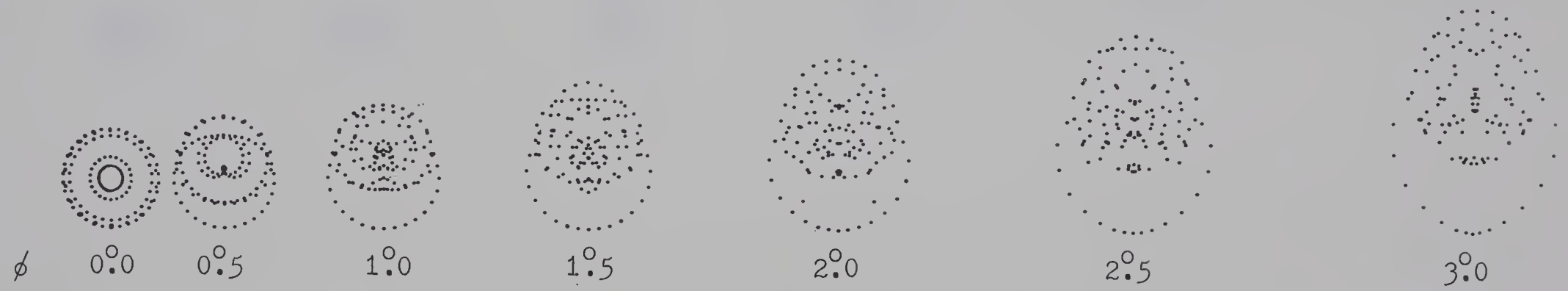

Fig. 25. Images at prime focus with correcting system (4358Å)

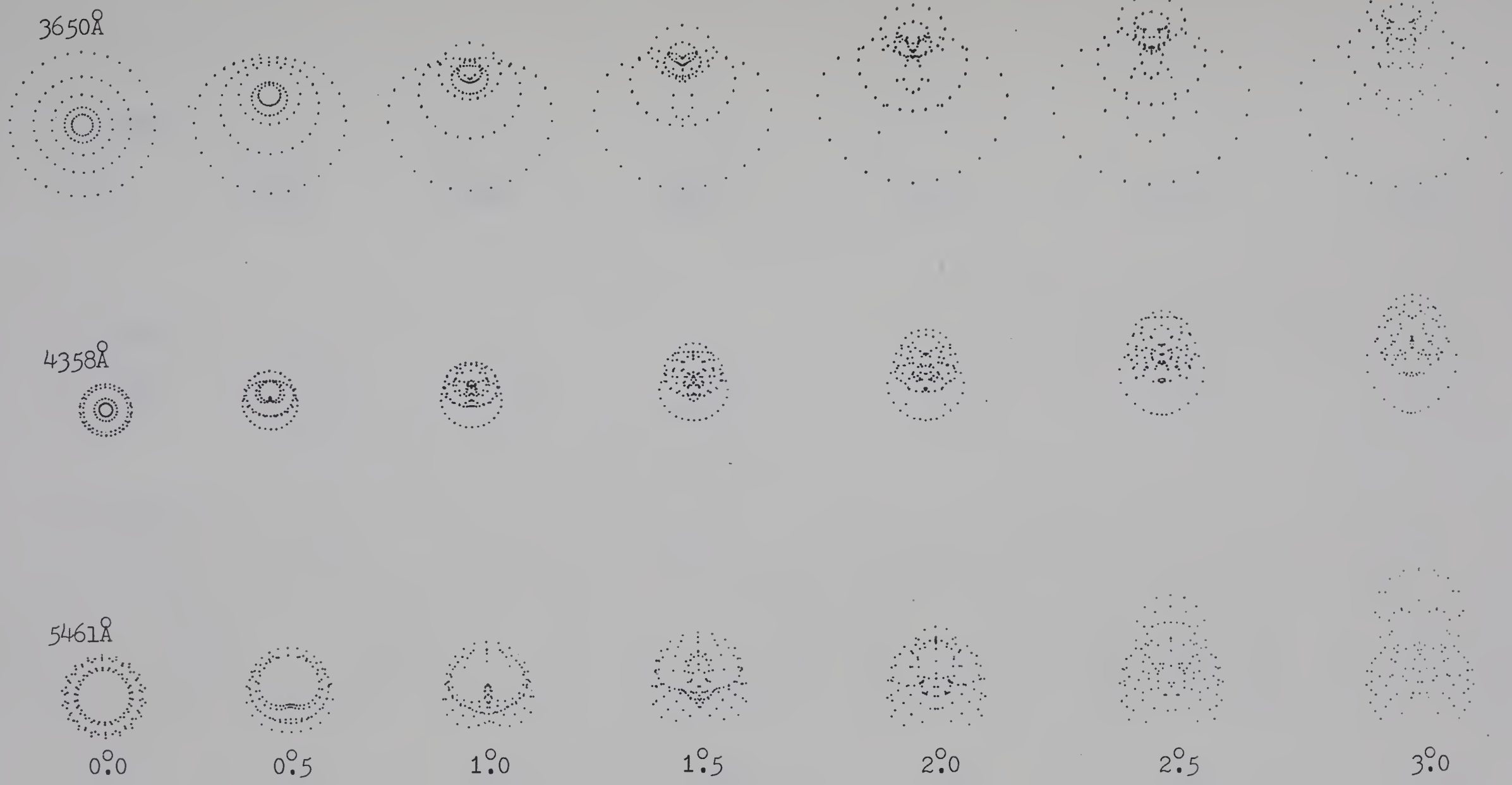

Fig. 26. Image variation with wavelength (Reflector-Corrector)

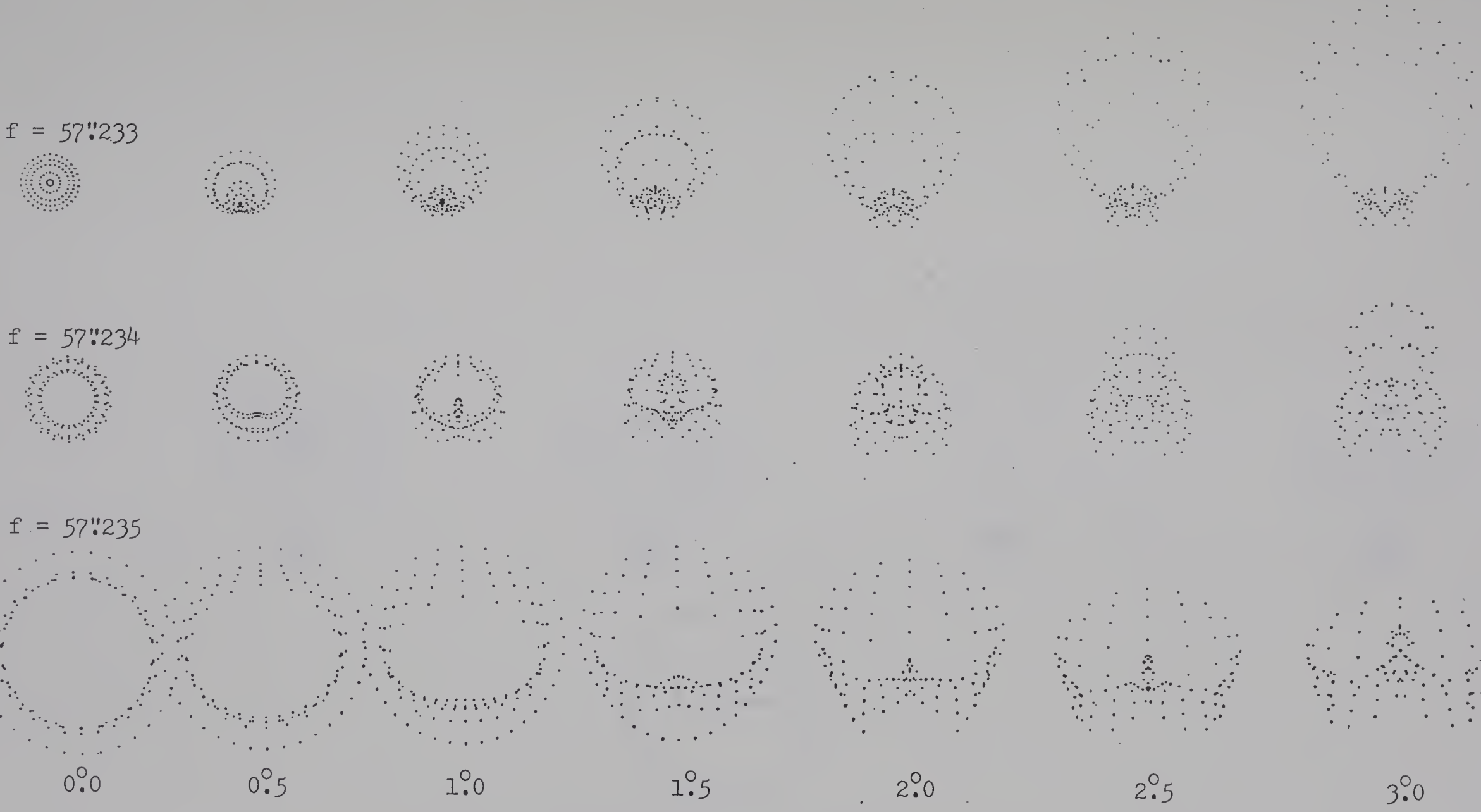

Fig. 27. Image variation with focal plane position (Reflector-Corrector)

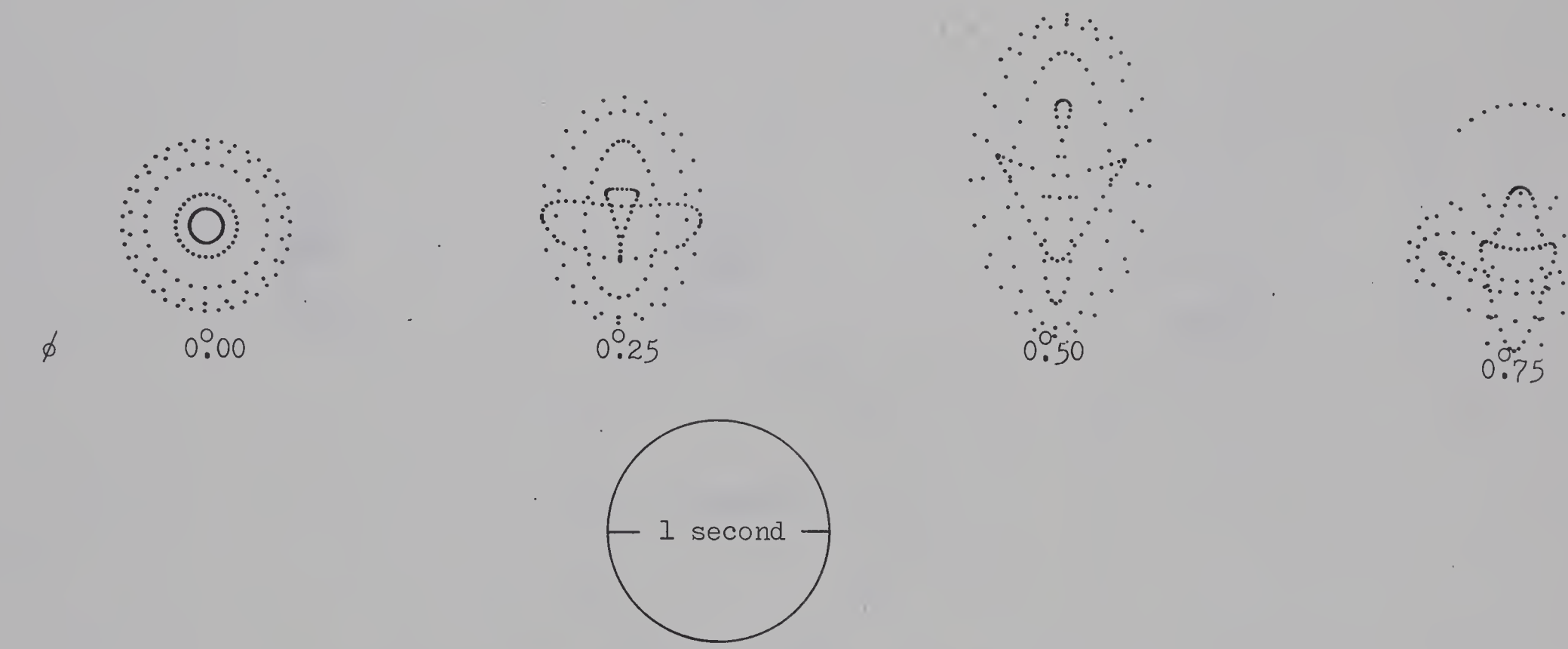

Fig. 28. Images of the corrected f/8 system

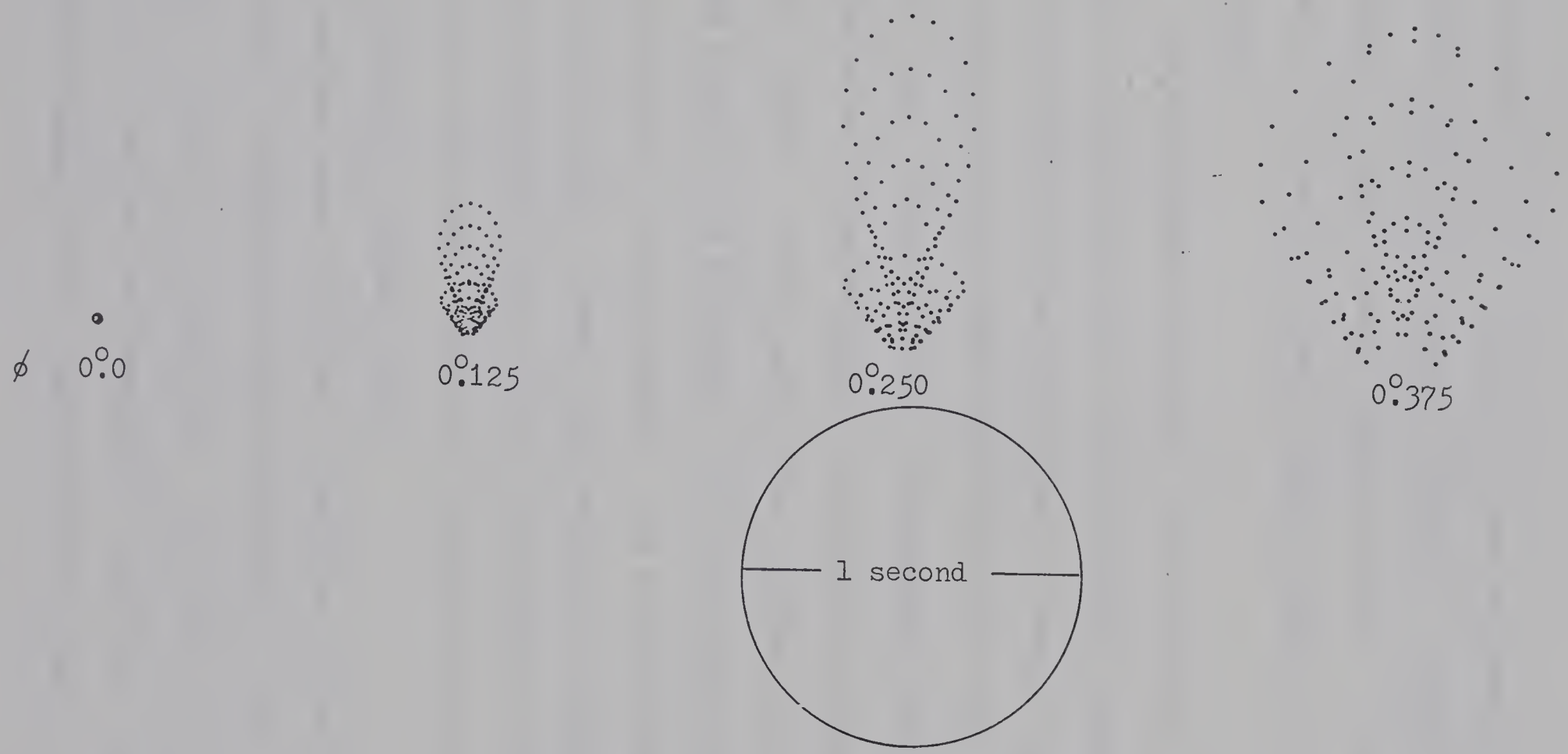

Fig. 29. Images of corrected f/18 system

APPENDIX II

COMPUTER PROGRAMS

Optimization of the correcting systems and generation of spot diagrams were done using computer programs. Although a separate program was used for each telescope system, it would be quite possible to create a general program capable of evaluating almost any system.

Two types of programs were used. The first type, used for optimizing a correcting system, is an interactive program which allows the operator to test any system by tracing light rays entering the system from any origin point and at any angle to the optical axis. Since several variables are changeable within the program, a system may be tested quickly by tracing a few marginal rays at various angles. On the basis of the results, the system can be changed slightly and retested. The second type of program, used for the generation of spot diagrams, uses a predetermined set of light ray origin points. These origin points are arranged around a set of concentric rings centred on the optical axis, in such a manner that each point represents an equal area of the disc defining the telescope's entrance pupil.

The programs trace a light ray through the system from surface to surface by using the surface intersection points and the directional cosines of the light ray. The three basic operations performed on the traced ray are translation, refraction, and reflection. A short summary of the equations used for each of these

operations is given below.

$\underline{e}$, $\underline{e}'$ are the vectors defined by the incident and refracted (reflected) light ray

α, β, γ are the directional cosines of the light ray

θ, θ' are the incident and refracted (reflected) angles

n, n' are the indices of refraction on the incident and refractive side of a surface

Translation:

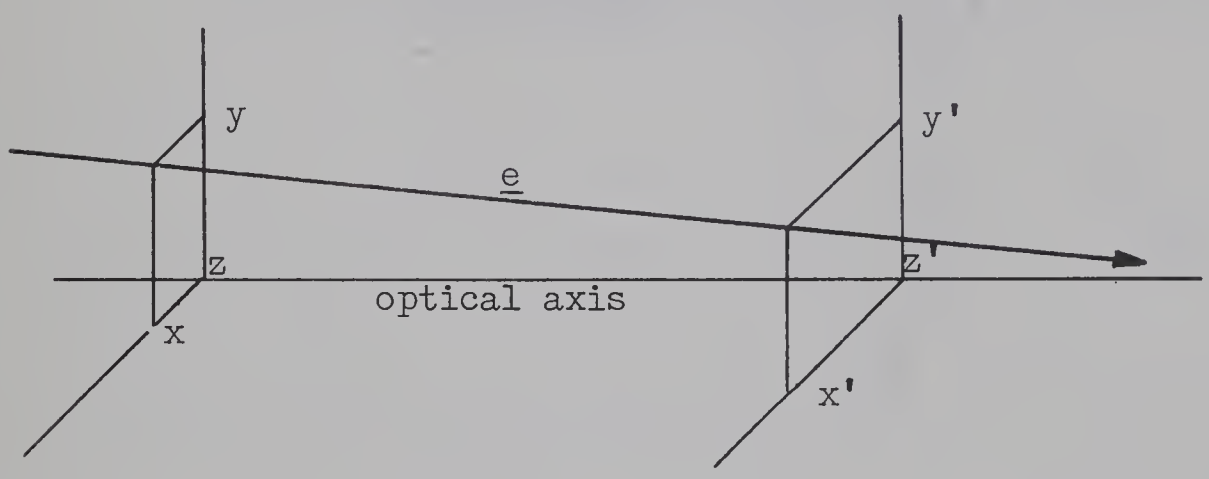

Fig. 30. Translation of light ray

$$\alpha' = \alpha; \quad \beta' = \beta, \quad \gamma' = \gamma$$

$$x' = x + \alpha\left[(x-x')^2 + (y-y')^2 + (z-z')^2\right]^{\frac{1}{2}}$$

$$y' = y + \beta\left[(x-x')^2 + (y-y')^2 + (z-z')^2\right]^{\frac{1}{2}}$$

$$z' = f(x',y')$$

If the surface to which the translation is being taken is relatively simple, as in the case of a sphere, the three equations can be solved in closed form. For more complicated surfaces, such as aspheric curves, it is often simpler to employ a re-iterative process within the program.

Refraction:

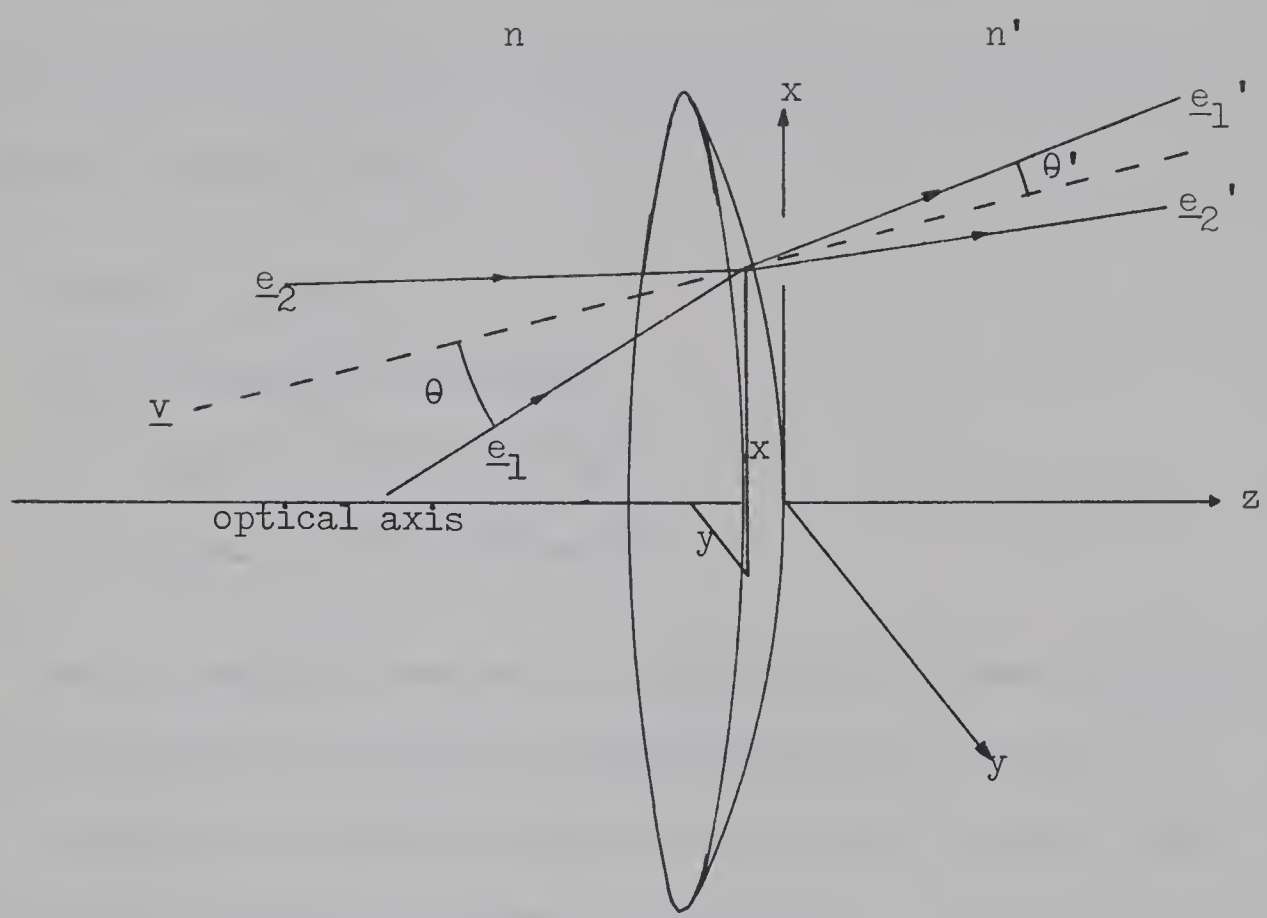

Fig. 31. Refraction of light ray

$\underline{v}$ = normal vector to the surface at the point of intersection

For refraction,

$$n'\underline{e}' = n\underline{e} + b\underline{v}$$

and taking the dot product of this equation with $\underline{v}$,

$$n(\underline{e}' \cdot \underline{v}) = n(\underline{e} \cdot \underline{v}) + b(\underline{v} \cdot \underline{v}),$$

but $\underline{e}' \cdot \underline{v} = \cos\theta'$, $\underline{e} \cdot \underline{v} = \cos\theta$, and $\underline{v} \cdot \underline{v} = 1$.

Therefore,

$$n'\cos\theta' = n\cos\theta + b \Rightarrow b = n'\cos\theta' - n\cos\theta$$

Using this substitution for b, and taking the cross product of the original equation with $\underline{v}$:

$$n'\sin\theta' = n\sin\theta$$
$$\Rightarrow n'^2(1-\cos^2\theta') = n^2\sin^2\theta$$
$$\Rightarrow n'\cos\theta' = (n'^2 - n^2\sin^2\theta)^{\frac{1}{2}}$$
$$\Rightarrow n'\cos\theta' = (n'^2 - n^2 + n^2\cos^2\theta)^{\frac{1}{2}}$$

As an example, consider the application of these formulae to the refraction of a light ray with directional cosines α, β, and γ, incident on an aspheric surface at a point (x,y,z). The equation of the aspheric surface is given by:

$$z = A_4(x^2+y^2)^2 + A_2(x^2+y^2),$$

and the equation of the normal vector at this point is given by:

$$z = \left[4A_4(x^3+xy^2) + 2A_2x\right] i + \left[4A_4(y^3+x^2y) + 2A_2y\right] j + k$$

The directional cosines are therefore:

$$\bar{\alpha} = \frac{4A_4(x^3+xy^2) + 2A_2x}{\left[4A_4(x^3+xy^2) + 2A_2x + 4A_4(y^3+x^2y) + 2A_2y + 1\right)^{\frac{1}{2}}]}$$

$$\bar{\beta} = \frac{4A_4(y^3+x^2y) + 2A_2y}{\left[4A_4(x^3+xy^2) + 2A_2x + 4A_4(y^3+x^2y) + 2A_2y + 1\right)^{\frac{1}{2}}]}$$

$$\gamma = (1 - \bar{\alpha}^2 - \bar{\beta}^2)^{\frac{1}{2}}$$

Taking the dot product of the incident light ray and the normal vector of the surface,

$$e\cdot v = \cos\theta = \alpha\cdot\bar{\alpha} + \beta\cdot\bar{\beta} + \gamma\cdot\gamma$$
$$= \alpha\cdot\bar{\alpha} + \beta\cdot\bar{\beta} + \left[(1-\alpha^2-\beta^2)(1-\bar{\alpha}^2-\bar{\beta}^2)\right]^{\frac{1}{2}}$$

We also have

$$n'\cos\theta' = (n'^2-n^2+n^2\cos^2\theta)^{\frac{1}{2}}$$
$$= (n'^2-n^2+n^2(\alpha\cdot\bar{\alpha} + \beta\cdot\beta + \left[(1-\alpha^2-\beta^2)(1-\bar{\alpha}^2-\bar{\beta}^2)\right]^{\frac{1}{2}})^2)^{\frac{1}{2}}$$

and from $n'\underline{e}' = n\underline{e} + b\underline{v}$,

$$\alpha' = \left[n\alpha + (n'\cos\theta' - n\cos\theta)\bar{\alpha}\right]/n'$$
$$= \frac{1}{n'}\left[n\alpha + \{(n'^2-n^2+n^2(\alpha\cdot\bar{\alpha} + \beta\cdot\beta + \left[(1-\alpha^2-\beta^2)(1-\bar{\alpha}^2-\bar{\beta}^2)\right]^{\frac{1}{2}})^2)^{\frac{1}{2}}\right.$$
$$\left.-n(\alpha\cdot\bar{\alpha} + \beta\cdot\bar{\beta} + \left[(1-\alpha^2-\beta^2)(1-\bar{\alpha}^2-\bar{\beta}^2)\right]^{\frac{1}{2}})\}\right]$$

$$\beta' = \left[n\beta + (n'\cos\theta' - n\cos\theta)\bar{\beta}\right]/n'$$
$$= \frac{1}{n'}\left[n\beta + \{(n'^2-n^2+n^2(\alpha\cdot\bar{\alpha} + \beta\cdot\beta + \left[(1-\alpha^2-\beta^2)(1-\bar{\alpha}^2-\bar{\beta}^2)\right]^{\frac{1}{2}})^2)^{\frac{1}{2}}\right.$$
$$\left.-n(\alpha\cdot\bar{\alpha} + \beta\cdot\bar{\beta} + \left[(1-\alpha^2-\beta^2)(1-\bar{\alpha}^2-\bar{\beta}^2)\right]^{\frac{1}{2}})\}\right]$$

Reflection:

The equations for reflection are identical to those of refraction with the substitutions n' = -n and n = 1.

Following are two of the programs used in the development of the correcting systems described in this work. The first is the interactive program used in the development of the f/8 Cassegrain corrector, and the second is the spot diagram generating program for the prime focus design.

Following the two programs is an example of numerical computer output generated by the programs.

```
C        THIS PROGRAM TRACES RAYS THROUGH AN F/8 CASSEGRAIN SYSTEM.  IN
C        ADDITION TO THE PARABOLIC PRIMARY AND HYBERBOLIC SECONDARY THIS
C        SYSTEM CONTAINS A PHOTOGRAPHIC CORRECTOR CONSISTING OF TWO
C        ASPHERIC PLATES AND A FIELD FLATTENER IN THE CONVERGENT BEAM.
C        THIS PROGRAM IS RUN FROM TERMINAL AND ALLOWS THE INPUT OF RAYS
C        ORIGINATING FROM ANY POINT AND ANY ANGLE.
C
      DOUBLE PRECISION DCOS,DATAN,DARCOS,DFLOAT,DSQRT,DSIN
      DOUBLE PRECISION X1,Y1,Z1,X2,Y2,Z2,ALPHA,BETA,GAMMA,ALPHAP,BETAP
      DOUBLE PRECISION GAMMAP,DIST,CTHETA,DZBYDX,DZBYDY,RAD,G
      DOUBLE PRECISION THETAX,THETAY,THETAZ,XTHETA,YTHETA,RADIUS,D,E,F
      DOUBLE PRECISION POWER,POW1,POW2,POW3,PTHETA
      DOUBLE PRECISION THICK,THICK1,THICK2,THICK3
      DOUBLE PRECISION DEX,DEX1,DEX2,DEX3,POS,POS1,POS2,POS3
      DOUBLE PRECISION FOCUS
      DOUBLE PRECISION A1,A2,A3,A
C
C        THE NEXT SECTION INITIALIZES THE PARAMETERS OF THE SYSTEM THAT
C        IS TO BE TESTED.  THE PROGRAM WILL PROMPT THE OPERATOR FOR THE
C        NECESSARY DATA.
C
C        START OF DESIGN INITIALIZATION MODULE
C
      WRITE(6,50)
50    FORMAT('1','TYPE IN THE POSITICNS OF THE  ASPHERIC CORRECTORS')
      WRITE(6,60)
60    FORMAT(' ','AND THE POSITION OF THE FIELD FLATTENER')
      READ(5,46)POS1,POS2,POS3
46    FORMAT(3F8.4)
      WRITE(6,51)
51    FORMAT('0','TYPE IN THE POWERS OF THE TWO ASPHERIC CORRECTORS')
      WRITE(6,61)
61    FORMAT(' ','AND THE RADIUS OF CURVATURE OF THE FIELD FLATTENER')
      READ(5,47)POW1,POW2,POW3
47    FORMAT(3F16.12)
      WRITE(6,70)
```

```
70    FORMAT('0','TYPE IN COEFFICIENTS OF SECOND ORDER CURVES')
      READ(5,47)A1,A2
      WRITE(6,52)
52    FORMAT('0','TYPE IN THE INDEX OF REFRACTION FOR EACH ELEMENT')
      READ(5,48)DEX1,DEX2,DEX3
48    FORMAT(3F10.6)
      WRITE(6,53)
53    FORMAT('0','TYPE IN THE THICKNESSES OF THE CORRECTORS')
      READ(5,49)THICK1,THICK2,THICK3
49    FORMAT(3F8.5)
      Z3=60.0000000000000
      RAD=57.295779513082320
C
C        END OF DESIGN INITIALIZATION MODULE
C
C        THE NEXT SECTION ESTABLISHES THE ANGLE THAT THE RAYS ARE TO
C        ENTER THE SYSTEM FOR THIS RUN AND THE POSITION OF THE FOCAL
C        PLANE.  THE NUMBER OF RAYS THAT ARE TO BE TESTED AT THIS ANGLE
C        IS ALSO DETERMINED.  THE PROGAM WILL PROMPT THE OPERATOR FOR
C        THE REQUIRED INFORMATION.
C
C        START OF OPTIMIZATION TEST DATA INPUT MODULE
C
      DO 999 J1=1,20
      WRITE(6,54)
54    FORMAT('1','ANGLE OF RAYS? (DOUBLE PREC)')
      READ(5,55)XTHETA
55    FORMAT(F20.16)
      XTHETA=90.0000000000000-XTHETA
      YTHETA=90.0000000000000D0
      E=90-XTHETA
      WRITE(6,56)
56    FORMAT('0','HOW MANY RAYS DO YOU WANT TO ENTER AT THIS ANGLE?')
      READ(5,57)KILL
57    FORMAT(I3)
      WRITE(6,58)
```

```
58    FORMAT('0','HOW FAR BEHIND THE MIFROR IS THE FOCAL PLANE?')
      READ(5,59)FOCUS
59    FORMAT(F20.16)
      WRITE(6,29)E
29    FORMAT('1','THE FOLLOWING LIGHT RAYS ARE AT AN ANGLE OF ',F7.3,'DE
     1GREES TO THE Z AXIS')
      WRITE(6,30)
30    FORMAT('-','                                                  X                Y
     1       Z         ANGLE TO X  ANGLE TO Y  ANGLE TO Z')
      WRITE(6,31)
31    FORMAT('+','                                                 _____            _____
     1 _____  __________  __________  __________')
      DO 998 J2=1,KILL
C
C        THE ORIGIN OF EACH RAY (X AND Y COORDINATE) TO BE TESTED MUST
C        BE ENTERED.  THE PROGRAM DOES NOT PROMPT FOR THIS ENTRY.
C
      READ(5,45)X1,Y1
45    FORMAT(2F16.12)
      Z1=Z3
      THETAX=XTHETA
      THETAY=YTHETA
C
C        END OF OPTIMIZATION TEST DATA INPUT MODULE
C
      ALPHA=DCOS(THETAX/RAD)
      BETA=DCOS(THETAY/RAD)
      GAMMA=DSQRT(1-ALPHA*ALPHA-BETA*BETA)
      THETAX=DARCOS(ALPHA)*RAD
      THETAY=DARCOS(BETA)*RAD
      THETAZ=DARCOS(GAMMA)*RAD
      WRITE(6,32)X1,Y1,Z1,THETAX,THETAY,THETAZ
32    FORMAT('0','LIGHT RAY ORIGIN POINT          ',F11.6,'  ',F11.6,'  ',
     1F11.6,'  ',F8.4,'     ',F8.4,'     ',F8.4,' ')
603   FORMAT(' ','INTERSECTION WITH CORRECTOR   ',F11.6,'  ',F11.6,'  ',
     1F11.6,'  ',F8.4,'     ',F8.4,'     ',F8.4,' ')
```

```
604   FORMAT(' ','BACK OF CORRECTOR              ',F11.6,'  ',F11.6,'  ',
     1F11.6,'  ',F8.4,'     ',F8.4,'     ',F8.4,' ')
605   FORMAT(' ','INTERSECTION WITH FLATTENER    ',F11.6,'  ',F11.6,'  ',
     1F11.6,'  ',F8.4,'     ',F8.4,'     ',F8.4,' ')
606   FORMAT(' ','BACK OF FLATTENER              ',F11.6,'  ',F11.6,'  ',
     1F11.6,'  ',F8.4,'     ',F8.4,'     ',F8.4,' ')
      DIST=Z1
C
C        THE INTERSECTION POINT WITH THE PRIMARY MIRROR IS DETERMINED.
C
      DO 33 I1=1,5
      X2=X1+ALPHA*DIST
      Y2=Y1+BETA*DIST
      Z2=(X2*X2+Y2*Y2)/240
      DIST=(Z1-Z2)/GAMMA
33    CONTINUE
      X1=X2
      Y1=Y2
      Z1=Z2
C
C        A CHECK IS MADE TO SEE IF THE LIGHT RAY WILL BE BLOCKED BY THE
C        SECONDARY MIRROR.
C
      E=X2*X2+Y2*Y2
      IF(E.LT.12.25) GO TO 995
C
C        ANOTHER CHECK IS MADE TO SEE IF THE LIGHT RAY MISSED THE
C        PRIMARY MIRROR.
C
      E=X1*X1+Y1*Y1
      IF(E.GT.100.01) GO TO 900
C
C        THE COMPONENTS OF THE MIRROR'S NORMAL VECTOR AT THE POINT OF
C        INTERSECTION ARE DETERMINED AND THE ANGLES AT WHICH THE RAY IS
C        REFLECTED ARE FOUND.
C
```

```
      DZBYDX=(X1/120)/DSQRT((X1/120)**2+(Y1/120)**2+1)
      DZBYDY=(Y1/120)/DSQRT((X1/120)**2+(Y1/120)**2+1)
      ALPHAP=-DZBYDX
      BETAP=-DZBYDY
      GAMMAP=DSQRT(1-ALPHAP*ALPHAP-BETAP*BETAP)
      CTHETA=-ALPHAP*ALPHA-BETAP*BETA+DSQRT((1-ALPHA*ALPHA-BETA*BETA)*(1
     1-ALPHAP*ALPHAP-BETAP*BETAP))
      ALPHA=ALPHA+2*ALPHAP*CTHETA
      BETA=BETA+2*BETAP*CTHETA
      GAMMA=DSQRT(1-ALPHA*ALPHA-BETA*BETA)
      THETAX=DARCOS(ALPHA)*RAD
      THETAY=DARCOS(BETA)*RAD
      THETAZ=DARCOS(GAMMA)*RAD
      WRITE(6,35) X1,Y1,Z1,THETAX,THETAY,THETAZ
35    FORMAT(' ','MIRROR INTERSECTION POINT     ',F11.6,'  ',F11.6,'  ',
     1F11.6,'  ',F8.4,'     ',F8.4,'     ',F8.4,' ')
C
C        THE POINT OF INTERSECTION WITH THE SECONDARY MIRROR IS FOUND.
C
C        E=ECCENTRICITY, F=SEMI MAJOR AXIS, D=SEMI MINOR AXIS
C
      DIST=40.22727272727272
      F=36.250000000000000-19.77272727272727
      E=36.250000000000000/F
      E=E*E-1.000000000000000
      D=DSQRT(36.250000000000000*36.250000000000000-F*F)
      DO 36 I1=1,7
      X2=X1+ALPHA*DIST
      Y2=Y1+BETA*DIST
      Z2=DSQRT((D*D+X2*X2+Y2*Y2)/E)+40.22727272727272-DSQRT(D*D/E)
      DIST=(Z2-Z1)/GAMMA
36    CONTINUE
      X1=X2
      Y1=Y2
      Z1=Z2
C
```

```
C        THE COMPONENTS OF THE NORMAL TO THE HYPERBOLOID AND THE ANGLES
C        OF THE REFLECTED RAY ARE DETERMINED
C
      ALPHAP=(X1/DSQRT(E   *(D*D+X1*X1+Y1*Y1)))/DSQRT((X1*X1+Y1*Y1)/(E
     1 *(D*D+X1*X1+Y1*Y1))+1)
      BETAP=(Y1/DSQRT(E   *(D*D+X1*X1+Y1*Y1)))/DSQRT((X1*X1+Y1*Y1)/(E
     1*(D*D+X1*X1+Y1*Y1))+1)
      GAMMAP=DSQRT(1-ALPHAP*ALPHAP-BETAP*BETAP)
      CTHETA=-ALPHAP*ALPHA-BETAP*BETA+DSQRT((1-ALPHA*ALPHA-BETA*BETA)*(1
     1-ALPHAP*ALPHAP-BETAP*BETAP))
      ALPHA=ALPHA+2*ALPHAP*CTHETA
      BETA=BETA+2*BETAP*CTHETA
      GAMMA=DSQRT(1-ALPHA*ALPHA-BETA*BETA)
      THETAX=DARCOS(ALPHA)*RAD
      THETAY=DARCOS(BETA)*RAD
      THETAZ=DARCOS(GAMMA)*RAD
      WRITE(6,37)X1,Y1,Z1,THETAX,THETAY,THETAZ
37    FORMAT(' ','SECONDARY INTERSECTION POINT  ',F11.6,'  ',F11.6,'  ',
     1F11.6,'  ',F8.4,'     ',F8.4,'     ',F8.4,' ')
C
C        THE POINT OF INTERSECTION WITH THE FIRST SURFACE OF THE FIRST
C        ASPHERIC PLATE IS FOUND AND THE REFRACTION OF THE LIGHT RAY
C        AT THIS SUPFACE DETERMINED.
C
      POS=POS1
      A=A1
      POWER=POW1
      DEX=DEX1
      THICK=THICK1
      DO 600 I1=1,5
      X2=X1+ALPHA*DIST
      Y2=Y1+BETA*DIST
      Z2=POS+POWER*(Y2*Y2+X2*X2)**2/(4*(DEX-1))-A*(X2*X2+Y2*Y2)
      DIST=(Z1-Z2)/GAMMA
600   CONTINUE
      X1=X2
```

```
      Y1=Y2
      Z1=Z2
      ALPHAP=(POWER*(X1**3+X1*Y1*Y1)-2*A*(DEX-1)*X1)/
     1DSQRT((POWER*(X1**3+X1*Y1*Y1)-2*A*(DEX-1)*X1)**2
     1+(POWER*(Y1**3+Y1*X1*X1)-2*A*(DEX-1)*Y1)**2
     1+(DEX-1)**2)
      BETAP=(POWER*(Y1**3+Y1*X1*X1)-2*A*(DEX-1)*Y1)/
     1DSQRT((POWER*(X1**3+X1*Y1*Y1)-2*A*(DEX-1)*X1)**2
     1+(POWER*(Y1**3+Y1*X1*X1)-2*A*(DEX-1)*Y1)**2
     1+(DEX-1)**2)
      CTHETA=ALPHA*ALPHAP+BETA*BETAP+DSQRT((1-ALPHA**2-BETA**2)*
     1(1-ALPHAP**2-BETAP**2))
      PTHETA=DSQRT(DEX**2-1+CTHETA**2)
      ALPHA=(ALPHA+ALPHAP*(PTHETA-CTHETA))/DEX
      BETA=(BETA+BETAP*(PTHETA-CTHETA))/DEX
      GAMMA=DSQRT(1-ALPHA**2-BETA**2)
      THETAX=DARCOS(ALPHA)*RAD
      THETAY=DARCOS(BETA)*RAD
      THETAZ=DARCOS(GAMMA)*RAD
      WRITE(6,603)X1,Y1,Z1,THETAX,THETAY,THETAZ
C         INTERSECTION WITH THE BACK OF THE CORRECTOR
C
C        THE POINT OF INTERSECTION ON THE BACK SURFACE OF THE FIRST
C        ASPHERIC PLATE IS FOUND, AND THE ANGLE OF THE REFRACTED RAY
C        DETERMINED.
C
      DIST=(Z1-POS+THICK)/GAMMA
      X1=X1+ALPHA*DIST
      Y1=Y1+BETA*DIST
      Z1=Z1-GAMMA*DIST
      ALPHA=ALPHA*DEX
      BETA=BETA*DEX
      GAMMA=DSQRT(1-ALPHA**2-BETA**2)
      THETAX=THETAX
      THETAX=DARCOS(ALPHA)*RAD
      THETAY=DARCOS(BETA)*RAD
```

```
      THETAZ=DARCOS(GAMMA)*RAD
      WRITE(6,604)X1,Y1,Z1,THETAX,THETAY,THETAZ
C
CCCC     THE POINT OF INTERSECTION WITH THE FIRST SURFACE OF THE SECOND
C        ASPHERIC PLATE IS FOUND AND THE REFRACTION OF THE LIGHT RAY
C        AT THIS SURFACE DETERMINED.
C
      POS=POS2
      A=A2
      POWER=POW2
      DEX=DEX2
      THICK =THICK2
      DIST=(Z1-POS)/GAMMA
      DO 601 I1=1,5
      X2=X1+ALPHA*DIST
      Y2=Y1+BETA*DIST
      Z2=POS+POWER*(Y2*Y2+X2*X2)**2/(4*(DEX-1))-A*(X2*X2+Y2*Y2)
      DIST=(Z1-Z2)/GAMMA
  601  CONTINUE
       X1=X2
       Y1=Y2
       Z1=Z2
       ALPHAP=(POWER*(X1**3+X1*Y1*Y1)-2*A*(DEX-1)*X1)/
     1DSQRT((POWER*(X1**3+X1*Y1*Y1)-2*A*(DEX-1)*X1)**2
     1+(POWER*(Y1**3+Y1*X1*X1)-2*A*(DEX-1)*Y1)**2
     1+(DEX-1)**2)
       BETAP=(POWER*(Y1**3+Y1*X1*X1)-2*A*(DEX-1)*Y1)/
     1DSQRT((POWER*(X1**3+X1*Y1*Y1)-2*A*(DEX-1)*X1)**2
     1+(POWER*(Y1**3+Y1*X1*X1)-2*A*(DEX-1)*Y1)**2
     1+(DEX-1)**2)
       CTHETA=ALPHA*ALPHAP+BETA*BETAP+DSQRT((1-ALPHA**2-BETA**2)*
     1(1-ALPHAP**2-BETAP**2))
       PTHETA=DSQRT(DEX**2-1+CTHETA**2)
       ALPHA=(ALPHA+ALPHAP*(PTHETA-CTHETA))/DEX
       BETA=(BETA+BETAP*(PTHETA-CTHETA))/DEX
       GAMMA=DSQRT(1-ALPHA**2-BETA**2)
```

```
      THETAX=DARCOS(ALPHA)*RAD
      THETAY=DARCOS(BETA)*RAD
      THETAZ=DARCOS(GAMMA)*PAD
      WRITE(6,603)X1,Y1,Z1,THETAX,THETAY,THETAZ
C
CC       THE POINT OF INTERSECTION ON THE BACK SURFACE OF THE SECOND
C        ASPHERIC PLATE IS FOUND, AND THE ANGLE OF THE REFRACTED RAY
C        DETERMINED.
C
      DIST=(Z1-POS+THICK)/GAMMA
      X1=X1+ALPHA*DIST
      Y1=Y1+BETA*DIST
      Z1=Z1-GAMMA*DIST
      ALPHA=ALPHA*DEX
      BETA=BETA*DEX
      GAMMA=DSQRT(1-ALPHA**2-BETA**2)
      THETAX=DARCOS(ALPHA)*RAD
      THETAY=DARCOS(BETA)*RAD
      THETAZ=DARCOS(GAMMA)*RAD
      WRITE(6,604)X1,Y1,Z1,THETAX,THETAY,THETAZ
C
CC       THE POINT OF INTERSECTION WITH THE FIELD FLATTENER AND THE ANGLE
C        OF THE REFRACTED RAY ARE NOW DETERMINED.
C
C          INTERSECTION WITH THE FIELD FLATTENER
      POS=POS3
C
CC       THE NEXT CARD HAS BEEN TEMPORARILY INSERTED FOR FINAL OPTIM-
C        IMIZATION AND OVERIDES THE ASSIGNED POSITION OF THE FIELD
C        FLATTENER.
C
      POS=-FOCUS+.21
      POWER=POW3
      DEX=DEX3
      THICK =THICK3
      DIST=(Z1-POS)/GAMMA
```

```
      DO 602 I1=1,5
      X2=X1+ALPHA*DIST
      Y2=Y1+BETA*DIST
      Z2=POS+(POWER-DSQRT(POWER**2-X2*X2-Y2*Y2))
      DIST=(Z1-Z2)/GAMMA
602   CONTINUE
      X1=X2
      Y1=Y2
      Z1=Z2
      ALPHAP=(X1/DSQRT(POWER**2-X1**2-Y1**2))
     1/DSQRT((X1**2+Y1**2)/(POWER**2-X1**2-Y1**2)+1)
      BETAP=(Y1/DSQRT(POWER**2-X1**2-Y1**2))
     1/DSQRT((X1**2+Y1**2)/(POWER**2-X1**2-Y1**2)+1)
      CTHETA=ALPHA*ALPHAP+BETA*BETAP+DSQRT((1-ALPHA**2-BETA**2)*
     1(1-ALPHAP**2-BETAP**2))
      PTHETA=DSQRT(DEX**2-1+CTHETA**2)
      ALPHA=(ALPHA+ALPHAP*(PTHETA-CTHETA))/DEX
      BETA=(BETA+BETAP*(PTHETA-CTHETA))/DEX
      GAMMA=DSQRT(1-ALPHA**2-BETA**2)
      THETAX=DARCOS(ALPHA)*RAD
      THETAY=DARCOS(BETA)*RAD
      THETAZ=DARCOS(GAMMA)*RAD
      WRITE(6,605)X1,Y1,Z1,THETAX,THETAY,THETAZ
C
CC       THE INTERSECTION WITH THE BACK OF THE FIELD FLATTENER AND THE
C        ANGLE OF THE REFRACTED RAY ARE FOUND.
C
      DIST=(Z1-POS+THICK)/GAMMA
      X1=X1+ALPHA*DIST
      Y1=Y1+BETA*DIST
      Z1=Z1-GAMMA*DIST
      ALPHA=ALPHA*DEX
      BETA=BETA*DEX
      GAMMA=DSQRT(1-ALPHA**2-BETA**2)
      THETAX=DARCOS(ALPHA)*RAD
      THETAY=DARCOS(BETA)*RAD
```

```
      THETAZ=DARCOS(GAMMA)*RAD
      WRITE(6,606)X1,Y1,Z1,THETAX,THETAY,THETAZ
C
C        THE POINT OF INTERSECTION WITH THE FOCAL PLANE IS DETERMINED.
C
      DIST=(Z1+FOCUS)/GAMMA
      X1=X1+ALPHA*DIST
      Y1=Y1+BETA*DIST
      Z1=Z1-GAMMA*DIST
      WRITE(6,34)  X1,Y1,Z1
34    FORMAT(' ','FOCAL PLANE INTERSECTION      ',F11.6,'  ',F11.6,'  ',
     1F11.6,' ')
      GO TO 996
900   WRITE(6,901)
901   FORMAT(' ','                                        ********** THIS LIG
     1HT RAY DID NOT INTERSECT THE MIRROR **********')
996   CONTINUE
      GO TO 997
995   WRITE(6,38)
38    FORMAT(' ','                                          ********** THIS LIGHT
     1 RAY WAS INTERCEPTED BY THE SECONDARY **********')
997   CONTINUE
998   CONTINUE
999   CONTINUE
500   CONTINUE
      STOP
      END
```

```
C         THIS PROGRAM TRACES RAYS THROUGH AN F/2.65 BAKER REFLECTOR-
CCC       CORRECTOR AND DISPLAYS THE RESULTS BOTH NUMERICALLY AND AS SPOT
C         DIAGRAMS GENERATED BY A CALCOMP PLOTTER.  THE PROGRAM TESTS
C         THE SYSTEM FOR RAYS ENTERING AT SEVERAL DIFFERENT ANGLES.  EACH
C         ANGLE GIVES THE IMAGES CORRESPONDING TO THOSE FOUND AT DIFFERENT
C         POSITIONS ON THE PHOTOGRAPHIC FIELD.  THE CORRECTOR-REFLECTOR
C         CONSISTS OF A FULL APERTURE ASPHERIC PLATE, A PARABOLIC MIRROR,
C         AND AN ACHROMATIZED DOUBLET IN THE CONVERGENT BEAM.
C
      DOUBLE PRECISION DCOS,DATAN,DARCOS,DFLOAT,DSQRT,DSIN
      DOUBLE PRECISION X1,Y1,Z1,X2,Y2,Z2,ALPHA,BETA,GAMMA,ALPHAP,BETAP
      DOUBLE PRECISION GAMMAP,DIST,CTHETA,DZBYDX,DZBYDY,RAD
      DOUBLE PRECISION THETAX,THETAY,THETAZ,XTHETA,YTHETA,RADIUS,D,E,F
      DOUBLE PRECISION POWER,POW1,POW2,POW3,PTHETA,POW4
      DOUBLE PRECISION THICK,THICK1,THICK2,THICK3
      DOUBLE PRECISION DEX,DEX1,DEX2,DEX3,POS,POS1,POS2,POS3
      DOUBLE PRECISION FOCUS
      DOUBLE PRECISION A1,A2,A3,A
      DOUBLE PRECISION TINY
      DIMENSION D1(160)
      DIMENSION D3(160)
      DIMENSION D4(160)
C
C         THE FIRST DATA CARD CONTAINS THE AXIAL POSITIONS OF THE ASPHERIC
C         CORRECTING SURFACE, THE FRONT AND REAR SURFACES OF THE FIRST
C         LENS, AND THE REAR SURFACE OF THE SECOND LENS.
C
      READ(5,46)POS1,POS2,POS3,POS4
46    FORMAT(4F8.4)
C
C         THE SECOND DATA CARD CONTAINS THE COEFFICIENT OF THE FOURTH
C         ORDER CURVE ON THE ASPHERIC ELEMENT AND THE RADII OF CURVATURE
C         OF THE THREE DIFFERENT LENS SURFACES.
C
      READ(5,47)POW1,POW2,POW3,POW4
47    FORMAT(4F16.12)
```

```
C
C        THE THIRD DATA CARD CONTAINS THE COEFFICIENT OF THE SECOND
C        ORDER CURVE ON THE ASPHERIC PLATE.
C
      READ(5,47)A1
C
C        THE FOURTH DATA CARD CONTAINS THE INDEX OF REFRACTION FOR EACH
C        OF THE THREE CORRECTING ELEMENTS.
C
      READ(5,48)DEX1,DEX2,DEX3
48    FORMAT(3F10.6)
C
C        THE FIFTH DATA CARD CONTAINS THE AXIAL THICKNESS OF EACH OF THE
C        THREE CORRECTING ELEMENTS.
C
      READ(5,49)THICK1,THICK2,THICK3
49    FORMAT(3F8.5)
C
C        THE SIXTH DATA CARD CONTAINS THE Z COMPONENT OF THE FOCAL PLANE.
C
      READ(5,59)FOCUS
59    FORMAT(F20.16)
      CALL PLOTS
      CALL PLOT(0.0,10.0,-3)
      AXIS=14
      PAD=57.295779513082320
C
C        THE NEXT SECTION GENERATES A SERIES OF LIGHT RAYS SPACED ALONG
C        CONCENTRIC CIRCLES AROUND THE OPTICAL AXIS.  THIS IS DONE IN
C        A WAY THAT CAUSES EACH OF THE GENERATED RAYS TO REPRESENT AN
C        EQUAL AREA AND HENCE AN EQUAL AMOUNT OF INCOMING LIGHT.
C
C        START OF CIRCULAR GRID INPUT MODULE.
C
      Z3=50.000000000000
      XTHETA=90.500000000000
```

```
      YTHETA=90.000000000000000
      DO 999 J1=1,7
      TINY=100
      NM=1
      XTHETA=XTHETA-.500000000000000
      E=90-XTHETA
      WRITE(6,29)E
29    FORMAT('1','THE FOLLOWING LIGHT RAYS ARE AT AN ANGLE OF ',F7.3,'DE
     1GREES TO THE Z AXIS')
      WRITE(6,30)
30    FORMAT('-','                                                  X
     1       Z        ANGLE TO X  ANGLE TO Y  ANGLE TO Z')
      WRITE(6,31)
31    FORMAT('+','                                                 _____
     1 _____    ----------  ----------  ----------')
      DO 998 J2=1,5
      READ(5,45)RADIUS,NUM
45    FORMAT(F4.1,1X,I2)
      NUMBER=NUM+1
      DO 997 J3=1,NUMBER
      D=DFLOAT(NUM)
      E=DFLOAT(J3)-1.000000000000000
      F=180/D
      E=E*F
      IF(E.GT.180.1) GO TO 996
      X1=RADIUS*DCOS(E/RAD)
      Y1=RADIUS*DSIN(E/RAD)
      Z1=Z3
      THETAX=XTHETA
      THETAY=YTHETA
C
CC       END OF CIRCULAR GRID INPUT MODULE.
C
      ALPHA=DCOS(THETAX/RAD)
      BETA=DCOS(THETAY/RAD)
      GAMMA=DSQRT(1-ALPHA*ALPHA-BETA*BETA)
```

```
      THETAX=DARCOS(ALPHA)*RAD
      THETAY=DARCOS(BETA)*RAD
      THETAZ=DARCOS(GAMMA)*RAD
      WRITE(6,32)X1,Y1,Z1,THETAX,THETAY,THETAZ
32    FORMAT('0','LIGHT RAY ORIGIN POINT        ',F11.6,'  ',F11.6,'  ',
     1F11.6,'  ',F8.4,'     ',F8.4,'     ',F8.4,' ')
603   FORMAT(' ','INTERSECTION WITH CORRECTOR   ',F11.6,'  ',F11.6,'  ',
     1F11.6,'  ',F8.4,'     ',F8.4,'     ',F8.4,' ')
604   FORMAT(' ','BACK OF CORRECTOR             ',F11.6,'  ',F11.6,'  ',
     1F11.6,'  ',F8.4,'     ',F8.4,'     ',F8.4,' ')
C
C        THE POINT OF INTERSECTION WITH THE FIRST SURFACE (THE BACK)  OF
C        THE FULL APERTURE ASPHERIC PLATE AND THE REFRACTION AT THIS
C        SURFACE ARE DETERMINED.
C
      POS=POS1
      A=A1
      POWER=POW1
      DEX=DEX1
      THICK=THICK1
      Z2=POS+THICK
      DIST=(Z1-Z2)/GAMMA
      X1=X1+ALPHA*DIST
      Y1=Y1+BETA*DIST
      Z1=Z2
      ALPHA=ALPHA/DEX
      BETA=BETA/DEX
      GAMMA=DSQRT(1-ALPHA**2-BETA**2)
      THETAX=THETAX
      THETAX=DARCOS(ALPHA)*RAD
      THETAY=DARCOS(BETA)*RAD
      THETAZ=DARCOS(GAMMA)*RAD
      WRITE(6,604)X1,Y1,Z1,THETAX,THETAY,THETAZ
C
C        THE POINT OF INTERSECTION WITH THE FIGURED SURFACE OF THE FULL
C        APERTURE PLATE AND THE REFRACTION AT THIS SURFACE ARE DETERMINED.
```

```
C
      DO 600 I1=1,5
      X2=X1+ALPHA*DIST
      Y2=Y1+BETA*DIST
      Z2=POS-POWER*((X2*X2+Y2*Y2)**2)+A*(X2*X2+Y2*Y2)
      DIST=(Z2-Z1)/GAMMA
600   CONTINUE
      X1=X2
      Y1=Y2
      Z1=Z2
      ALPHAP=-(POWER*(X2**3+X2*Y2*Y2)*4-2*A*X2)/
     1DSQRT((4*POWER*(X2**3+Y2*Y2*X2)-2*A*X2)**2
     1+(4*POWER*(Y2**3+Y2*X2*X2)-2*A*Y2)**2+1)
      BETAP=-(POWER*(Y2**3+Y2*X2*X2)*4-2*A*Y2)/
     1DSQRT((4*POWER*(X2**3+Y2*Y2*X2)-2*A*X2)**2
     1+(4*POWER*(Y2**3+Y2*X2*X2)-2*A*Y2)**2+1)
      CTHETA=ALPHA*ALPHAP+BETA*BETAP+DSQRT((1-ALPHA**2-BETA**2)*
     1(1-ALPHAP**2-BETAP**2))
      PTHETA=DSQRT(1-DEX**2+(DEX**2)*(CTHETA**2))
      ALPHA=DEX*ALPHA+ALPHAP*(PTHETA-DEX*CTHETA)
      BETA=DEX*BETA+BETAP*(PTHETA-DEX*CTHETA)
      GAMMA=DSQRT(1-ALPHA**2-BETA**2)
      THETAX=DARCOS(ALPHA)*RAD
      THETAY=DARCOS(BETA)*RAD
      THETAZ=DARCOS(GAMMA)*RAD
      WRITE(6,603)X1,Y1,Z1,THETAX,THETAY,THETAZ
C
C        THE POINT OF INTERSECTION WITH THE PRIMARY MIRROR AND THE
C        ANGLE OF THE REFLECTED RAY ARE FOUND.
C
      DIST=Z1
      DO 33 I1=1,5
      X2=X1+ALPHA*DIST
      Y2=Y1+BETA*DIST
      Z2=(X2*X2+Y2*Y2)/240
      DIST=(Z1-Z2)/GAMMA
```

```
33     CONTINUE
       X1=X2
       Y1=Y2
       Z1=Z2
C
C          A CHECK IS MADE TO SEE IF THE LIGHT RAY MISSED THE PRIMARY.
C
       E=X1*X1+Y1*Y1
       IF(E.GT.100.01) GO TO 900
       DZBYDX=(X1/120)/DSQRT((X1/120)**2+(Y1/120)**2+1)
       DZBYDY=(Y1/120)/DSQRT((X1/120)**2+(Y1/120)**2+1)
       ALPHAP=-DZBYDX
       BETAP=-DZBYDY
       GAMMAP=DSQRT(1-ALPHAP*ALPHAP-BETAP*BETAP)
       CTHETA=-ALPHAP*ALPHA-BETAP*BETA+DSQRT((1-ALPHA*ALPHA-BETA*BETA)*(1
      1-ALPHAP*ALPHAP-BETAP*BETAP))
       ALPHA=ALPHA+2*ALPHAP*CTHETA
       BETA=BETA+2*BETAP*CTHETA
       GAMMA=DSQRT(1-ALPHA*ALPHA-BETA*BETA)
       THETAX=DARCOS(ALPHA)*RAD
       THETAY=DARCOS(BETA)*RAD
       THETAZ=DARCOS(GAMMA)*RAD
       WRITE(6,35) X1,Y1,Z1,THETAX,THETAY,THETAZ
35     FORMAT(' ','MIRROR INTERSECTION POINT     ',F11.6,'   ',F11.6,'   ',
      1F11.6,'   ',F8.4,'     ',F8.4,'     ',F8.4,' ')
C
C          THE POINT OF INTERSECTION WITH THE FIRST SURFACE OF THE FLINT
C          COMPONENT AND THE REFRACTION AT THIS SUPFACE ARE DETERMINED.
C
       POS=POS2
       POWER=POW2
       DEX=DEX2
       THICK =THICK2
       DIST=(POS-Z1)/GAMMA
       DO 601 I1=1,5
       X2=X1+ALPHA*DIST
```

```
      Y2=Y1+BETA*DIST
      Z2=POS2+POW2-DSQRT(POW2**2-X2*X2-Y2*Y2)
      DIST=(Z2-Z1)/GAMMA
601   CONTINUE
      X1=X2
      Y1=Y2
      Z1=Z2
      CTHETA=DSQRT((1-(X2/POW2)**2-(Y2/POW2)**2)
     1*(1-ALPHA*ALPHA-BETA*BETA))
     1-(X2*ALPHA/POW2 +Y2*BETA/POW2)
      PTHETA=DSQRT(DEX2**2-1+CTHETA**2)
      ALPHA=(ALPHA-(PTHETA-CTHETA)*X2/POW2)/DEX2
      BETA =(BETA -(PTHETA-CTHETA)*Y2/POW2)/DEX2
      GAMMA=DSQRT(1-ALPHA**2-BETA**2)
      THETAX=DARCOS(ALPHA)*RAD
      THETAY=DARCOS(BETA)*RAD
      THETAZ=DARCOS(GAMMA)*RAD
      WRITE(6,603)X1,Y1,Z1,THETAX,THETAY,THETAZ
C
C        INTERSECTION WITH THE REAR SURFACE OF THE FLINT ELEMENT AND THE
C        REFRACTION THAT OCCURS AT THIS SURFACE ARE DETERMINED.
C
      POS=POS3
      POWER=POW3
      DEX=DEX3
      THICK =THICK3
      DIST=(POS-Z1)/GAMMA
      DO 602 I1=1,5
      X2=X1+ALPHA*DIST
      Y2=Y1+BETA*DIST
      Z2=POS3+POW3-DSQRT(POW3**2-X2*X2-Y2*Y2)
      DIST=(Z2-Z1)/GAMMA
602   CONTINUE
      X1=X2
      Y1=Y2
      Z1=Z2
```

```
      CTHETA=DSQRT((1-(X2/POW3)**2-(Y2/POW3)**2)
     1*(1-ALPHA*ALPHA-BETA*BETA))
     1-(X2*ALPHA/POW3 +Y2*BETA/POW3)
      CTHETA=DSQRT((1-(X2/POW3)**2-(Y2/POW3)**2)*
     1(1-ALPHA**2-BETA**2))-X2*ALPHA/POW3-Y2*BETA/POW3
      PTHETA=DSQRT(1-DEX2**2+(DEX2**2)*(CTHETA**2))
      ALPHA=DEX2*ALPHA-(PTHETA-DEX2*CTHETA)*X2/POW3
      BETA=DEX2*BETA-(PTHETA-DEX2*CTHETA)*Y2/POW3
      WRITE(6,604)X1,Y1,Z1,THETAX,THETAY,THETAZ
C
C        THE INTERSECTION WITH THE FIRST SURFACE OF THE CROWN ELEMENT
C        AND THE REFRATION AT THIS SURFACE ARE DETEPMINED.
C
      DIST=.001
      DO 606 I1=1,5
      X2=X1+ALPHA*DIST
      Y2=Y1+BETA*DIST
      Z2=POS3+POW3-DSQRT(POW3**2-X2*X2-Y2*Y2)+.001
      DIST=(Z2-Z1)/GAMMA
606   CONTINUE
      X1=X2
      Y1=Y2
      Z1=Z2
      CTHETA=DSQRT((1-(X2/POW3)**2-(Y2/POW3)**2)
     1*(1-ALPHA*ALPHA-BETA*BETA))
     1-(X2*ALPHA/POW3 +Y2*BETA/POW3)
      PTHETA=DSQRT(DEX3**2-1+CTHETA**2)
      ALPHA=(ALPHA-(PTHETA-CTHETA)*X2/POW3)/DEX3
      BETA =(BETA -(PTHETA-CTHETA)*Y2/POW3)/DEX3
      GAMMA=DSQRT(1-ALPHA**2-BETA**2)
      THETAX=DARCOS(ALPHA)*RAD
      THETAY=DARCOS(BETA)*RAD
      THETAZ=DARCOS(GAMMA)*RAD
      WRITE(6,603)X1,Y1,Z1,THETAX,THETAY,THETAZ
C
C        THE POINT OF INTERSECTION WITH THE REAR SURFACE OF THE CROWN
```

```
ELEMENT AND THE REFRACTION AT THAT SURFACE ARE DETERMINED.
C
      DIST=.1
      DO 812 I8=1,7
      X2=X1+ALPHA*DIST
      Y2=Y1+BETA*DIST
      Z2=POS4+POW4+DSQRT(POW4**2-X2*X2-Y2*Y2)
      DIST=(Z2-Z1)/GAMMA
812   CONTINUE
      CTHETA=DSQRT((1-(X2/POW4)**2-(Y2/POW4)**2)*
     1(1-ALPHA**2-BETA**2))-X2*ALPHA/POW4-Y2*BETA/POW4
      PTHETA=DSQRT(1-DEX3**2+(DEX3**2)*(CTHETA**2))
      ALPHA=DEX3*ALPHA-(PTHETA-DEX3*CTHETA)*X2/POW4
      BETA=DEX3*BETA-(PTHETA-DEX3*CTHETA)*Y2/POW4
      X1=X2
      Y1=Y2
      Z1=Z2
      GAMMA=DSQRT(1-ALPHA**2-BETA**2)
      THETAX=DARCOS(ALPHA)*RAD
      THETAY=DARCOS(BETA)*RAD
      THETAZ=DARCOS(GAMMA)*RAD
      WRITE(6,604)X1,Y1,Z1,THETAX,THETAY,THETAZ
C
C        THE POINT OF INTERSECTION WITH THE FOCAL PLANE IS FOUND.
C
      DIST=(FOCUS-Z1)/GAMMA
      X1=X1+ALPHA*DIST
      Y1=Y1+BETA*DIST
      Z1=Z1+GAMMA*DIST
      WRITE(6,34) X1,Y1,Z1
34    FORMAT(' ','FOCAL PLANE INTERSECTION      ',F11.6,'  ',F11.6,'  ',
     1F11.6,' ')
C
C        IN THE NEXT SECTION THE PLOT OF THE SPOT DIAGRAM FOR EACH OF
C        THE INVESTIGATED ANGLES IS GENERATED.
C
```

```
      IF(X1.GT.TINY) GO TO 120
      TINY=X1
120   CONTINUE
      D1(NM)=X1
      D3(NM)=Y1
      D4(NM)=-Y1
      NM=NM+1
      GO TO 996
900   WRITE(6,901)
901   FORMAT(' ','                                          *************** THIS LIG
     1HT RAY DID NOT INTERSECT THE MIRROR ***************')
996   CONTINUE
997   CONTINUE
998   CONTINUE
      D1(NM)=TINY
      D3(NM)=0.0
      D4(NM)=0.0
      NM=NM+1
      D1(NM)=.0000375
      D3(NM)=.0000375
      D4(NM)=.0000375
      NN=NM-2
      CALL PLOT(AXIS,0.0,-3)
      AXIS=AXIS+1.0
      CALL LINE(D3,D1,NN,1,-1,1)
      CALL LINE(D4,D1,NN,1,-1,1)
999   CONTINUE
      CALL PLOT(0.0,0.0,999)
      STOP
      END
```

	X	Y	Z	ANGLE TO X	ANGLE TO Y	ANGLE TO Z
LIGHT RAY ORIGIN POINT	0.500000	0.0	60.000000	90.0000	90.0000	0.0
********** THIS LIGHT RAY WAS INTERCEPTED BY THE SECONDARY **********						
LIGHT RAY ORIGIN POINT	-0.500000	0.000000	60.000000	90.0000	90.0000	0.0
********** THIS LIGHT RAY WAS INTERCEPTED BY THE SECONDARY **********						
LIGHT RAY ORIGIN POINT	1.500000	0.0	60.000000	90.0000	90.0000	0.0
********** THIS LIGHT RAY WAS INTERCEPTED BY THE SECONDARY **********						
LIGHT RAY ORIGIN POINT	0.750000	1.299038	60.000000	90.0000	90.0000	0.0
********** THIS LIGHT RAY WAS INTERCEPTED BY THE SECONDARY **********						
LIGHT RAY ORIGIN POINT	-0.750000	1.299038	60.000000	90.0000	90.0000	0.0
********** THIS LIGHT RAY WAS INTERCEPTED BY THE SECONDARY **********						
LIGHT RAY ORIGIN POINT	5.500000	0.0	60.000000	90.0000	90.0000	0.0
MIRROR INTERSECTION POINT	5.500000	0.000000	0.126042	95.2484	90.0000	5.2484
SECONDARY INTERSECTION POINT	1.813930	0.000000	40.253245	91.9693	90.0000	1.9693
INTERSECTION WITH CORRECTOR	0.515785	0.000000	2.500116	91.2896	90.0000	1.2896
BACK OF CORRECTOR	0.511280	0.000000	2.300000	91.9565	90.0000	1.9565
INTERSECTION WITH CORRECTOR	0.111588	0.000000	-9.400124	91.3331	90.0000	1.3331
BACK OF CORRECTOR	0.106936	0.000000	-9.600000	92.0225	90.0000	2.0225
INTERSECTION WITH FLATTENER	0.005286	0.000000	-12.478499	91.3286	90.0000	1.3286
BACK OF FLATTENER	0.000647	0.000000	-12.678500	92.0157	90.0000	2.0157
FOCAL PLANE INTERSECTION	0.000296	0.000000	-12.688500			
LIGHT RAY ORIGIN POINT	5.277211	1.549529	60.000000	90.0000	90.0000	0.0
MIRROR INTERSECTION POINT	5.277211	1.549529	0.126042	95.0353	91.4768	5.2484
SECONDARY INTERSECTION POINT	1.740453	0.511043	40.253245	91.8895	90.5547	1.9693
INTERSECTION WITH CORRECTOR	0.494892	0.145313	2.500116	91.2374	90.3633	1.2896
BACK OF CORRECTOR	0.490565	0.144044	2.300000	91.8773	90.5511	1.9565
INTERSECTION WITH CORRECTOR	0.107068	0.031438	-9.400124	91.2791	90.3755	1.3331
BACK OF CORRECTOR	0.102605	0.030127	-9.600000	91.9405	90.5697	2.0225
INTERSECTION WITH FLATTENER	0.000572	0.000168	-12.478499	91.2747	90.3743	1.3286
BACK OF FLATTENER	0.000621	0.000182	-12.678500	91.9340	90.5678	2.0157
FOCAL PLANE INTERSECTION	0.000284	0.000083	-12.688500			
LIGHT RAY ORIGIN POINT	4.626894	2.673524	60.000000	90.0000	90.0000	0.0
MIRROR INTERSECTION POINT	4.626894	2.673524	0.126042	94.4135	92.8347	5.2484
SECONDARY INTERSECTION POINT	1.525975	0.980684	40.253245	91.6566	91.0646	1.9693
INTERSECTION WITH CORRECTOR	0.433906	0.278854	2.500116	91.0849	90.6972	1.2896
BACK OF CORRECTOR	0.430116	0.276419	2.300000	91.6459	91.0576	1.9565